CAPITAL UNIVERSITY OF SCIENCE AND TECHNOLOGY, ISLAMABAD

Modeling of MIMO Radio Channels for Mobile-to-Mobile and Umbrella Cell Based Cellular Communication Systems

by

Mohd Yaqoob Wani

A thesis submitted in partial fulfillment for the degree of Doctor of Philosophy

in the

Faculty of Engineering

Department of Electrical Engineering

September 2017

Modeling of MIMO Radio Channels for Mobile-to-Mobile and Umbrella Cell Based Cellular Communication Systems

By
Mohd Yaqoob Wani
(PE093005)

Dr. Mohammad N Patwary
Faculty of Computing, Engineering & Sciences
Staffordshire Unversity, UK

Dr. Taimoor Abbas
Faculty of Engineering
Lund University, Sweden

Dr. Noor Muhammad Khan
Thesis Supervisor

Dr. Noor Muhammad Khan
Head, Department of Electrical Engineering

Dr. Imtiaz Ahmad Taj
Dean, Faculty of Engineering

DEPARTMENT OF ELECTRICAL ENGINEERING
CAPITAL UNIVERSITY OF SCIENCE AND TECHNOLOGY
ISLAMABAD
2017

CERTIFICATE OF APPROVAL

This is to certify that the research work presented in the thesis, entitled **"Modeling of MIMO Radio Channels for Mobile-to-Mobile and Umbrella Cell Based Cellular Communication Systems"** was conducted under the supervision of **Dr. Noor Muhammad Khan**. No part of this thesis has been submitted anywhere else for any other degree. This thesis is submitted to the **Department of Electrical Engineering, Capital University of Science and Technology** in partial fulfillment of the requirements for the degree of Doctor in Philosophy in the field of **Electrical Engineering**. The open defence of the thesis was conducted on **13 September, 2017.**

Student Name :   Mr. Mohd Yaqoob Wani
                        (PE-093005)

The Examining Committee unanimously agrees to award PhD degree in the mentioned field.

Examination Committee :

(a) External Examiner 1:   Dr. Mukhtar Ullah, Professor
                            Muslim Youth University,
                            Islamabad

(b) External Examiner 2:   Dr. Shahid Khattak
                            Professor
                            CIIT, Abbottabad

(c) Internal Examiner :   Dr. Muhammad Ashraf
                            Associate Professor
                            CUST, Islamabad

Supervisor Name :   Dr. Noor Muhammad Khan
                            Professor
                            CUST, Islamabad

Name of HoD :   Dr. Noor Muhammad Khan
                            Professor
                            CUST, Islamabad

Name of Dean :   Dr. Imtiaz Ahmad Taj
                            Professor
                            CUST, Islamabad

AUTHOR'S DECLARATION

I, **Mr. Mohd. Yaqoob Wani (Registration No. PE-093005)**, hereby state that my PhD thesis entitled, '**Modeling of MIMO Radio Channels for Mobile-to-Mobile and Umbrella Cell Based Cellular Communication Systems**' is my own work and has not been submitted previously by me for taking any degree from Capital University of Science and Technology, Islamabad or anywhere else in the country/ world.

At any time, if my statement is found to be incorrect even after my graduation, the University has the right to withdraw my PhD Degree.

(Mr. Mohd. Yaqoob Wani)

Dated: 13- September, 2017   Registration No : PE093005

PLAGIARISM UNDERTAKING

I solemnly declare that research work presented in the thesis titled "**Modeling of MIMO Radio Channels for Mobile-to-Mobile and Umbrella Cell Based Cellular Communication Systems**" is solely my research work with no significant contribution from any other person. Small contribution/ help wherever taken has been duly acknowledged and that complete thesis has been written by me.

I understand the zero tolerance policy of the HEC and Capital University of Science and Technology towards plagiarism. Therefore, I as an author of the above titled thesis declare that no portion of my thesis has been plagiarized and any material used as reference is properly referred/ cited.

I undertake that if I am found guilty of any formal plagiarism in the above titled thesis even after award of PhD Degree, the University reserves the right to withdraw/ revoke my PhD degree and that HEC and the University have the right to publish my name on the HEC/ University Website on which names of students are placed who submitted plagiarized thesis.

(Mr. Mohd. Yaqoob Wani)
Registration No. PE093005

Dated: 13- September, 2017

This thesis is dedicated to my parents.

For their endless love, support and encouragement.

PLAGIARISM UNDERTAKING

I solemnly declare that research work presented in this thesis titled "**Modeling of MIMO Radio Channels for Mobile-to-Mobile and Umbrella Cell Based Cellular Communication Systems**" is solely my research work with no significant contribution from any other person. Small contribution/help wherever taken has been dully acknowledged and that complete thesis has been written by me.

I understand the zero tolerance policy of the HEC and Capital University of Science and Technology towards plagiarism. Therefore, I as an author of the above titled thesis declare that no portion of my thesis has been plagiarized and any material used as reference is properly referred/cited.

I undertake that if I am found guilty of any formal plagiarism in the above titled thesis even after award of PhD Degree, the University reserves the right to withdraw/revoke my PhD degree and that HEC and the University have the right to publish my name on the HEC/University website on which names of students are placed who submitted plagiarized work.

(**Mohd Yaqoob Wani**)

Registration No: PE093005

Acknowledgements

First of all, I would like to thank Almighty Allah for giving me the opportunity and courage to pursue higher education. I would like to express my sincere gratitude to Professor Dr. Noor M. Khan for his persistent, continuous, dedicated and pertinent guidance that kept me motivated to complete thesis. During my studies Dr. Noor not only helped me in resolving the mysteries of wireless channel modeling but also made me realize the importance of dedication, consistency and time management. It has been an honor to have him as my supervisor for my PhD thesis. He has always encouraged my research work and has advised me patiently by providing insightful suggestions.

I would also like to thank all the faculty members of electrical engineering department of the Capital University of Science and Technology, for that they provided an environment, which was conducive for honing my theoretical knowledge and enhancing my practical skills. In addition, they ensured me that I have learnt how to utilize the concepts and skills in solving active research problems.

I also want to thank all the members of the Acme Center for Research in Wireless Communications (ARWiC) research group who have always provided me a pleasant environment to think of innovative ideas and continue research. I would like to express my gratitude especially to Dr. Muhammad Riaz for his brotherly advice and timely support; whenever I needed it the most. He was always the beacon of hope for me and lifted my spirits, when I was affected by research blues. I am also grateful to Mr Mirza Yasir, who was always available in organizing and managing research meetings and administrative matters.

I dedicate this PhD thesis to my friends and family, especially my sweet wife, lovely children, Ab. Basit, Aima Yaqoob and Saba Yaqoob, who are the pride and joy of my life. I love you more than anything and I appreciate all your patience and support during my PhD studies.

List of Publications

1. M. Yaqoob Wani, M. Riaz and Noor M Khan, "Modeling and Characterization of MIMO Mobile-to-Mobile Communication Channels Using Elliptical Scattering Geometry", *Wireless Personal Communications*, vol. 91, no.2, pp. 509–524, Jun. 2016, publisher, Springer. [Impact factor: 0.951]

2. M. Yaqoob Wani and Noor M Khan, "Characterization of 3D Elliptical Spatial Channel Model for MIMO Mobile-to-Mobile Communication Environment" , accepted in *Wireless Personal Communications*,vol. X, no.X, pp. 1–20, Jun. 2017, publisher, Springer. [Impact factor: 0.951]

3. M. Yaqoob Wani, M. Riaz and Noor M Khan, "Geometrical Modeling of Scattering Environment For Highways in Umbrella Cell Based MIMO Communication Systems" submitted in *Wireless Personal Communications*, July 8, 2017. [Impact factor: 0.951]

Abstract

Mobile-to-mobile (M2M) and fixed-to-mobile (F2M) communication technology has shown astonishing intrusion in battle-fields, cellular and vehicular networks, intelligent transportation systems and internet of things. Mobile nodes involved in these infrastructures demand a high data rate connectivity over radio fading links.

This dissertation concentrates on the geometrical modeling of the spatial characteristics of two-dimensional (2D) and three-dimensional (3D) radio fading channel for multiple-input-multiple-output (MIMO) M2M and MIMO F2M communication scenarios. Closed-form expressions for the joint and marginal space-time correlation functions among MIMO antenna array elements and probability density function (PDF) of angle-of-arrival (AoA) of the multipaths in nonisotropic environments are presented.

Initially, the emphasis has been on the 2D propagation scenario; where, mobile subscribers are equipped with low elevated multiple antenna array structures and they intend to communicate on the move without any base station (BS). These mobile subscribers usually reside on structured-bounded highways or in the "long and narrow" streets and canyons; where, the distribution of scattering objects along the roadside regions are non-isotropic in nature. It is observed that elliptical geometry is an appropriate shape, which correlates more accurately the layout of such propagation environments than the circular shape. In the proposed model, it is assumed that the mobile stations reside at the centers of two different ellipses and the scatterers are distributed uniformly along the boundaries of the ellipses. The ellipses are independently rotatable along the horizontal plane corresponding to the direction of mobile stations. The lengths of major and minor axes and the eccentricities of the ellipses are assumed to be dependant on the physical measurement of the propagation environments. Using the proposed geometrical model, the closed-form expression of PDF of AoA/AoD is obtained for non-isotropic scattering environments. Based on this AoA/AoD, mathematical expression of joint and marginal PDFs of space-time correlations among the MIMO antenna elements are derived. The 2D eccentricity based channel model is then extended to 3D elliptical-based cylindrical channel model to accommodate the high-rise structures present along the roadside premises of highways, streets or canyons. In this model, the scattering objects are assumed to be placed on the surfaces of the elliptical-based

cylinders around both transmitter and receiver nodes. The horizontal dimension of the physical propagation medium is modeled by eccentricity and height of the scatterers are modeled by the height of cylinders. Mobile stations are placed at the centers of the cylinders equipped with multiple antenna arrays. The dimension of cylinders are independently adjustable and rotatable according to the physical dimension of the propagation medium and the direction of motion of MS's. Here again the mathematical expressions for correlations among MIMO M2M links are formulated and the obtained theoretical results are simulated and compared with the measured data. In the last part of thesis, a 3D elliptical based geometrical channel model is proposed to model umbrella-cell in a cellular communication environment, which provides trustworthy communication links for speedy vehicles on the highways. In the proposed model, mobile subscriber is assumed to be located at the center of the elliptical cylinder equipped with low-rise antenna array and the scatterers are assumed to be uniformly distributed on the surface of the cylinder; whereas, the BS is on the top of high-rise tower with multiple antenna structure and is assumed to be scatter-free. Using the proposed model an expression for space-time correlation among antenna elements is derived.

Contents

List of Figures

List of Tables

Abbreviations

AoA	Angle-of-Arrival
AoD	Angle-of-Departure
ToA	Time-of-Arrival
M2M	Mobile-to-Mobile
F2M	Fixed-to-Mobile
F2F	Fixed-to-Fixed
PDF	Probability density function
BS	Base station
MS	Mobile station
ITS	Intelligent transportation systems
VANET	Vehicular ad hoc networks
LoS	Line-of-Sight
NLoS	Non-Line-of-Sight
IVC	Inter-vehicle communications
CCF	Cross correlation function
CF	Correlation function
LoS	Line of sight
MANET	Mobile ad hoc networks
ISI	Inter-symbol interference
QoS	Quality of service
MSC	Mobile switching center
WSS	Wide sense stationary
3D	Three dimentional
2D	Two dimentional

MIMO   Multiple input multiple output

SISO   Single input single output

MS_t Transmit mobile stations

MS_r Receive mobile stations

ARWiC   ACME Center for Research in Wireless Communication

Symbols

a_t	Major axis of ellipse around $\mathrm{MS_t}$
a_r	Major axis of ellipse around $\mathrm{MS_r}$
b_t	Minor axis of ellipse around $\mathrm{MS_t}$
b_r	Minor axis of ellipse around $\mathrm{MS_r}$
ϵ_t	Eccentricity of ellipse around $\mathrm{MS_t}$
ϵ_r	Eccentricity of ellipse around $\mathrm{MS_r}$
$\mathbf{J}$	Jacobian matrix
$(.)^H$	Hermitian transpose
$E(.)$	Expectation
$J_0(.)$	Zeroth order Bessel fuction
D	Transmitter-Receiver separation distance
$R_{d,r}$	Variable radius of ellipse around $\mathrm{MS_r}$
$R_{d,t}$	Variable radius of ellipse around $\mathrm{MS_t}$
$\psi_t^{(p)}$	The elevation angle of pth transmit antenna element (relative to x-axis)
$\psi_r^{(q)}$	The elevation angle of qth receive antenna element (relative to x-axis)
$\beta_t^{(m)}$	The elevation angle of departure (EAoD)
$\beta_r^{(n)}$	The elevation angle of arrival (EAoA)
$\alpha_t^{(m)}$	The azimuth angle of departure (AAoD)
$\alpha_r^{(n)}$	The azimuth angle of arrival (AAoA)
$\theta_t^{(p)}$	The azimuth angle of pth transmit (relative to x-axis)
$\theta_r^{(q)}$	The azimuth angle of qth receive antenna element (relative to x-axis)
δ_t	Separation between transmit antenna elements
δ_r	Separation between receive antenna elements

$A_t^{(q)}$	Receive antenna element
$A_r^{(p)}$	Transmit antenna element
v_t	Velocity of transmitter
v_r	Velocity of receiver
f_{tmax}	Maximum Doppler frequency
f_{dmax}	Doppler frequency as a result of relative velocity of MSs
$S_t^{(m)}$	mth scattering object around MS_t
$S_r^{(n)}$	nth scattering object around MS_r
d_{pm}	Distance from transmitter MS_t to the scattering point $S_t^{(m)}$
d_{mn}	Distance from scattering point $S_t^{(m)}$ to the scattering point $S_r^{(n)}$
d_{nq}	Distance from scattering point $S_r^{(n)}$ to the receiver MS_r
T_{coh}	Coherence time
T_s	Symbol period
c	Speed of light
C	Capacity
$\mathbf{H}$	Channel matrix
λ	Wavelength
ρ	Signal to noise ratio
P	Number of transmit antenna array elements
Q	Number of receive antenna array elements
I	Identity matrix

Chapter 1

Introduction

This chapter begins with an overview of fixed-to-fixed (F2F), fixed-to-mobile (F2M) and mobile-to-mobile (M2M) communication environments. The chapter also highlights the significance of the proposed research topic and emphasis is given on various communication systems where high speed mobile users intend to achieve high data rates like in vehicular ad hoc networks (VANETs) of M2M and umbrella cellular structure of F2M environments. The chapter ends with an organization of the dissertation.

1.1 Overview of Communication Channels

Wireless communication received tremendous advancements after Guglielmo Marconi placed a foundation stone of wireless communication in the late 1800s. As a result, a new era of communication started that drew the attention of a large number of researchers and engineers who developed state-of-the-art methods for the transmission of audio and multimedia applications over wireless links. In the 19th and early 20th century, wireless communication technology witnessed significant improvements in coverage and throughput. These improvements were mainly based on the better understanding of the propagation environment, through which electromagnetic waves travel from transmitter to the receiver.

Based on this radio propagation environment, the wireless communication channels can be broadly divided into three main types (i) Fixed-to-fixed (F2F), (ii) Fixed-to-mobile (F2M) and, (iii) Mobile-to-mobile (M2M) communication channels. In F2F environment, both communicating nodes are stationary and are equipped with single or multiple directional antenna arrays. In F2F communication systems both transmitter and receiver antenna arrays are predominantly installed on the high-rise structures or mountains in such a way that the LoS component exist in between them, as depicted in Fig. 1.1. This wireless network is more cost efficient than the land cable network and also has the ability to withstand perfectly during unpleasant weather conditions. In modern telecommunication systems, a beam of radio waves in microwave frequency band is used in F2F wireless links that facilitates broadcasters to send data from studio to transmitter unit. Telecommunication operators also use F2F microwave directional links to transfer huge amount of data at high-speed from/to base-stations to/from the core networks [3].
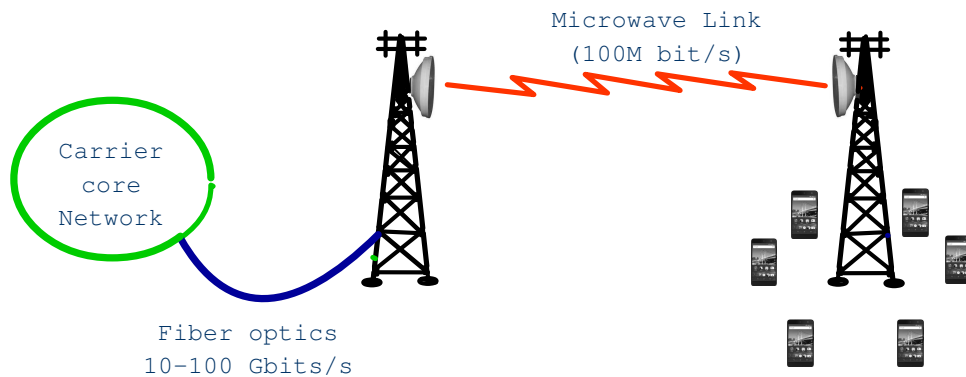
FIGURE 1.1: A simplified rendering of an F2F microwave link

Whereas, in F2M radio communication system, a base station (BS) is considered to be stationary with a high-rise antenna mounted on the top of a tall structure or tower while the MSs are equipped with low elevated antennas surrounded by the buildings, vegetation, mountains, etc., and are supposed to be in motion. Cellular mobile communication is one of the major applications of the F2M communication systems. In most of the F2M systems, the BS is assumed to be scatter-free while the MS is usually surrounded by local scatterers. A typical F2M wireless communication system is depicted in Fig. 1.2. Various emerging systems demand that the wireless nodes should communicate directly with each
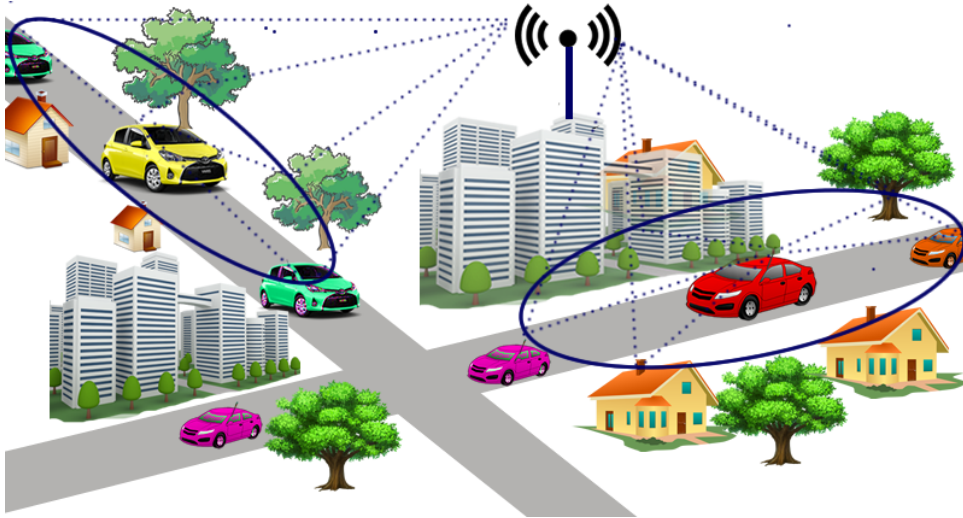
FIGURE 1.2: A simplified rendering of an F2M communication scenario
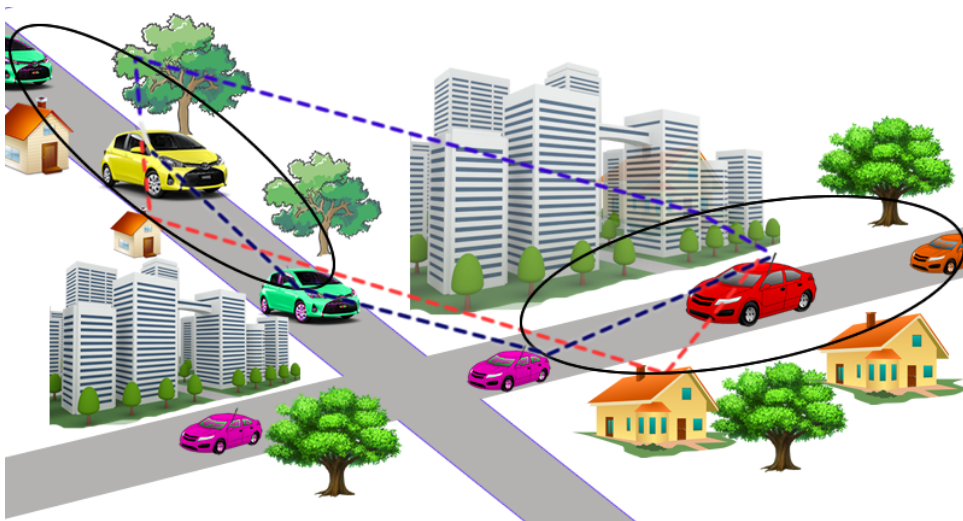
FIGURE 1.3: A simplified rendering of an M2M communication scenario

other without having a centralized BS; such a communication system is known as M2M communication environment as depicted in Fig. 1.3. In M2M communication environment both nodes of the communication link are supposed to be on the move. Mobile ad hoc networks (MANETs), VANETs, intelligent transportation systems (ITS), inter-vehicle communications (IVCs), and relay-based cooperative networks are the applications of M2M communication system [4]. In these systems, the MSs are equipped with low elevated antennas and are surrounded by the scattering objects like high-rise buildings, trees, vehicles, mountains and other structures. In such environments, transmitted signal propagates along multiple paths and terminates at receiver antennas with random phases and amplitudes.

Therefore, mobile communicating nodes are severely affected by the multipath fading. In addition to this, the motion of surrounding vehicles, movements of tree leaves, motion of transmitter and receiver causes the time-varying dispersion in the transmitted signal spectrum. This dispersion in frequency is called Doppler shift or Doppler spread. Each multipath is independently subjected to Doppler shift and hence experiences an independent frequency shift. The expression of the Doppler frequency (f_d) can be written as $V_r f_c \cos(\gamma)/c$, where, V_r is the relative velocity of the MS, f_c is the carrier frequency, γ is AoA and c is the velocity of light. The Doppler shift is proportional to the carrier frequency, relative velocities of the mobile nodes and AoA of multipath signals [5]. Fig. 1.4, illustrates the Doppler effect in a typical F2M multipath fading environment where fast moving mobile subscribers mostly reside. Especially, in case of macrocellular communication environment, fast-moving vehicles get severely effected by the large Doppler spreads. In addition to it, the high speed of the vehicles not only creates the
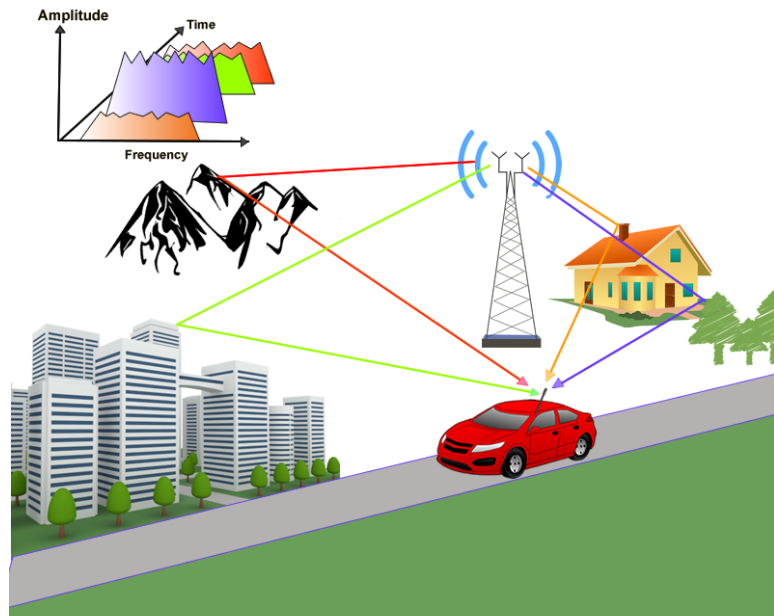
FIGURE 1.4: A simplified illustration of Doppler effect in F2M environment

serendipitous and unpremeditated situations in communication but also increases the rate of occurrence of handoff, which in turn imposes burden on mobile switching center (MSC). These situations mostly occur on highways under an umbrella macrocell and can not be properly modeled using existing models [6]. In [7–17],

different techniques have been proposed to handover the fast-moving vehicles to an umbrella cell. Moreover, in M2M or F2M propagation environments, line-of-sight (LoS) component is mostly unavailable. Therefore, signals are propagated by means of reflection, diffraction, refraction and scattering mechanisms. These delayed multipath components arrive from different directions in different time instants and combine constructively or destructively creating a faded envelope at the receiver terminal. In past, the multipath propagation in wireless communication channel was considered to be an obstacle in designing trustworthy communication links. However, this paradigm has been changed in modern communication systems, researcher tried to take advantage of these multipath signals to improve the reliability and capacity of the wireless communication systems. This is achieved through space-time processing in which multiple antennas are employed at both terminals of the communication link [18]. Multiple antennas can offer significant increase in spectral efficiency and data throughput without additional bandwidth or transmit power [19]. Information theory has shown that if the multipath signal propagation is properly exploited with MIMO, enormous theoretical capacity can be achieved [20–26]. However, different coding schemes like space-time trellis codes, space-time block codes, layered space-time codes, etc., have been introduced to exploit the advantages of MIMO antenna structures [27–29]. The spectral efficiencies of the MIMO system are based on the assurance that an opulent scattering environment provides uncorrelated data links with different spatial signatures from each transmit antenna to each receive antenna. Whereas, the correlation in the space, frequency and time domains are dependent on the spread in angle of arrival (AoA)/angle of departure (AoD), delay spread and the Doppler spread. Therefore, MIMO system capacity rely on the richness and statistical distributions of the scattering objects in the propagation medium. Therefore, for the beneficial design of a MIMO-M2M or MIMO-F2M communication systems, extensive knowledge of the statistical characteristics of the fading channel coefficients and the capacity analysis of the propagation links between the communicating nodes are extremely important. The capacity of a MIMO wireless communication system not only depends on the antenna array elements but also depends significantly on the rank of

the correlation matrix of the wireless channel [30–33]. The correlations among antenna elements exert adverse effects on its capacity and error rate performance of the MIMO system[31, 34]. At an arbitrary time instant k, the normalized capacity $C(k)$ or capacity per unit bandwidth of a MIMO system having P antenna elements at the transmitter and Q antenna elements at the receiver, can be expressed as [23, 35, 36],

$$C(\mathbf{k}) = \log_2 \det \left(\mathbf{I}_Q + \tfrac{\rho}{P} \mathbf{H}(\mathbf{k}) \mathbf{H}(\mathbf{k})^H \right) \text{bps/Hz} \qquad (1.1)$$

where, $\mathbf{I}_Q$ is the $Q \times Q$ identity matrix, $(\cdot)^H$ is called hermitian transpose, $\det(\cdot)$ is matrix determinant, ρ is the mean signal-to-noise ratio (SNR) for each receiver antenna element, $\mathbf{H}(\mathbf{k})_{Q \times P}$ is called MIMO channel matrix at the time instant, k, that can be obtained by appropriate channel model. According to the information theory, reliable and error-free communication can be achieved if the data rate is kept below the channel capacity. Therefore, to predict the performance of MIMO communication systems, the simulation of realistic MIMO channel model is essential.

1.2 Spatial and Temporal Correlation of MIMO Channels

In MIMO wireless communication systems, maximum throughput can only be achieved when multiple data streams are transmitted through multiple antenna array elements into the uncorrelated wireless channels. In a real world scenario, the MIMO channels are usually not fully uncorrelated to each other; however, exhibit some correlations among them. Signals interact with the scatterers present in the propagation medium in a complex way. These scatterers reflect, diffract and scatter the transmitted signal in all possible directions and create multipaths (i.e. multiple copies of transmitted signal). These multipaths impinge at receiver antenna array elements constructively or destructively resulting in a faded

signal envelope at each antenna element [37]. At the receiver end strong signal processing algorithms are used to separate desired data streams from the faded envelopes. Therefore, the performance of MIMO system considerably depends on the richness of scatterers, correlations among MIMO links, space-time coding and channel state information (CSI). In MIMO systems, if channels are uncorrelated that means multiple spatially separated channels are available between the transmitter and receiver then capacity closer to the Shannon can be achieved via each channel. In reality, the multipaths in such scattering environment force the radio propagation channels to interact each other through various degrees of freedom. This phenomenon of interaction is called spatial correlation [38, 39]. The spatial correlation is inversely proportional to the angular spread of the AoA/AoD of the multipaths. In addition to spatial correlation, mutual coupling of antenna array elements also contribute in the channel correlations [40]. Spread in AoA/AoD is
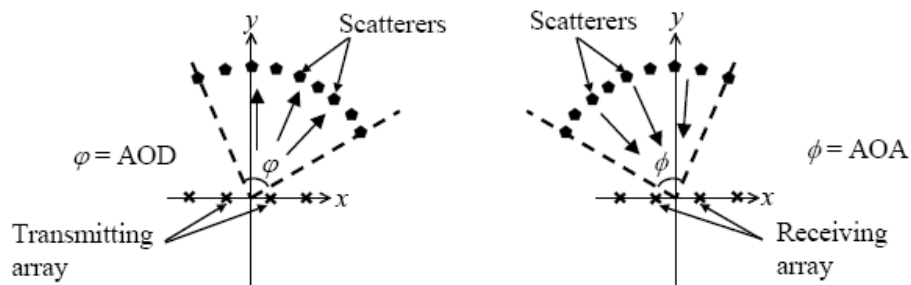
FIGURE 1.5: AoA/AoD of the multipaths

the range of angular directions where the multipath signals arrive at receiver (or leave the transmitter) antenna array as shown in Fig. 1.5. A wider AoA (or AoD) means that the multipath signals arrive at the receiver (or leave the transmitter) in different paths that may have most probably, different spatial signatures. Therefore, receive or transmit channel correlations depend on the antenna element spacing, scattering distributions and AoA (or AoD) of the multipath signals. In addition to spatial correlations, the channel gets trapped into another correlation variation known as temporal correlated when the transmitter, receiver or scatterers present in the medium are in motion. The relative motion between transmitter, receiver or the scatter objects exhibits dispersion in the carrier frequency this is called Doppler shift as discussed in Section 1.1. In mobile communications, the

temporal correlation can be obtained by taking the inverse Fourier transform of the Doppler power spectrum density (PSD).

1.3   Significance of the Research Topic

Extensive developments have been seen in the last few decades in the area of wireless communication systems. While, it has been the topic of interest since 1960s, however, a huge surge of research in this field erupted in the last few decades, because of the rapid expansion of wireless applications. Challenges that might be faced by future wireless communication systems in all aspects of life are reliable wireless communication with high data rate, error-free linkages and quality of service (QoS) surety. Achieving high data rate over radio fading channels is not an easy task for several vilifications. As already discussed in detail in Section 1.1, the wireless channel is a husky time-varying propagation environment. Because of the harsh behavior of the propagation environment, signal transmitted on a wireless channel is subjected to interference, propagation path loss, Doppler spread, delay spread, shadowing, fading, interference by neighboring wireless devices and atmospheric conditions, etc. While it is possible to increase data rates by providing more bandwidth or increasing power of the transmitted signal; however, the constraints in wireless communication systems like signal power and bandwidth hinder the achievements of such high data rates. On one hand, the bandwidth or spectrum is prohibitively expensive and on the other hand, increasing transmit power adds interference to other systems. Thus, neither the spectrum nor the power can be increased. Therefore, space-time processing is considered a viable approach to increase the capacity in terms of the data rate with good QoS. However, to attain high capacity with good QoS over space-time processing-based MIMO links, an exact understanding of the physical propagation environment is required, so that maximum capacity closer to the one defined by Shannons information theory can be achieved [41]. Spectral efficiency of a wireless communication link or increase in capacity can also be achieved by dividing the large geographical area into small cells in such a way that each cell is allocated a chunk of frequency band, which may
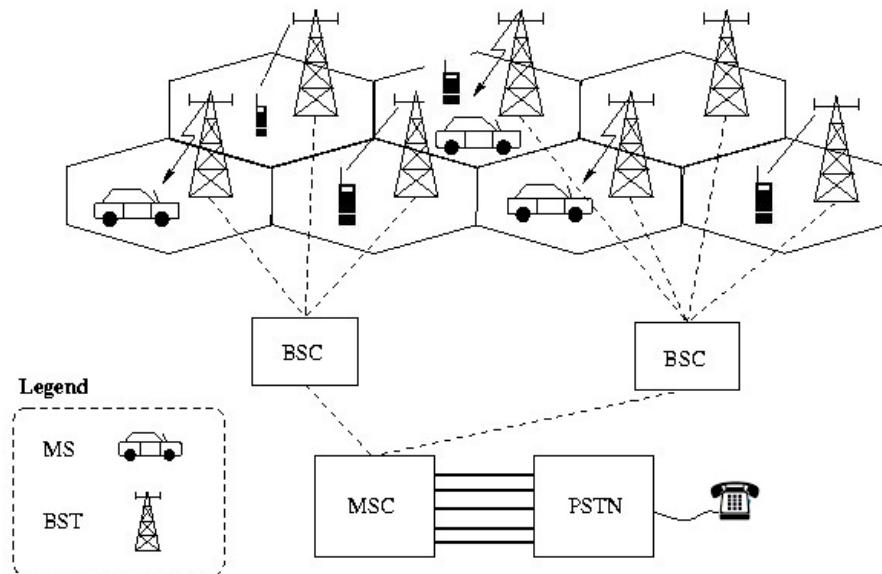
FIGURE 1.6: Cellular mobile communications

be reused in distant cells while controlling co-channel interference as depicted in Fig. 1.6. The frequency-reuse concept in cellular mobile communication systems improves spectral efficiency significantly. This system-level concept becomes the basis of all modern cellular mobile communication systems.

Cellular mobile communication has shown exponential increase in the number of mobile users since last decade. As a system intends to increase the number of its subscribers, it is forced to increase its capacity. Data requirements of a single user are usually increased due to additional value-added services in cellular mobile communication systems. In cellular mobile communications, the capacity can be increased either by increasing the bandwidth or by reducing the cell size so that the frequency (or channel) may be reused more frequently. This small size of the cell architecture creates most crucial dilemma in the cellular mobile communication i.e, it increases the occurrence rate of handoff [42]. Handoff is a process of shifting the channel from one time-slot, frequency or spreading code to other while the mobile unit is progressing a call [43]. The handoff process becomes very serious issue for speedy vehicles on highways across the microcells [44], as it imposes extra burden on MSC of the cellular mobile communication system [45]. To overcome the frequent handoff problem, the fast moving vehicle are handed over to umbrella

cell, which not only decreases the frequency of the handoffs but also maximizes the radio coverage [16, 45–48]. In an umbrella cell, a high powered antenna is mounted on high-rise structure to cover large area along a highway [49]. The umbrella cell is dedicated to provide coverage to high speed users on the highway for long distances, therefore, the frequency of handoffs is minimized [5]. Apart from handoff problem, the non-stationary and time-variant behavior of wireless channel immensely degrades the performance of the cellular mobile communication for high speed vehicle. Therefore, challenge in F2M or M2M wireless communication is the time-variation nature of the propagation medium. This time-variation creates difficulty in obtaining the exact channel state information (CSI). The precise CSI is mandatory at the receiver for better capacity, QoS and error free communication [50]. One of the well known method of estimating CSI is based on the use of known training sequences.

In mobile communication scenario, the channel statistics are random and are dependent on the distribution of scattering objects present in the propagation medium, antenna configuration and Doppler spreads, etc. Therefore, before installing the communication systems in such scenario, it is imperative to have understanding of the channel characteristics that can be used for the design, performance analysis and the development of wireless communication systems. Field-trials (i.e., empirical models) can be take as one of the ways to assess the statistics of a radio fading channel. In this channel assessment technique, all environmental effects of a specific area on the quality of the communication link are taken into account. The empirical models can provide accurate statistics of the channel parameters, but they are cite-specific and are also neither cost efficient nor time efficient [51]. However, computer simulations are alternative solutions that can reproduce the desired channel characteristics if channel models used in the simulation are well designed. In this regard, various channel models are available in the literature that can be used for the analysis and development of a communication system. Among these models, stochastic and geometry-based stochastic channel models (GBSCM) rely on some valid assumptions. Computer simulation results that are based on these models are accurate enough to provide the fading statistics of the real-world

propagation channels. In addition to it, the channel models are very cost effective as well as time effective as compared to field trials. Moveover, GBSCM are flexible and can provide better understanding for SISO and MIMO systems in mobile communication environments [52]; therefore, it is highly desirable to have suitable GBSCM's that are not only equipped with spatial characteristics of radio channel but should also provide the sufficient knowledge about the correlations among the antenna elements of MIMO communication link. Keeping in view the advantages of GBSCM's 2D and 3D channel models have been proposed in this dissertation for M2M/F2M MIMO communication link.

1.4   Research Objectives

Keeping in view the discussion presented in Section 1.3, the proposed research study aims to address the following major research objectives:

- To propose a geometrical shape that resembles with the layout of streets, canyons and highways.

- To derive a mathematical expression for the PDF of AoA/AoD of the signals when a MS resides in streets or canyons.

- To propose an appropriate generic geometrical model for MIMO M2M communications.

- To propose an appropriate geometrical model for MIMO M2M communications that can address the effect of AoA of the signals scattered from high-rise buildings and road-side vegetation, etc.

- To propose a geometrical channel for an umbrella cell of cellular mobile communication, when a fast moving mobile subscriber is on call in macro-cellular system.

- To derive a mathematical expression for correlation functions among MIMO antenna elements.

1.5 Organization of the Dissertation Report

The rest of the dissertation is organized as follows:

Chapter 2, reports substantial discussion of various wireless communication channel models and presents their critical analysis in the wake of designing a high-capacity MIMO system. Section 2.1 starts with a discussion on the importance of channel models for MIMO systems and then proceeds to the critical analysis of the well-known modeling techniques in subsection 2.1.1 and 2.1.2. Then the importance of elliptical geometry in channel modeling is highlighted in 2.1.3. In the end of Section 2.1, a problem statement is presented on the basis of the provided literature survey. Finally, Section 2.2 provides research contributions of the thesis and methodology to accomplish the proposed research target.

Chapter 3, presents a geometrically based 2D elliptical channel model for MIMO M2M communication scattering environment and the chapter starts with an introduction given in Section 3.1 and Section 3.2 describes in detail the proposed spatial channel model. Section 3.3 and Section 3.4 provides mathematical derivation of the PDF of AoA expression and space-time correlation functions, respectively. Finally, Section 3.5 describes theoretical results of the obtained closed-form expressions of the space-time correlation functions.

Chapter 4, begins with an introduction in Section 4.1 and Section 4.2 describes the proposed 3D geometric stochastic channel model for MIMO M2M propagation scattering environment. Section 4.3 provides a detailed derivation of proposed system model. Moreover, mathematical expression of the joint and marginal space-time correlation functions among MIMO antenna elements is given in Section 4.4. Finally, Section 4.5 portrays the theoretical results with their detailed discussion.

Chapter 5, presents a 3D elliptic cylindrical geometrical channel model for scattering environment under the umbrella-cell. In Section 5.1 introduction of the chapter is presented and Section 5.1 the describes the system model of the proposed geometrical channel model. The Section 5.3 and Section 5.3 provides the details of mathematical derivation of the space-time correlation function. Finally,

In Section 5.5, the describes theoretical results of the obtained space-time correlation function is presented and in Section 5.6 provides the conclusion of the chapter.

Chapter 6, summarizes the developed research work and the obtained theoretical results in Section 6.1 and provides the future directions and recommendations in Section 6.2.

Chapter 2

Literature Survey, Problem Statement and Research Contributions

This chapter reports substantial discussion of various wireless communication channel models and presents their critical analysis in the wake of designing a high-capacity MIMO system. Section 2.1 starts with a discussion on the importance of channel models for MIMO systems and then proceeds to the critical analysis of the well-known modeling techniques in subsection 2.1.1 and 2.1.2. Then the importance of elliptical geometry in channel modeling is highlighted in 2.1.3. In the end of Section 2.1, a problem statement is presented on the basis of the provided literature survey. Section 2.2 provides research contributions of the thesis and methodology to accomplish the proposed research target. Section 2.3 describes the strengths and limitations of the proposed work and finally, 2.4 provides a brief conclusion of the chapter.

2.1   Literature Survey

Continuous demand for high data rates in all aspects of wireless communication systems has been a constant driving force in research arena. Since the last few decades a new era of communication has emerged rapidly where the transmitter and/or receiver nodes want to communicate with each other on the move, this is called mobile communication. Resulting mobile communication systems are the promising candidates to facilitate real-time data, audio and video transmission among the mobile subscribers and also between the fast moving vehicles on the highways, racetracks, etc., to alleviate hazards of accidents and provide error free communication links [53]. The fundamental requirements of these mobile communication systems is to provide high capacity wireless links with better quality of service (QoS), utilizing limited resources. High mobility of mobile subscribers and rich scattering environments have significant impact on the capacity of such systems [54]. However, in rich propagation scattering environments, the channel characteristics are unpredictable and multipath components cause the received signal to be in deep fade. Single-input-single-output (SISO) communication links are the very basic systems; however, they are too vulnerable to avoid effects caused by multipaths. Therefore, traditional SISO communication link may not provide the required capacity with good QoS in such communication scenarios. Recently, rich scattering environment has been recognized a feasible situation for the high data-rate applications, if multiple antenna arrays are employed instead of single antenna structure at both ends of wireless link [23]. MIMO systems, therefore, exploit this rich scattering environment in constructive manner and provide spatial multiplexing that can guarantee astonishing increase in throughput [23, 26, 32, 35, 55]. The promised large capacity gain of a MIMO system can be achieved contingent upon good understanding of spatial characteristics of the radio fading channel as well as upon proper observation of correlations among antenna elements [26].

2.1.1 Early Work on Channel Modeling:

Various techniques are adopted to model the wireless channel to estimate its statistics on the basis of communication scenario and the distribution of the scattering objects in the propagation environments. Mostly, communication channels are modeled in the literature using empirical, deterministic, stochastic and geometry-based stochastic channel modeling (GBSCM) approaches [56–59]. Statistical distributions of empirical channel models are based on the experimental measurements and observations for a particular communication scenario. The accuracy of these models depends on the number of field measurement campaigns for a specific propagation environment. Due to this reason, an empirical model can not be considered a suitable generalized model for all propagation scenarios. Deterministic channel modeling approach is employed when locations of the transmitter, receiver and scatterers are known.

The deterministic channel model characterizes the parameters of the propagation channel deterministically, e.g., ray tracing approach. This channel modeling needs a complete knowledge of geography of the location of scattering objects present in the desired propagation environment. Also, the laws of electromagnetic wave propagation are used to estimate the received signal power at a specific site [60]. The estimation of propagation radio waves is based on complicated electromagnetic formulas, and ray tracing technique that needs huge computational power. The accuracy of the deterministic channel model depends on the reproduction of the propagation environments. In addition to it, for the localizations of scatterers huge information of the geometry is required [61, 62]. Therefore, deterministic channel modeling approach can predict the performance of the wireless system perfectly under above specific conditions. Since, in M2M or F2M communication environment, the communicating nodes are on the move and their locations are not fixed; therefore, deterministic channel modeling approach is not appropriate for these communication scenarios [63].

The stochastic channel modeling approach is based on the PDFs of various parameters like AoA/AoD, time-of-arrival/departure (ToA/D), Doppler shift, delay,

pathloss, etc., which give insight about the statistical behavior of the channel and is, thus, an empirical approach to analyze the parameters of the channel in a stochastic manner [64]. Stochastic channel modeling can be further classified into non-geometrical stochastic models (NGSMs) and GBSCM [65, 66]. In NGSM approach, AoA, AoD, location of scatterers and other physical parameters of the channel are completely in a stochastic manner without following any underlying geometry. Although, these models require least information about propagation environment and less processing power but the generated analysis usually processes least accuracy. In contrast, the impulse response in GBSCM is characterized by the fundamental laws of wave propagation applied to specific transmitter, receiver and scatterer geometries that are chosen in a stochastic manner [67, 68]. The vibrant behavior of the M2M and F2M wireless channel makes the propagation channel non-stationary, therefore, NGSM modeling approach is incapable of modeling the impact of physical scattering phenomenon in such a dynamic propagation environment. Nevertheless, such non-stationary propagation environments can be modeled by GBSCM approach under the assumption of quasi-stationary scattering [69]. Since, these models are based on some assumptions; therefore, they are less accurate compared to empirical channel models, if specific propagation scenario is considered only. Results obtained by the GBSCM channel model must be validated against measurement campaign before its use for a particular propagation environment. These are the special categories of stochastic channel models, based on the fundamental laws of waves propagation and the physical geometry of scattering environment. Therefore, they can predict the achievable capacity of a system, and hence can be applied to design and analyze the large systems. In addition, GBSCMs may be utilized for various propagation scenarios by adjusting the model input parameters of the same framework and are mathematically trackable [70–72]. On the basis of physical dimensions of propagation environments, PDFs of various parameters of F2M and M2M wireless channel may be derived geometrically. Moreover, the motion of the scattering objects, transmitter or the receiver can be modeled easily in GBSCM approach for non-stationary environments [73].

However, understanding the importance of the GBSCM, various geometrical channel models have been proposed in the literature for F2M and M2M communication environments.

2.1.2 Geometrical Channel Models for M2M and F2M Environments:

Akki and Haber were the pioneer researchers who proposed a fundamental channel model for M2M urban and suburban communication environments [74]. Using their model, they derived expressions for the PDFs of received envelope and time-correlations in channel coefficients. Using these correlations, the authors also obtained expression for the power spectral density (PSD). Patzöld *et al.* [75], extended the work in [74], and presented a frequency non-selective circular two-ring model for MIMO M2M communication environment. Assuming infinite scatterers around the MSs (MSs), the authors derived expressions for transmit and receive correlation functions and provided a framework for the channel capacity. Another concept that scatterers are not located exactly at the boundary of the circular rings but at varying distances from the center of the rings, was presented in the form of two-erose-ring model in [76]. The authors also derived formulas for the complex envelope of the diffused antenna components. However, the empirical results were presented on the basis of simulation for the space-time correlation function assuming an isotropic scattering environment. The work in [76], was extended by Riaz *et al.* [77], for the derivation of mathematical expressions for the time-autocorrelation function and Doppler spectrum. In [78, 79], geometrical channel models have been proposed by employing circular disc and circular strip shapes for M2M scattering environment. In the previously discussed 2D-channel models, the authors have assumed isotropic scattering environments around the MS's. Whereas, Chelli *et al.*, have provided the analytical expressions of auto-correlation function (ACF) and CCF under the non-stationary and non-isotropic scattering environments based on the geometrical T-junction model [80].

In the above-mentioned 2D geometrical channel models, signal propagation has been considered only along azimuth plane ignoring the elevation plane. Hence, 2D geometrical channel models may be appropriate in some of the rural areas, but may not be decorous for streets, canyons, urban or metropolitan areas. Because in such areas, the source of communication is predominantly with scattered waves, which are diffracted, reflected down the streets or canyons by the edges of the surrounding infrastructure. Therefore, geometrical channel models that consider the effect of elevation angle and azimuth angle of the signals are suitable models for such urban environments.

Therefore, for such propagation scenarios, 3D geometrical channel models are proposed in the literature for M2M and F2M communication environments. In initially proposed 3D geometrical channel models for M2M communication [81–83], the authors assumed a wide sense stationary (WSS) scattering environment and provided closed-form expressions for the time-autocorrelation function and Doppler spectrum. Zajić *et al.* in [84, 85], have assumed that the MSs are located at the center of cylinders with low elevated multiple antenna arrays and the scatterers are uniformly distributed along the surfaces of cylinders. The authors have proposed a general analytical solution of 3D space-time cross-correlation function (CCF) for MIMO M2M communication environment. It was proved that the 3D CCF is the product of 2D space-time correlation functions of M2M communication channel. Furthermore, the model was simulated for isotropic and non-isotropic environments. The authors in [86] extended previously proposed 3D geometrical channel models by introducing LoS component and concentric-cylinders. They have derived expressions for first and second order channel statistics and compared the analytical result with measurement results obtained from highway of Midtown Atlanta. Nurilla *et al.*[87], have also provided 3D MIMO M2M communication channel model for semicircular tunnel. In this proposed channel model, the authors have assumed that the MS are inside the tunnel with elevated MIMO antenna arrays and the scatterers are randomly distributed on the tunnel wall. They have derived expressions for space-time-frequency cross-correlation function (STF-CCF).

In addition to 3D M2M MIMO channel models, researchers have also proposed 3D geometrical channel for SISO/MIMO F2M communication environments. Macrocell of cellular mobile network is well-known application of F2M communication systems. In this scenario, MS is fixed with low elevated antenna structure and is in the vicinity of local scatterers; whereas, base station is located on the top of any high-rise tower and is scatter free. In F2M communication scattering environment, the most dominant zones in urban and suburban regions where the fast moving mobile subscribers of cellular mobile network mostly reside are metropolitan areas, streets, canyons or highways. These fast moving mobile subscribers on one hand demand high data-rate applications and experience frequent handoffs on the other hand. This exerts an extra burden on MSC. The frequency of handoffs is usually minimized by handing over these fast moving subscribers to umbrella cells. That not only manages the handoff problem but also increases coverage and QoS. Keeping in view the importance of umbrella cell an appropriate geometrical channel model is required that can be used to design a system to provide the maximum throughput and QoS. In this regard, various 2D and 3D geometrical channel have been proposed in the literature. One ring based 2D geometrical channels models have been proposed for F2M communication employing multiple antenna arrays at both ends of communication link [88–93]. The authors analyzed the models for various channel characteristic like AoA, ToA, Doppler spread and cross-correlations among the MIMO links. This 2D circular-based geometrical channel model is extended by Feng *et al.* in [2], and have proposed a 3D cylindrical geometrical model for fast-moving train under the deep cutting scenario and have derived closed form expression for space-time correlation among MIMO antenna elements. Furthermore, authors in [70, 94], have assumed scatterers are uniformly distributed hemispherically around the MS and have derived PDF of AoA/AoD and closed-form expression for RMS angular spread in the horizontal plane as seen from the base station.

2.1.3 Significance of Elliptical Geometrical Shape in Channel Modeling:

Above discussed 2D and 3D geometrical channel models may be applicable in some scenario of mobile communication; however, these models are not appropriate to model metropolitan streets, highways with road-side vegetation, embankments, deep-cut railway tracks and canyons that are the demanding candidate for MIMO M2M/F2M communication in non-isotropic propagation environments. The layout of such propagation environments resemble more closely with elliptical shape than circular, so can be modeled more realistically with elliptical geometrical shape. Because, the roads, canyons or the highways where the mobile subscriber mostly reside are longer in length and smaller in width. The major and minor axis can model the length and the width of such propagation environments realistically than radius of circle.

Keeping in view the significance of elliptical shape, various elliptical based geometrical channel models have been proposed in the literature for SISO and MIMO F2F/F2M/M2M communication scattering environments. Liberti *et al.* [95] proposed a channel model for SISO F2F communication system. In this model, low elevated transmitter and receiver antennas are supposed to be located at the foci (boundary) of ellipse and the scatterers are located inside elliptical boundary. The authors derived the expressions for the statistics of the direction-of-arrival (DoA), path delay, and power of multipath components. This work has been extended for F2M communication environment in [96–101], where the authors assumed that MS is surrounded by uniformly distributed scatterers in circular or elliptical scattering environments. They derived expressions for the PDFs of joint ToA/AoA, marginal AoA and ToA. Furthermore, for SISO M2M wireless communication channels, Baltizis *et al.* in [102, 103], considered that the MS are located at the center of ellipses and uniformly distributed inside ellipses. The authors derived formulas for the calculation of the angular spread, delay variation and PDF of AoA. The authors assumed uniform distribution of scatterers around the transmitter and receiver nodes, located at the center of the ellipses. The above

proposed 2D elliptical geometrical channel model considered azimuth AoA/AoD of multipaths only however, in reality high-rise buildings, vegetation and other infrastructure present along the roadside premises are the sources of multipaths in the azimuth and elevation planes. After understanding this usefulness of 3D-space of AoA/AoD, Riaz *et al.* proposed an ellipsoid geometrical channel model for SISO M2M environments, where they derived expressions for the PDFs of ToA and AoA in both azimuth and elevation planes [104, 105]. The authors assumed the signals are equally likely from all directions of the ellipsoid that contradicts the realistic propagation environment. Because the probability of AoA of scattered signals from the sky-top of urban areas is almost zero, Ahmed *et al.* in [106, 107], proposed modified geometrical channel model of [104, 105], with top surface open and derived PDFs for AoA and AoD.

As discussed earlier that the geometrical channel models for F2M and M2M SISO systems can be used to predict the performance in some of the urban/suburban areas but can not analyze more appropriately the obtainable data-rates and QoS in rich scattering environments. Whereas, the elliptical geometrical shape is more suitable candidate for MIMO systems, as it captures significant geographic areas that are the rich scattering regions of such propagation environments [108, 109]. The majority multipath components are expected from the roadside scatters regions that provides beneficial situation for the MIMO capacity [110]. The concept of using elliptical geometry was also utilized in [111, 112], a MIMO M2M communication channel model was proposed and the expression of the correlation functions among MIMO links were derived. Soltani *et al.* [113] also explored the impact of mobile scattering clusters on the Doppler spectrum while assuming the mobile nodes at the foci of single ellipse.

In the proposed elliptical channel models mentioned in the last paragraph for modeling MIMO M2M communication links, the authors assumed that the transmitter and the receiver are located at the foci of the single ellipse with SISO or MIMO antenna structures. Such proposed geometrical channel models can be beneficial when mobile subscribers reside in one street or canyon but may not be useful for a situation when MSs reside in different streets, canyons or highways.

2.1.4 Problem Statement:

In the earlier subsections, various geometrical channel models are discussed for F2M and M2M communication environments. Out of these models, the two-ring and the two-disc circular channel models for SISO and MIMO links show potential to become viable foundations for future research in M2M/F2M communication environments. However, these models may not be appropriate to model scattering environments like streets, highways and canyons that host M2M/F2M links most of the times. Nevertheless, the realistic approach to model the streets, highways and canyons for M2M communication scenario recommended in the literature [57, 96, 98, 114] is the elliptical shape based channel modeling. Baltzis *et al.* developed elliptical models in [102, 103] for SISO M2M communication environments. These models can be made more efficacious if multiple antenna arrays are introduced at the transmitter and receiver nodes. Although some models [108, 109] were proposed in the literature for the M2M communication environment using MIMO links; however, these models lacked in considering the non-isotropic phenomenon that usually emerges when the MSs communicate with each other with their low-height antennas in streets and canyons. Secondly, these models are based on single-ellipse geometry; therefore, may be useful only if the MS reside in a single street or canyon, but may not be beneficial when the MSs are in two different streets, canyons, or highways with different scattering environments. Patzöld *et al.* [75, 115] introduced MIMO antenna arrays using two-ring circular channel model for M2M communication environment, while considering isotopic scattering environment and derived closed-form expressions for correlations among the MIMO links. The authors, however, suggested von-Mises distribution for the PDF of AoA without developing any geometry for the case of non-isotropic scattering environment. This motivates us to propose an eccentricity based MIMO M2M channel model that fits well with the physical layout of the streets or canyons, which are non-isotropic scattering environments in nature. To model urban and suburban scattering environment, where, the scatterers usually lie along roadside in the elevation plane like high-rise buildings and trees, 3D geometrical channel models are required for both M2M and F2M communication environments that

can accommodate the effect of these scattering objects. Moreover, fast moving mobile subscribers in F2M macrocellular environments of cellular communication are more demanding candidates for high-data rate and frequent handoff services. A well designed umbrella-cell is useful for such fast moving mobile subscribers while they are on call. This umbrella-cell helps the cellular communication network to reduce the frequency of handoff and also assist in the traffic management and channel assignment in the system [45, 116]. In addition to it, umbrella-cell serves the mobile subscribers who are on the move in the shadowed regions of the microcells by improving their signal-to-noise ratios so that they may remain connected with the cellular network. The umbrella-cell also increases the radio coverage as well as provides more number of channels in the desired cellular region. Keeping in view the shape of the region covered by the umbrella cell, of umbrella-cell, a feasible 3D elliptical-based channel model is required that can be used predict the quality and performance of the MIMO communication link in case of high data-rates, and can be utilized in designing better MIMO systems for highways bounded by high-rise buildings. In other words an F2M channel model is used that can serve the fast-moving subscribers on highways by reducing the frequency of handoff, which in turn decreases burden on the MSC.

2.2 Research Methodology and Thesis Contribution:

In order to address the issue of non-isotropic M2M communication scenario that mostly develops in streets and canyon of a large metropolitan city. A 2D eccentricity-based geometrical channel model is proposed and mathematical expression is derived for the PDF of AoA/AoD, which is further verified through simulation results. Moreover, marginal correlation functions at transmitter and receiver antennas for M2M communication channel are derived, which are then used to develop joint transmit-receive correlation functions. As noted in the literature survey, the high rise elevated scattering objects have significant impact on the angle of arrival

of the multipath signals at the mobile and thus on the capacity of communication links. To accommodate this fact, the proposed MIMO M2M 2D-elliptical geometrical channel model is extended to a 3D elliptical-based cylindrical geometry. In this proposed 3D channel model, eccentricity is used to model the physical dimensions the propagation medium in azimuth plane while the height of the elliptical cylinders are utilized to model scattering objects alonf the elevation plane. Using this 3D proposed channel model, expressions for the joint and marginal cross correlation functions (CCFs) are derived for non-isotropic scattering environments. The derived expressions are plotted using various parameters to observe their effect with varying antenna spacing. The obtained correlation plot is then compared with measured data, which shows a close agreement of the plot with the trend of the measured data. Moreover, by changing various parameters of the proposed channel model, some existing 2D and 3D channel models are deduced. Furthermore, in order to address the second issue of channel modeling for fast-moving subscribers on highways, a 3D geometrical channel model is proposed for umbrella cells in F2M macrocellular environments. This system incorporates the novel idea of modeling scattering environments around fast-moving vehicles on highways equipped with smart antenna systems. In this case, It is assumed that the fast moving subscriber is located at the center of elliptical cylinder and is equipped with low elevated multiple-antenna array whereas, the base-station is located on the top of a high-rise structure elevated with multiple antenna array. Using the proposed model, expressions for the joint and marginal of space-time correlation function are derived among the MIMO antenna elements. These correlation functions are helpful to design and develop MIMO systems for high-speed mobile subscribers with high data rate applications.

2.3   Strengths and Limitations of the Proposed Work:

In mobile communication environments, the fast moving subscribers usually reside in streets, canyons or on highways while they are on the call or using any real-time data-hungry applications. The capacity of the communication link in such propagation environments depends largely on scattering objects that are located on the road side regions. The proposed GBSCMs address the issue of propagation in M2M environment where the mobile subscribers being in two different streets or highway are communication with each other. The proposed GBSCMs exploit the advantage of the fact that the physical layout of such propagation environments has close resemblance with the shape of ellipses because its boundary capture most of the roadside objects, which can be assumed to be the dominant sources for the multipaths. For this purpose minor and major axes of the ellipse are set to model the width and length of the roads, while the height of the elliptical-cylinder is adjusted according to the elevations of roadside scattering objects. Therefore, for a specific urban or suburban regions, the elliptical-based GBSCMs proposed in this dissertation can estimate the statistics of the MIMO M2M/F2M propagation channels more appropriately than the existing circular-based channel models. Moreover, the geometries of the proposed eccentricity-based GBSCMs are flexible in all dimensions. Consequently, various published GBSCMs can be obtained by adjusting the eccentricity and the height of elliptical-cylinders of the proposed models. Nevertheless, like many theoretical models, the proposed MIMO channel models for M2M and F2M umbrella-cell communication scenarios have a few limitations, due to the assumptions made in its architecture for the ease of mathematical derivations of correlation functions among the MIMO antenna elements, these assumptions are listed below:

1. Each multipath component of the propagating signal undergoes two bounces in M2M and single bounce in F2M communication environments.

2. Infinite number of scatterers are uniformly distributed on the proposed 2D and 3D geometries.

3. Power is equally reflected from all the scatterers.

4. Each scatterer behaves as an isotropic antenna.

5. The scatterers are fixed and MSs are quasi-stationary for a short period of time.

Certain assumptions may not be valid in some of the real-life propagation scenarios, therefore, the results obtained by the GBSCMs must be validated through measurement campaigns before its use for a particular propagation scenario. Moreover, the model proposed for M2M MIMO communication envelopment may not be suitable for those scenarios where two mobiles reside closer to each other having a strong LoS link. Similarly the model proposed for F2M umbrella-cell based communication system may not work satisfactorily for flat-rural open areas where the highways are not bounded by scatterers.

2.4 Conclusion:

This chapter provides comprehensive and comparative study of various channel modeling approaches proposed in the literature. It is deduced from the comparative study that GBSCM approach is more flexible and appropriate to model the mobile communication propagation environments. In this regard, various geometrical channel models have been proposed in the literature for SISO/MIMO M2M/F2M communication environments. Out of these models, elliptical-based geometry is considered to be the more demanding candidate for modeling of radio fading channels in the streets, canyons or highways environments. Because the fast moving mobile subscribes are more frequently on the call in the streets, canyons and highways in metropolitan regions. Furthermore, these mobile subscribers are also demanding candidates for high date rates and QoS communications. Hence, MIMO structured communication is the most feasible solution for these situations.

Therefore, a well designed MIMO M2M elliptical based GBSCM can be very useful for the performance, analysis and design of the communication systems in such propagation envelopments.

Chapter 3

Modeling and Characterization of MIMO Mobile-to-Mobile Communication Channels Using Elliptical Scattering Geometry

This chapter presents a geometrically based 2D elliptical channel model for MIMO M2M communication scattering environment and starts with Section 3.1 that provides introduction and importance of GBSCM. Section 3.2 describes the detail of proposed spatial channel model. Section 3.3 and Section 3.4 provides mathematical derivation of the PDF of AoA expression and space-time correlation functions, respectively. Section 3.5 describes theoretical results of the obtained closed-form expressions of the space-time correlation functions. Finally, a descriptive conclusion is given in Section 3.6.

3.1 Introduction

Continuous demands for high data rates in all aspect of wireless communication systems are becoming a constant driving force in today's research arena. Situations

become even more demanding for M2M communication networks where both ends of the link are surrounded by huge number scattering objects. Such rich scattering environments are unfriendly to conventional communication systems, however, a MIMO system takes the benefits of multipath environments and offer a significant increase in data rate, provided antenna array elements have low correlations among each other [23, 32, 35]. Therefore, understanding of spatial characteristics of radio fading channel and correlations among various elements of the multiple antennas is extremely important for the efficient design of a MIMO system. In this regard various channels models have been reported in the literature exploiting empirical, deterministic and GBSCMs [57, 58]. In regular-shape GBSCMs, elliptical-based channel modeling technique provides a feasible platform to model the streets, canyons and highways where, mostly the fast moving subscribers reside while they are on call or using real-time data-hungry applications. Therefore, for the design and performance analysis of MIMO M2M communication systems for such particular scenarios, an eccentricity-based channel model is proposed in this chapter. An empirical formula has been derived for AoA distribution emerged as the result of non-isotropic arriving signals. Utilizing the AoA and the proposed geometrical model with some assumptions, a closed-form expression for the joint transmit-receive correlation function has been derived.

3.2   System Model

In this section, the system architecture of the proposed geometrically-based two-elliptical channel model for MIMO M2M communication environment is presented as shown in Fig. 3.1. Each of the transmitting and receiving MSs is denoted by M_i, where the subscript $i = $ t or r to denote MS_t and MS_r, respectively. The MSs are located at the centers of the ellipses having major axes a_t and a_r and minor axes b_t and b_r with eccentricities ϵ_t and ϵ_r, respectively. The MSs are separated by a distance $d\left(\text{such that } D \gg (a_t + a_r)\right)$ and are surrounded by uniformly distributed scatterers present on the boundaries of the ellipses. The ellipses are made rotatable with the directions of motion of the MSs such that their major axes a_t and a_r
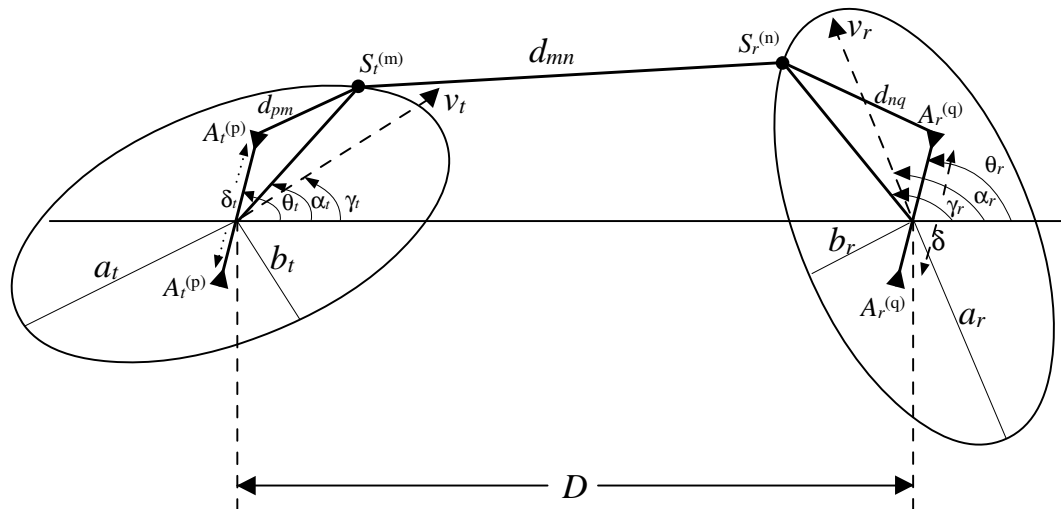
FIGURE 3.1: Proposed Elliptical Channel Model for MIMO Mobile-to-Mobile Communication Environment.

make angles γ_t (or γ_r) , respectively, with the x-axis. Both MSs, being at the same height are equipped with multiple antennas with configuration $P \times Q$, where P and Q are the number of antennas mounted on MS_t and MS_r, respectively. For simplicity, only $P = Q = 2$ antenna elements are considered. However, the results can be derived for any configuration. The transmit and receive antenna elements are denoted by $A_t^{(p)}$ and $A_r^{(q)}$ and the separations between antenna elements on MS_t and MS_r are denoted by δ_t and δ_r, respectively. The description of the other parameters involved in the proposed geometrical model are narrated in Table 4.1.

TABLE 3.1: Definitions of the channel parameters used in the system model.

Symbols	Description.
D	The distance between center to center of elliptical cylinders surrounding MS_t and MS_r.
$R_{d,t}, R_{d,r}$	The variable radius of the transmitter and receiver ellipses, respectively.
$\delta_t(p, \tilde{p})$	The spacing between p^{th} and $\tilde{p}^{th}$ antenna elements at Tx.
$\delta_r(q, \tilde{q})$	The spacing between q^{th} and $\tilde{q}^{th}$ antenna elements at Tx.
$\theta_t^{(p)}, \theta_r^{(q)}$	The azimuth angle of pth transmit and q^{th} receive antenna element (relative to x-axis), respectively.
v_t, v_r	The velocities of the Tx and Rx, respectively.
γ_t, γ_r	The moving directions of the Tx and Rx, respectively.
$\alpha_t^{(m)}, \alpha_r^{(n)}$	The azimuth angles of departure (AAoD) and the azimuth angles of arrival (AAoA), respectively.
$d_{pm}\ d_{\tilde{p}m}\ d_{mn}\ d_{nq}$ $d_{n\tilde{q}}$	The distances $\mathrm{d}\left(A_t^{(p)}, S_t^{(m)}\right)$, $\mathrm{d}\left(A_t^{(\tilde{p})}, S_t^{(m)}\right)$, $\mathrm{d}\left(S_t^{(m)}, S_r^{(n)}\right)$, $\mathrm{d}\left(S_r^{(n)}, A_r^{(q)}\right)$, and $\mathrm{d}\left(S_r^{(n)}, A_r^{(\tilde{q})}\right)$

It is assumed that $\delta_t \ll b_t$ and $\delta_r \ll b_r$. The symbols $S_t^{(m)}$ and $S_r^{(n)}$ in Fig. 3.1, denote the mth and nth scattering objects around MS_t and MS_r, respectively.

Moreover, the MS_t and MS_r are moving with velocities v_t and v_r making angles γ_t and γ_r with the x-axis. Angle-of-departure (AoD) and angle-of-arrival (AoA) of the mth and nth multipath signals are designated as $\alpha_t^{(m)}$ and $\alpha_r^{(n)}$, respectively. The tilt angles of the transmit and receive antennas are denoted by θ_t and θ_r. The proposed two-elliptical model is based on the following general assumptions,

1. Double bounce scattering model is considered between communicating MSs.

2. Infinite number of scatterers are uniformly distributed on the boundaries of ellipses.

3. Power is equally reflected from all the scatterers.

4. Each scatterer behaves as an isotropic antenna.

5. The scatterers are fixed and MSs are quasi-stationary for a short period of time.

3.3   Distribution of AoA/AoD

For the ease of derivation, in most of the geometrical channel modeling approaches uniform distribution of scattering objects is assumed thereby relating the scatterer distribution with the AoA. A relationship between arc-lengths and the arriving angles of the multipath signals at the center of the proposed geometry has been presented in the literature for circular scattering models [96]. However, such relationship between the two parameters does not exist for the elliptical geometry. In this section, we find a connection between the arc-lengths with the distribution of AoA of the multipath signals numerically as well as theoretically for the proposed elliptical geometry where scatterers are located at its boundary. Researchers usually use different scattering distributions like Gaussian, Laplacian, Uniform and von Mises distributions for the PDF of AoA/AoD in their proposed geometric
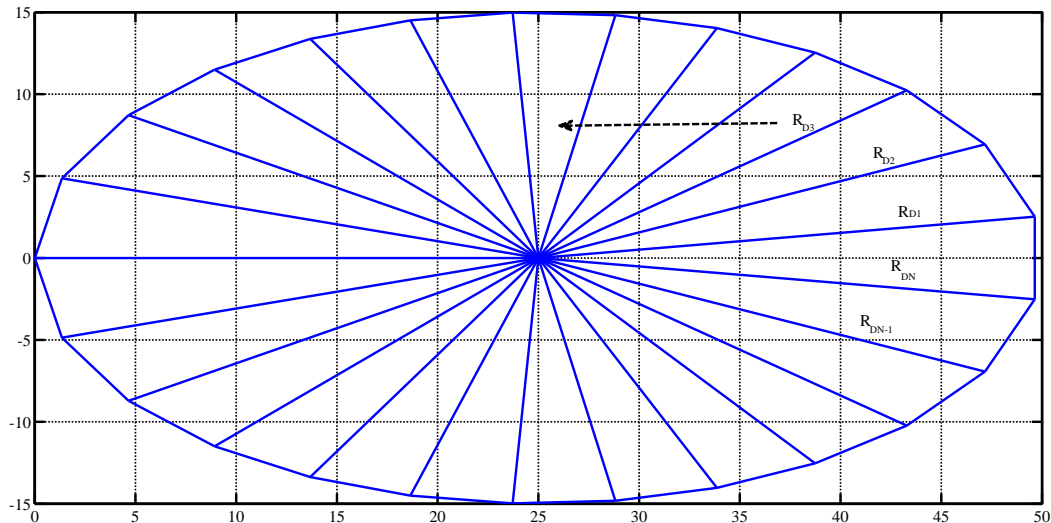
FIGURE 3.2: Equal distribution of scattering points on the boundary of the ellipse for a specific dimension.

channel models. The physical scattering environment around the MSs can either be isotropic or non-isotropic like in circular or elliptical models, respectively. The von Mises PDF is considered matching well in fitting the measured results of azimuth dispersion in mobile radio channels [117]. Abidi *et al.* in [118], introduced von Mises distribution for non-isotropic scattering environments, which is given as:

$$p(\alpha) = \frac{1}{2\pi I_o(\kappa)} \exp[\kappa \cos(\alpha - \mu)], \tag{3.1}$$

where $I_o(.)$ is the modified Bessel function of first kind of order zero, $\mu \in (-\pi, \pi)$ represents the mean angle and κ controls the spread of scatters around the mean μ. Above mathematical expression of the von Mises provided convenience to express closed-form solutions for correlations functions and other coefficients of the wireless channel. Taking this advantage, authors in [101, 111] derived closed-form expressions of the correlation function among different MIMO channel coefficients for non-isotropic scenarios. In order to obtain the distribution of the AoA of the multipath signals in the proposed scattering model depicted in Fig. 3.1. One need to concentrate on the non-isotropicity present in the proposed system model. This requires establishing a relationship of any of the above-mentioned probability distribution models with dimension (shape and size) of the physical scattering environment that creates non-isotropicity.
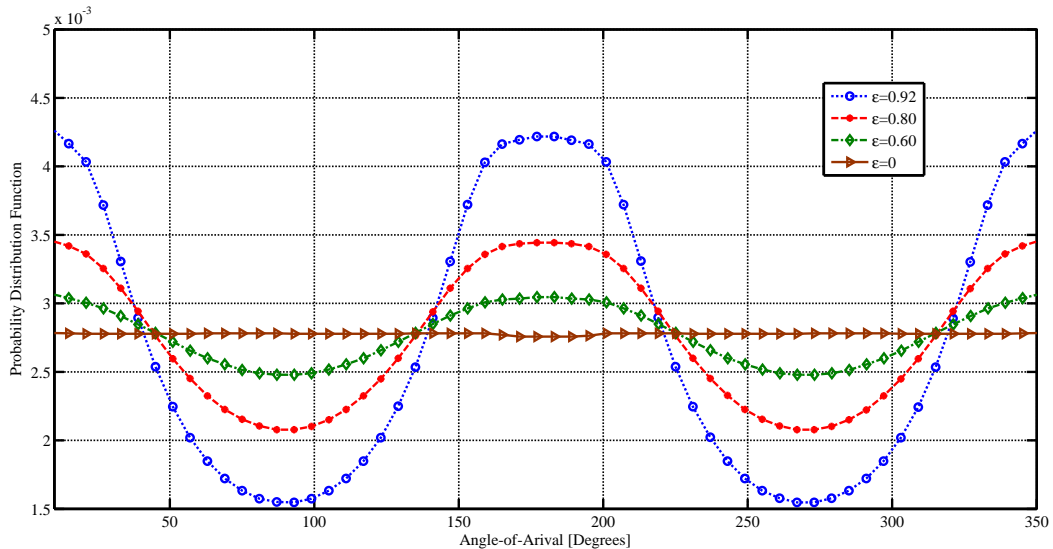
FIGURE 3.3: Rate of occurrence of the AoA using scatterers present on elliptical boundary of various eccentricities around MS_t and MS_r.

For the calculation of AoA distribution, an arbitrary elliptical region around the MS_r shown in Fig. 3.2, is considered. Some N point-objects are created as scattering points on the boundary of the ellipse around either of the MSs of the communication link. The scattering objects are located at points (x_1, y_1), (x_2, y_2), (x_3, y_3), ..., (x_N, y_N) in the Cartesian coordinates system. Equal spacing between these points is calculated by dividing the perimeter of the ellipse by N number of scattering points as shown in Fig. 3.2. Knowing the arc-length and using the coordinates of the scattering points, straight lines are drawn from the center of the ellipse to the coordinates of the scattering objects. Using cosine laws, angle between two consecutive lines (e.g., R_{D1} and R_{D2}) is measured. Using the same procedure, angle between rest of the pairs of these lines are measured. The resultant angles are then used to draw histogram for different values of the eccentricities ϵ_r of the ellipse around MS_r, as shown in Fig. 3.3. The figure shows that the PDF of AoA of multipath signals changes to uniform as the geometry of the scattering objects changes from an elliptical to a circular shape. The following empirical formula for the PDF of AoA is also fitted and is validated by the calculated result as shown in Fig. 3.4.

$$p(\alpha_i) = \frac{1}{2\pi I_o(\epsilon_i^2)} e^{\epsilon_i^2 \cos 2\alpha_i} \tag{3.2}$$
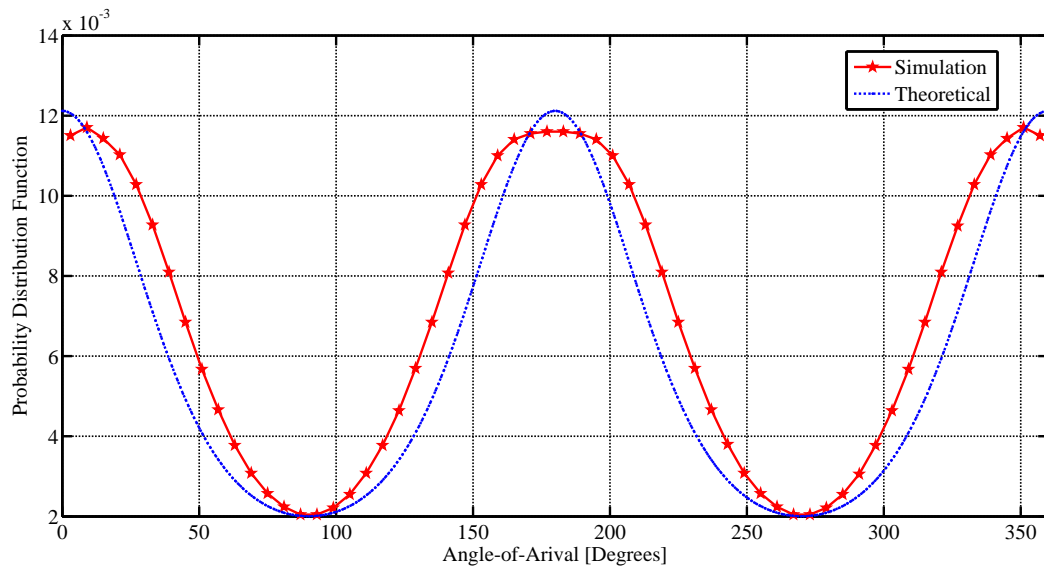
FIGURE 3.4: Comparison of theoretical results of expression for the PDF of AoA with the simulation results obtained from data set of the proposed elliptical geometry

.

where $I_o(\cdot)$ is the modified bessel function of zeroth order and $\epsilon_i = \sqrt{1 - b_i^2/a_i^2}$ is the eccentricity of the elliptical loci around MS_i. The subscript $i \in (\text{t}, \text{r})$

3.4 Derivation of the Correlation function

In this section, an expression for CCF using the proposed elliptical channel model for MIMO M2M communication environment is derived. Let the MSs are located at certain points (i.e., X_o, Y_o) in the Cartesian coordinates systems. The generalized equation for each ellipse, having semi-major a_i and semi-minor b_i axes, can be expressed as,

$$\frac{\big((x_i - X_o)\cos\alpha_i + (y_i - Y_o)\sin\alpha_i\big)^2}{a_i^2}$$
$$+\frac{\big(-(x_i - X_o)\sin\alpha_i + (y_i - Y_o)\cos\alpha_i\big)^2}{b_i^2} = 1 \tag{3.3}$$

The variable radius, $R_{d,i}$, of the ellipse varies from its minimum to maximum according to the length of minor and major axes of the ellipse, respectively. An
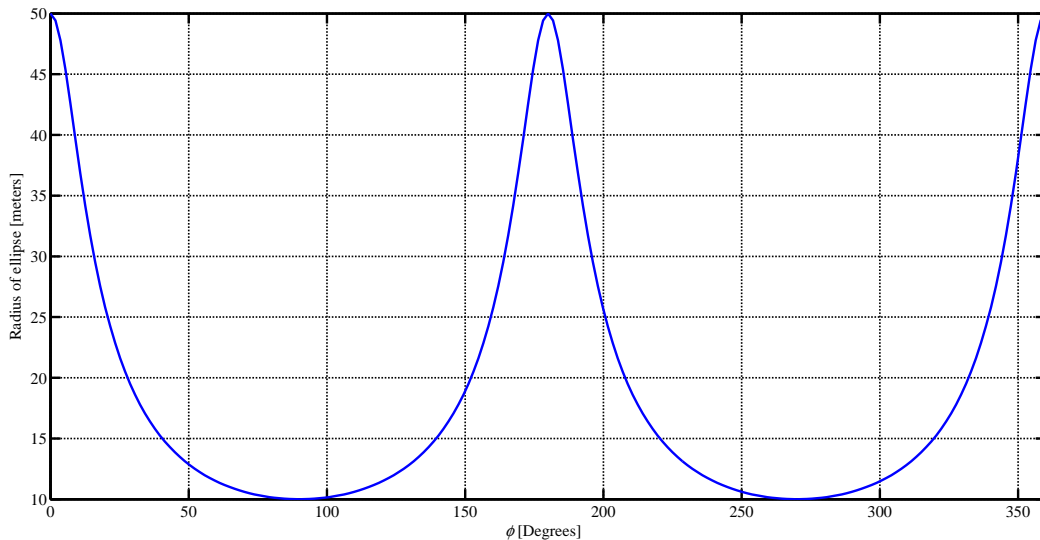
FIGURE 3.5: Radius of ellipse with respect to AoA.

expression for this Variable radius is given by,

$$R_{d,i} = \frac{a_i b_i}{\sqrt{a_i^2 \sin^2 \alpha_i + b_i^2 \cos^2 \alpha_i}} \tag{3.4}$$

The variable radius of the ellipse given in (3.4) is plotted against AoA/AoD shown in Fig. 3.5. This variable radius can be linked with the distribution of the scattering points lying on the boundary of the ellipse. From these results, it can be concluded that when scatterers are uniformly distributed on the boundary of the ellipse, of any arbitrary eccentricity, the AoA emerges as shown in Fig. 3.3.

In the proposed geometry depicted in Fig. 3.1, it can be observed that a signal, which is transmitted from the transmit antenna element $A_t^{(p)}$, first strikes at the scatterer $S_t^{(m)}$ of the scattering ellipse surrounding the transmitter and then travels to the scatterer $S_r^{(n)}$ of the scattering ellipse surrounding the receiver, and finally reaches the receiving antenna element $A_r^{(q)}$. Mathematically, this propagation length of the signal can be expressed as,

$$D = d_{pm} + d_{mn} + d_{nq} \tag{3.5}$$

where,

d_{pm} = distance from transmitter M_t to the scattering point $S_t^{(m)}$

d_{mn} = distance from scattering point $S_t^{(m)}$ to the scattering point $S_r^{(n)}$

d_{nq} = distance from scattering point $S_r^{(n)}$ to the receiver M_r

As each of the MS is moving with velocity v_t (or v_r) causing maximum Doppler shift $f_{tmax} = v_t/\lambda$ (or $f_{rmax} = v_r/\lambda$), exploiting the proposed geometrical model, an expression for the channel of the communication link from $A_t^{(1)}$ to $A_r^{(1)}$ can be described as in [21, 115],

$$h_{11}(t) = \lim_{M,N \to \infty} \frac{1}{\sqrt{MN}} \sum_{m,n=1}^{M,N} f_{mn} e^{j[2\pi(f_t^{(m)}+f_r^{(n)})t+\theta_r+\theta_{mn}+\theta_o]} \qquad (3.6)$$

where

$f_{mn} = x_m y_n z_{pq}$

$x_m = e^{j\pi(\delta_t/\lambda)\cos(\alpha_t^{(m)}-\theta_t)}$

$y_n = e^{j\pi(\delta_r/\lambda)\cos(\alpha_r^{(p)}-\theta_r)}$

$z_{pq} = e^{j\frac{2\pi}{\lambda}(R_{d,t}\cos\alpha_t^{(m)}-R_{d,r}\cos\alpha_r^{(n)})}$

$f_t^{(m)} = f_{tmax}\cos(\alpha_t^{(m)}-\gamma_t)$

$f_r^{(n)} = f_{rmax}\cos(\alpha_r^{(n)}-\gamma_r)$

$\theta_o = -\frac{2\pi}{\lambda}D$

$\theta_r = -\frac{2\pi}{\lambda}(R_{d,t}+R_{d,r})$

where θ_r is the constant phase that depends on specific orientations of the ellipses. Similarly, θ_o is also a constant phase as interspacing between the MSs is fixed. Due to the constant behavior of these phases, there will be no effect on the statistics of the proposed model, therefore these phases can be neglected. Using the proposed geometrical channel model, one can find the other diffused components $\left(\text{i.e., } h_{12}(t), h_{21}(t) \text{ and } h_{22}(t)\right)$. Space-time correlation function between the transmission links $A_t^{(1)} - A_r^{(1)}$ and $A_t^{(2)} - A_r^{(2)}$ can be expressed as in [115],

$$\rho_{11,22}(\delta_t, \delta_r, \tau) = E\{h_{11}(t)h_{22}^*(t+\tau)\} \qquad (3.7)$$

where the operator $E\{\cdot\}$ is known as the expectation and is applied on all the random phases, AoA and AoD (i.e., $\alpha_t^{(m)}$, $\alpha_r^{(n)}$ and θ_{pq}) in the equation. By substituting the values of the major axis x_m and minor axis y_n of the ellipse and their conjugate transpose in (3.6) then we get the following expression for the above CCF as,

$$
\begin{aligned}
\rho_{11,22}(\delta_t, \delta_r, \tau) = {} & \lim_{M,N\to\infty} \frac{1}{MN} \sum_{m=1}^{M} \sum_{n=1}^{N} E\Bigg\{ x_m x_{\acute{m}} y_n y_{\acute{n}} z_{mn} z_{\acute{m}\acute{n}}^* \\
& \times \exp\left[\left\{ j\left(2\pi(f_t^{(m)} + f_r^{(n)} - f_t^{(\acute{m})} - f_r^{(\acute{n})})t + \theta_{mn} - \theta_{\acute{m}\acute{n}} - (f_t^{(\acute{m})} + f_r^{(\acute{n})})\tau \right) \right\}\right] \Bigg\}
\end{aligned}
$$

(3.8)

Using boundary condition i.e., $f_t^{(m)} + f_r^{(n)} = f_t^{(\acute{m})} + f_r^{(\acute{n})}$ iff $m = \acute{m}$ and $n = \acute{n}$, it follows that (3.8) in reduced form can be written as,

$$
\rho_{11,22}(\delta_t, \delta_r, \tau) = \frac{1}{MN} \sum_{m=1}^{M} \sum_{n=1}^{N} x_m^2 y_n^2 \exp\left[-j2\pi(f_t^{(m)} + f_r^{(n)})\tau \right]
$$

(3.9)

In the above equation, x_m and $f_t^{(m)}$ are the functions of AoD, $\alpha_t^{(m)}$, while y_n and $f_r^{(n)}$ are the functions of AoA, $\alpha_r^{(n)}$. It has already been assumed that there are infinite number of scatterers, which reside around the MSs i.e., $M, N \to \infty$. In such a case, the discrete random variables $\alpha_t^{(m)}$ and $\alpha_r^{(n)}$ become continuous random variables and take the form α_t and α_r. These continuous random variables are represented by certain statistical distributions, denoted by $p(\alpha_t)$ and $p(\alpha_r)$, respectively.

Power received at the receiver through each diffused component corresponding to differential angles $d\alpha_t$ and $d\alpha_r$ is proportional to $p(\alpha_t)p(\alpha_r)d\alpha_t d\alpha_r$. As the AoA, α_r, and AoD, α_t, are statistically independent random variables, therefore, the joint transmit-receive space-time correlation function (CCF) in (3.9) can be decomposed and that can be written in the form of the product of transmit and receive correlation functions as,

$$\rho_{11,22}(\delta_t, \delta_r, \tau) = \rho_t(\delta_t, \tau)\rho_r(\delta_r, \tau) \tag{3.10}$$

where the transmit correlation function $\rho_t(\delta_t, \tau)$ can be expressed as,

$$\rho_t(\delta_t, \tau) = \int_{-\pi}^{\pi} x_m^2(\delta_t, \alpha_t) \exp\left[-j2\pi f_t(\alpha_t)\tau\right] p(\alpha_t) \mathrm{d}\alpha_t \tag{3.11}$$

Putting the values of $x_m(\delta_t, \alpha_t)$ and $f_t(\alpha_t)$ from (3.6) and $p(\alpha_t)$ from (3.2) in (3.11),

$$\rho_t(\delta_t, \tau) = \frac{1}{2\pi I_o(\epsilon_t^2)} \int_{-\pi}^{\pi} \exp[j2\pi(\delta_t/\lambda)\cos(\alpha_t - \theta_t)] \exp[-j2\pi$$
$$\times f_{t_{max}} \cos(\alpha_t^{(m)} - \gamma_t)\tau] \exp[\epsilon_t^2 \cos 2\alpha_t] \mathrm{d}\alpha_t \tag{3.12}$$

Expanding the trigonometric functions in the above equation and rearranging the terms,

$$\rho_t(\delta_t, \tau) = \frac{1}{2\pi I_o(\epsilon_t^2)} \int_{-\pi}^{\pi} \exp\left[2\pi\left\{j(\delta_t/\lambda)\cos(\theta_t) - j(V_t/\lambda)\tau\cos(\gamma_t) + \epsilon_t^2\right\}\cos(\alpha_t)\right]$$
$$\times \exp\left[2\pi\left\{j(\delta_t/\lambda)\sin(\theta_t) - j(V_t/\lambda)\tau\right\}\sin(\gamma_t)\right]\mathrm{d}\alpha_t \tag{3.13}$$

Substituting,

$x_1 = 2\pi\left\{j(\delta_t/\lambda)\cos\theta_t - j(V_t/\lambda)\tau\cos\gamma_t + \epsilon_t^2\right\}$ and

$x_2 = j2\pi\left\{(\delta_t/\lambda)\sin\theta_t - (V_t/\lambda)\tau\sin\gamma_t\right\}$, (3.13) takes the form,

$$\rho_t(\delta_t, \tau) = \frac{1}{2\pi I_o(\epsilon_t^2)} \int_{-\pi}^{\pi} \exp\left[x_1\cos\alpha_t \; + \; x_2\sin\alpha_t\right]\mathrm{d}\alpha_t \tag{3.14}$$

The above equation is integrated by comparing it with eq. (3.338-4) in [119],

$$\rho_t(\delta_t, \tau) = \frac{1}{2\pi I_o(\epsilon_t^2)} J_o\left(2\pi\sqrt{x_1^2 + x_2^2}\right) \tag{3.15}$$

where $J_o(\cdot)$ is the bessel function of zeroth order. Putting back the values of x_1 and x_2, (3.15) can be expressed in simplified form as,

$$
\begin{aligned}
\rho_t(\delta_t, \tau) = \frac{1}{I_o(\epsilon_t^2)} J_o \bigg(2\pi \Big(& \epsilon_t^4 - (\delta_t/\lambda)^2 - (\tau f_{t_{\max}})^2 - 2\epsilon_t^2 \tau f_{t_{\max}} \cos \gamma_t \\
& + j2\epsilon_t^2 \tfrac{\delta_t}{\lambda} \cos \theta_t + 2\tau \tfrac{\delta_t}{\lambda} f_{t_{\max}} \cos (\gamma_t - \theta_t) \Big)^{1/2} \bigg)
\end{aligned}
\tag{3.16}
$$

Similar equation can be derived for the correlation function at the receiver end. Thus joint correlation function in (3.10) can be expressed as,

$$
\begin{aligned}
\rho_{11,22}(\delta_t, \delta_r, \tau) = \frac{1}{I_o(\epsilon_t^2) I_o(\epsilon_r^2)} J_o \bigg(& 2\pi \Big(\epsilon_t^4 - (\delta_t/\lambda)^2 - (\tau f_{t_{\max}})^2 - 2\epsilon_t^2 \tau f_{t_{\max}} \cos \gamma_t \\
+ j2\epsilon_t^2 \frac{\delta_t}{\lambda} \cos \theta_t + 2\tau \frac{\delta_t}{\lambda} f_{t_{\max}} & \cos (\gamma_t - \theta_t) \Big)^{1/2} \bigg) J_o \bigg(2\pi \Big(\epsilon_r^4 - (\delta_r/\lambda)^2 \\
- (\tau f_{r_{\max}})^2 - 2\epsilon_r^2 \tau f_{r_{\max}} \cos \gamma_r & + j2\epsilon_r^2 \frac{\delta_r}{\lambda} \cos \theta_r + 2\tau \frac{\delta_r}{\lambda} f_{r_{\max}} \cos (\gamma_r - \theta_r) \Big)^{1/2} \bigg)
\end{aligned}
\tag{3.17}
$$

which is a generalized expression for the joint correlation function of MIMO M2M communication links for more realistic channel models that targets environments like streets and canyons.

The following remarks can be made about (3.17):

- If elliptical geometrical shapes are replaced with circular ones, the eccentricities of the ellipses around transmitter and receiver i.e., ϵ_t and ϵ_r, would approach to zero. In such a case, the scattering environment will become

isotropic and the expression for the joint correlation function in (3.17) reduces to, which is the result presented in [75, 85, 120, 121]

$$\rho_{11,22}(\delta_t, \delta_r, \tau) = J_o\left(2\pi\left(-(\delta_t/\lambda)^2 - (\tau f_{t_{\max}})^2 - 2\tau\frac{\delta_t}{\lambda}f_{t_{\max}}\cos\left(\gamma_t - \theta_t\right)\right)^{1/2}\right)$$
$$\times J_o\left(2\pi\left(-(\delta_r/\lambda)^2 - (\tau f_{r_{\max}})^2 - 2\tau\frac{\delta_r}{\lambda}f_{r_{\max}}\cos\left(\gamma_r - \theta_r\right)\right)^{1/2}\right)$$
$$(3.18)$$

- For a SISO case, substituting the spacing between antenna element equal to zero:

$$\rho_{11,22}(0, 0, \tau) = J_o\left(2\pi f_{t_{\max}}\tau\right) J_o\left(2\pi f_{r_{\max}}\tau\right) \tag{3.19}$$

which is the well known result presented in [74, 122] for SISO M2M communication environment.

- If the transmitting MS_t is supposed to be fixed; the maximum Doppler would occur only due to the motion of the receiving MS_r; then (3.19) reduces to,

$$\rho(\tau) = J_o\left(2\pi f_{r_{\max}}\tau\right) \tag{3.20}$$

which is the well known CCF of the Jake's model [123, 124].

3.5   Results and Description

In this section, description of the obtained theoretical results for the derived correlation function is presented. From (3.17), it is clear the correlation function depends on various parameters like eccentricities of the ellipses, separation between antenna elements, velocities of the MSs and carrier frequency of the arriving signals. It can be observed that the correlation between antenna elements is maximum at $\tau = 0$ and decays with an increasing value of τ. It implies that the MIMO capacity will be minimum at the beginning as the correlation is maximum
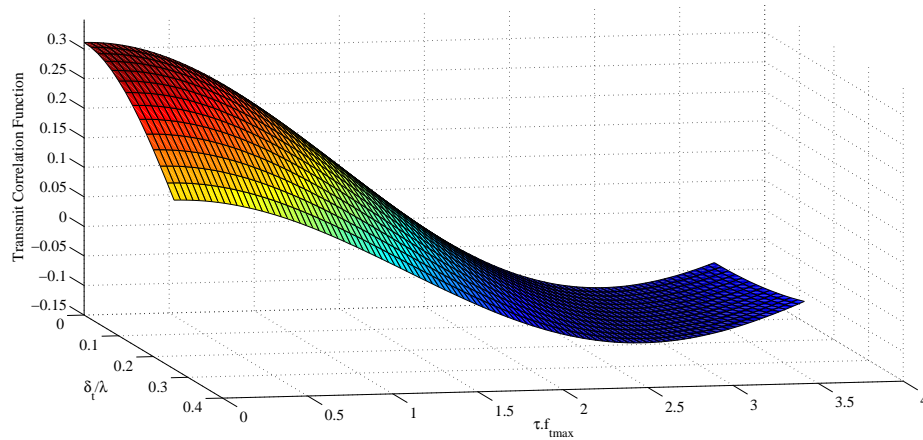
FIGURE 3.6: Correlation function of the non-isotropically arriving signals using MIMO two-elliptical channel model ($a_t = 50$m, $b_t = 20$m, D = 100m, $f_c = 800$MHz $v_t = 100$km/hr, $\gamma_t = 0^o$, $\theta_t = 90^o$, $c = 3 \times 10^8 m/s$).
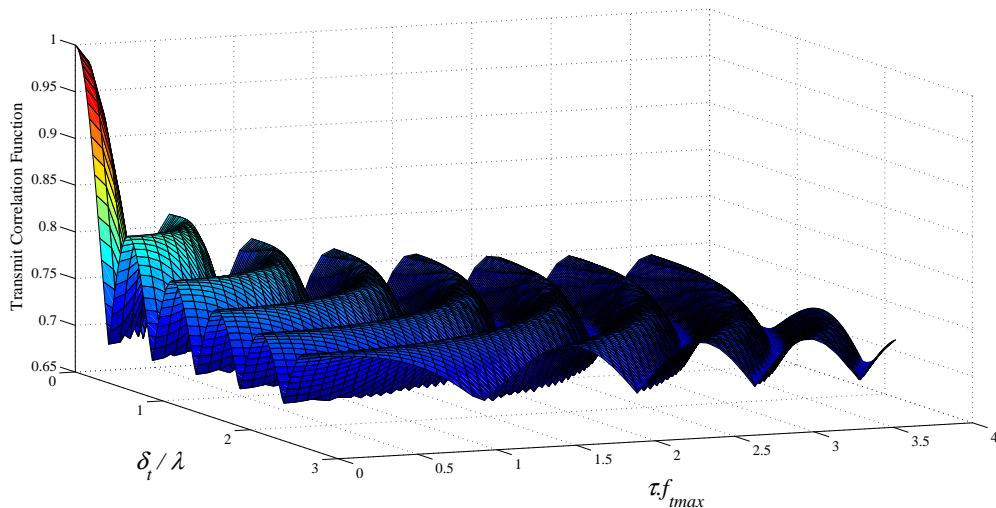
FIGURE 3.7: Correlation function of the isotropically arriving signals using MIMO two-ring channel model ($a_t = b_t = 50$m, D = 100m, $f_c = 800$MHz $v_t = 100$km/hr, $\gamma_t = 0^o$, $\theta_t = 90^o$, $c = 3 \times 10^8 m/s$)

.

there and will thus show an increasing trend with decreasing values of correlation.

Since in the proposed elliptical model, the scattering objects are assumed to be uniformly spaced on the elliptical loci, the AoA distribution at the receiver, MS_r would thus be non-isotropic as shown in Fig. 3.3. For such non-isotropic environment where a non-isotropic AoA distribution emerges from the varying distances of the scattering points from the MS_r, expression for the correlation function is
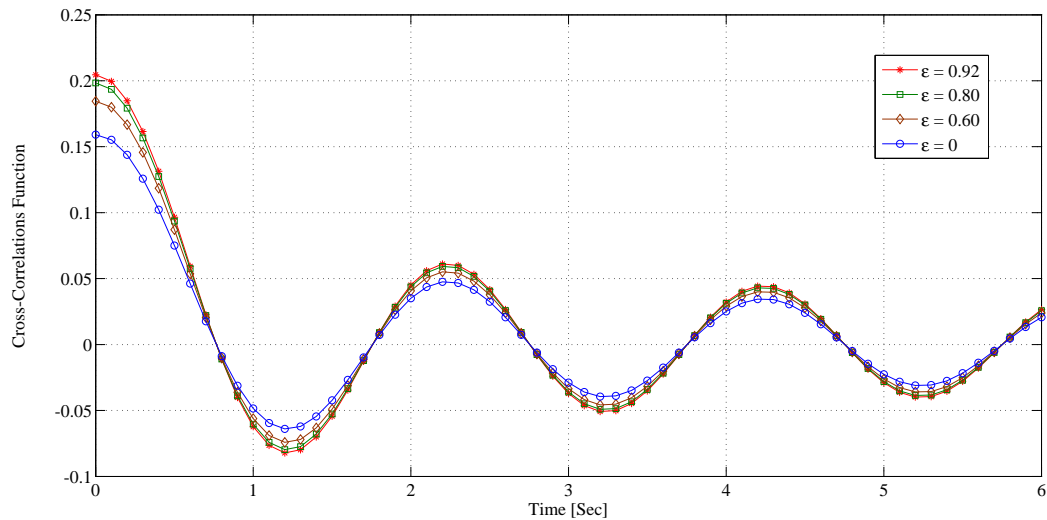
FIGURE 3.8: Comparison of correlation function on the basis of different values of eccentricity ($a_t = 50$m, $b_t = 20$m, D = 100m, $f_c = 800$MHz $v_t = 100$km/hr, $\gamma_t = 0^o$, $\theta_t = 90^o$, $c = 3 \times 10^8 m/s$).

derived as given in (3.17). Various correlation plots with 3D and 2D views are generated for the parameters specified in the captions of the figures. The result presented in Fig. 3.6, shows excellent agreement with the simulation results given in [115]. This is basically the elliptical geometrical shape that forces the correlation functions, $\rho_t(\delta_t, \tau)$, to be having this typical trend. However, the causes of such trend have not be documented in [115]. If the value of the major axis of an ellipse is fixed and increase its minor from its minimum value to a value equal to its major axis making eccentricity equal to zero, then the ellipse will be transformed into a circle. In this case, the correlation function, $\rho_t(\delta_t, \tau)$, shows an isotropic behavior of the arriving signals as shown in Fig. 3.7. This result also perfectly matches the theoretical results of the correlation curves shown in [115].

From the above figures, it is verified that the circular geometrical model is the special case of our proposed elliptical model. The 2D curves of the correlation function for different values of eccentricities are shown in Fig. 3.8. It can be seen that the correlation increases with an increase in eccentricity of the ellipse and becomes maximally uncorrelated when the ellipse is transformed into a circle.

The effect of spacing between antenna elements, δ_t, on the correlation function is shown in Fig. 3.9. The plots are taken for different values of antenna spacing i.e.,
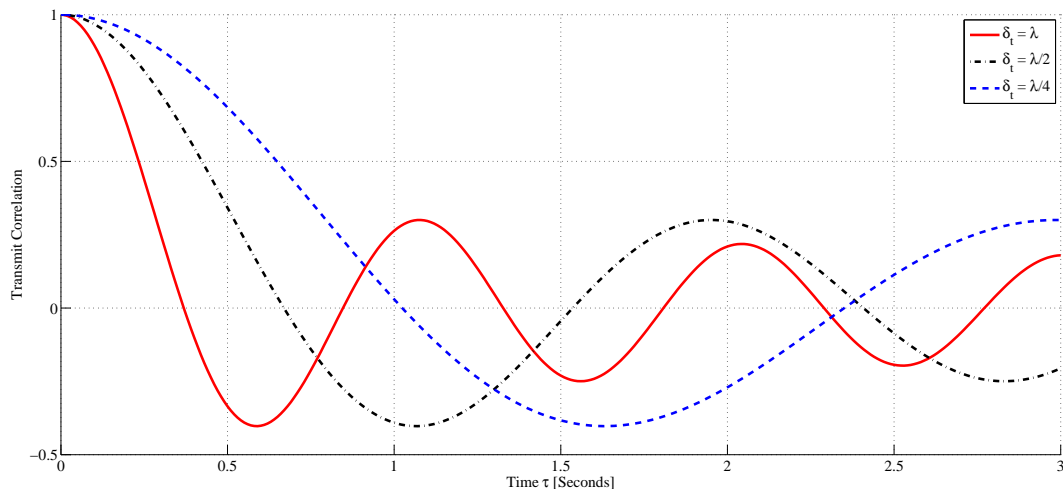
FIGURE 3.9: Effect of spacing between antenna elements on the antenna correlation, ($a_t = 50$m, $b_t = 20$m, $f_c = 300$MHz $v_t = 100$km/hr, $\gamma_t = 0^o$, $\theta_t = 90^o$, $c = 3 \times 10^8 m/s$).

$\delta_t = \lambda/\Delta$ where, $\Delta = 2, 4, 8$. The plots conform that the correlation is lesser for larger values of antenna spacing and vice versa.

It can be seen from the mathematical expressions (3.16) and (3.17) that correlation between antenna array elements also depends upon velocities of the transmit and receive MSs. In simulations, the effect of motion of the transmit MS is shown in Fig. 3.10, for different velocities i.e., $v_t = 100$km /hr, 150km/hr, and 200km/hr. From these correlation curves, it is observed that as the velocity of the transmit MS is low, the correlation is higher while low correlation is observed as the transmit MS moves at high speed. Keeping in view, the coherence time (T_{coh}) of the channel dependents on the Doppler frequency (f_{dmax}). Therefore, for the design of MIMO M2M communication systems, the velocities of the MSs should be taken under consideration.

In order to show the effect of the frequency on the transmit correlation a graph is depicted as in Fig. 3.11. It is observed from the graph that the correlation curves drops abruptly at higher frequency while as the correlation curve has a slow trend of decaying for low frequency. Therefore, a longer time is required to observe the correlation curves for higher carrier frequency.
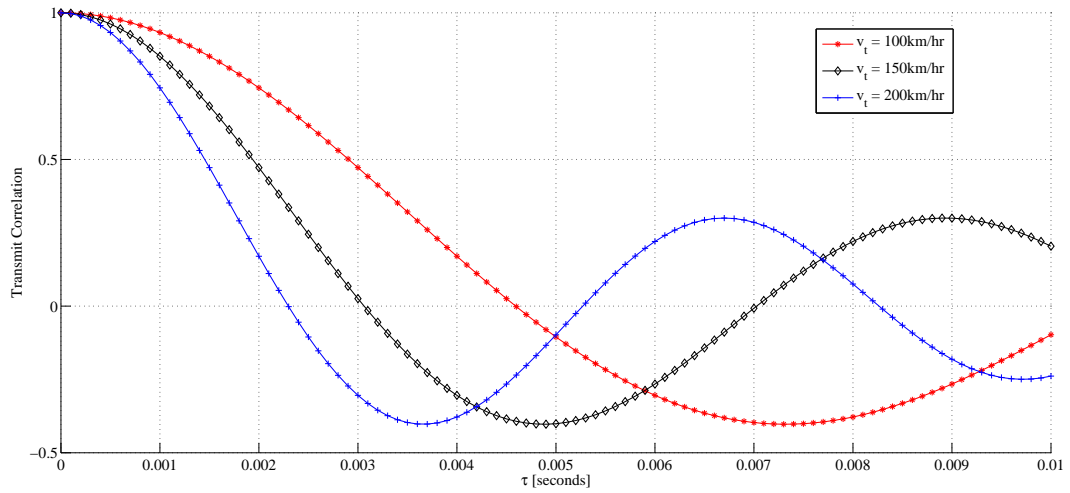
FIGURE 3.10: Effect of velocity (v_t) on transmit correlation, $(a_t = 50\text{m}, b_t = 20\text{m}, f_c = 900\text{MHz } v_t = 100\text{km/hr}, \gamma_t = 0^o, \theta_t = 90^o, c = 3 \times 10^8 m/s)$.
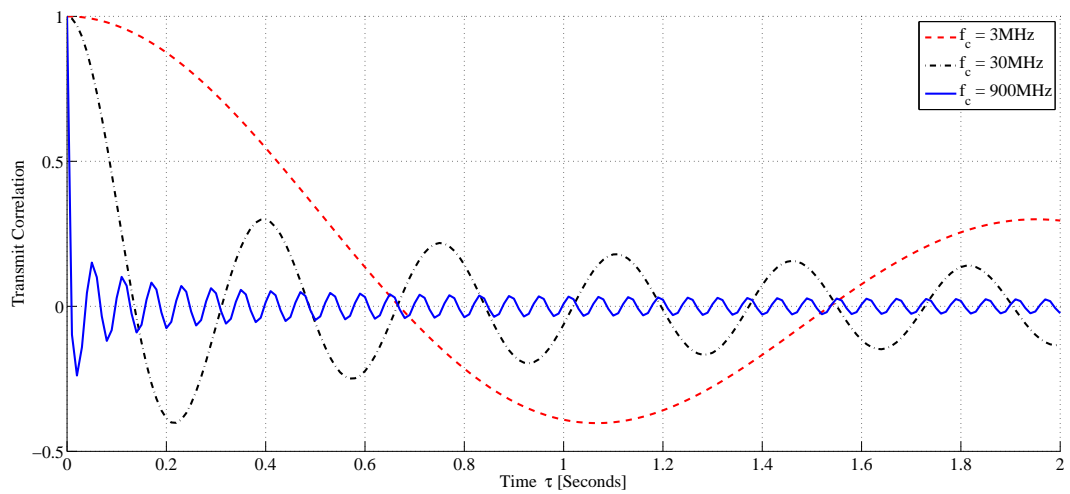
FIGURE 3.11: Effect of carrier frequency on the transmit correlation, $(a_t = 50\text{m}, b_t = 20\text{m}, \gamma_t = 0^o, \delta_t = .5\lambda, \theta_t = 60^o, v_t = 100km/hr \ c = 3 \times 10^8 m/s)$.

3.6 Conclusion

In this chapter, a 2-D elliptical geometrical scattering model for MIMO M2M communication channel is developed. The elliptical geometrical shape is supposed to be a more realistic approach than circular geometry to model the streets and canyons. It is assumed that both MSs are located at the centers of ellipses and surrounded by uniformly distributed scatterers present on the elliptical boundaries. Due to having elliptical boundaries, the distances of the scattering objects from the MSs are not equal, which forces the AoA distribution at either of the MSs to be non-isotropic. An empirical formula is provided for the AoA distribution emerged as the result of such non-isotropic arriving signals. Obtained results of empirical formula are compared with the numerical curves of the elliptical geometry that resulted into an acceptable agreement. Utilizing the non-isotropic AoA and the proposed geometrical model, a closed-form expression for the joint transmit-receive correlation function is derived. Since, the AoA and AoD are statistically independent, therefore, the joint expression for the correlation function can be expressed as a product of transmit and receive correlation functions. Various plots have been provided to analyze the correlation functions among the diffused components of the M2M MIMO communication link. It can be seen from the curves that the correlation depends on spacing between antenna elements, eccentricity of the ellipses, velocities of the MSs and the frequency of the arriving signals. Furthermore, the correlation curves obtained from the mathematical expression of the proposed model have been compared with the existing results in the literature. In order to validate the proposed model, the elliptical geometrical shape has been transformed into a circular one. The resulting comparative analysis verified that the circular geometrical models in [75, 85, 120, 121], are the special cases of our proposed model.

Chapter 4

Characterization of 3D Elliptical Spatial Channel Model for MIMO Mobile-to-Mobile Communication Environment

This chapter begins with Section 4.1 that introduces importance of GBSCM in mobile communications. Section 4.2 describes the proposed 3D geometric stochastic channel model for MIMO M2M propagation scattering environment. Section 4.3 provides a detailed derivation of the proposed system model. Moreover, mathematical expression for the joint and marginal space-time correlation functions among MIMO antenna elements is given in Section 4.4. Section 4.5 portrays the theoretical results with their detailed discussion and finally, Section 4.6 provides the conclusion of the chapter.

4.1 Introduction

Mobile-to-mobile (M2M) communication technology gives rise to various innovative advancements over a short span of time in vehicular, railway and defence

sectors. These communication scenarios demand audio, data, live video streaming, teleconferencing and other value added services with high data rates and good QoS [125, 126]. Providing high capacity data links to mobile subscribers with limited resources is a constant driving force in the research arena. This becomes even more challenging when the mobile subscribers are at high speed in the streets, canyons and highways with rich scatterers along the road side regions. In rich scattering environments MIMO is considered to be a promising candidate for high capacity data links provided that the minimum correlation exists among the antenna elements [127]. Therefore, a suitable channel model is required that can be used to estimate the performance of the MIMO M2M communication systems in such propagation environments. In this regard, empirical, stochastic and GBSCM modeling techniques are being adopted to model the wireless propagation channels. Out of these models, regular-shaped GSCM's (RS-GSCM's) are considered potential candidate to model MIMO M2M propagation channels in such propagation scenarios. However, the physical layout of the streets, canyons, deep-cut railway tracks and highways are mostly narrow in width and longer in length that have close resemblance to the elliptical shape. Therefore, the proposed eccentricity-based cylindrical channel model for MIMO M2M communication environments is the appropriate solution to model such channels. Where, the height of elliptic cylinder can model the high-rise buildings, vegetation and other infrastructure present along the roadside premises are the sources of multipaths in the elevation planes. In the proposed channel model scatterers are assumed to be uniformly distributed on the surface of cylinders while as MSs are located at the base center of the cylinders. Both MSs are holding low-rise multiple antenna arrays and there is no LoS path between MSs. The expression of space-time correlation function is formulated, which is simulated for various channel parameters. Finally, for the validation of proposed model, correlation results are compared with the measurement data, which shows a close agreement.

4.2 System Model

In this section, we present the system architecture of the proposed elliptical-base cylindrical channel model for MIMO M2M communication environment as shown in Fig. 4.1. In this proposed channel model, transmitting and receiving MSs are denoted by MS_t and MS_r respectively. These MSs are assumed to be located at the centers bottom surface of the elliptical cylinders, having major axes a_t and a_r and minor axes b_t and b_r with eccentricities ϵ_t and ϵ_r, respectively. The mobile nodes are moving independently with the velocities of v_t and v_r making angles α_t and α_r with the x-axis. The center to center distance between the two elliptical cylindrical is represented by D $\left(\text{such that } D \gg a_t + a_r\right)$ and to avoid the channel may not experience the keyhole behavior the distance should not be greater than $4R_{d,t}R_{d,r}Q/(\lambda(Q-1)(P-1))$ [128]. The azimuth plane dimension of the physical propagation channel around the MSs are adjusted in the system model by eccentricities ϵ_t and ϵ_r of the ellipses. Whereas, the surrounding scatter height around transmitter and receiver are represented by h_t and h_r respectively. The scatters present in the close vicinity of mobile nodes are assumed to be uniformly distributed on the surfaces of elliptical cylinders. Moreover, the elliptical cylinders are rotatable congruous to the directions of motion of the MSs such that their major axes a_t and a_r make angles α_t (or α_r) respectively, with the x-axis. Mobile nodes are equipped with low height antennas arrays with configuration $P \times Q$, where P and Q are the number of antennas mounted on MS_t and MS_r, respectively. For simplicity, we take $P = Q = 2$. However, the results can be derived for any configuration. The transmit and receive antenna array elements are denoted by $A_t^{(p)}$ and $A_r^{(q)}$, and the distance between the antenna array elements are denoted by δ_t and δ_r, which are very small as compared to the minor axes of the surrounding ellipses respectively. The description of the other parameters involved in the proposed geometrical model are narrated in Table 4.1.

TABLE 4.1: Definitions of the channel parameters used in the system model

Symbols	Description.
D	The distance between center to center of elliptical cylinders surrounding MS_t and MS_r.
$R_{d,t}, R_{d,r}$	The variable radius of the transmitter and receiver ellipses, respectively.
$\delta_t(p, \tilde{p})$	The spacing between p^{th} and $\tilde{p}^{th}$ antenna elements at Tx.
$\delta_r(q, \tilde{q})$	The spacing between q^{th} and $\tilde{q}^{th}$ antenna elements at Tx.
$\theta_t^{(p)}, \theta_r^{(q)}$	The azimuth angle of pth transmit and q^{th} receive antenna element (relative to x-axis), respectively.
$\psi_t^{(p)}, \psi_r^{(q)}$	The elevation angle of pth transmit and q^{th} receive antenna element (relative to x-y plane), respectively.
v_t, v_r	The velocities of the Tx and Rx, respectively.
γ_t, γ_r	The moving directions of the Tx and Rx, respectively.
$\alpha_t^{(m)}, \alpha_r^{(n)}$	The azimuth angles of departure (AAoD) and the azimuth angles of arrival (AAoA), respectively.
$\beta_t^{(m)}, \beta_r^{(n)}$	The elevation angle of departure (EAoD) and the elevation angle of arrival (EAoA), respectively.
$d_{pm}\ d_{\tilde{p}m}\ d_{mn}\ d_{nq}$ $d_{n\tilde{q}}$	The distances $d\left(A_t^{(p)}, S_t^{(m)}\right)$, $d\left(A_t^{(\tilde{p})}, S_t^{(m)}\right)$, $d\left(S_t^{(m)}, S_r^{(n)}\right)$, $d\left(S_r^{(n)}, A_r^{(q)}\right)$, and $d\left(S_r^{(n)}, A_r^{(\tilde{q})}\right)$
d_{max}^{pq}	$d_{pm} + d_{mn} + d_{nq}$.
$d_{max}^{\tilde{p}\tilde{q}}$	$d_{\tilde{p}m} + d_{mn} + d_{n\tilde{q}}$.

4.3 Derivation of the Reference Model

The derivations of the various characteristic of the MIMO M2M fading channel are based on the reference model depicted in Fig. 4.1. It can be observed that a signal
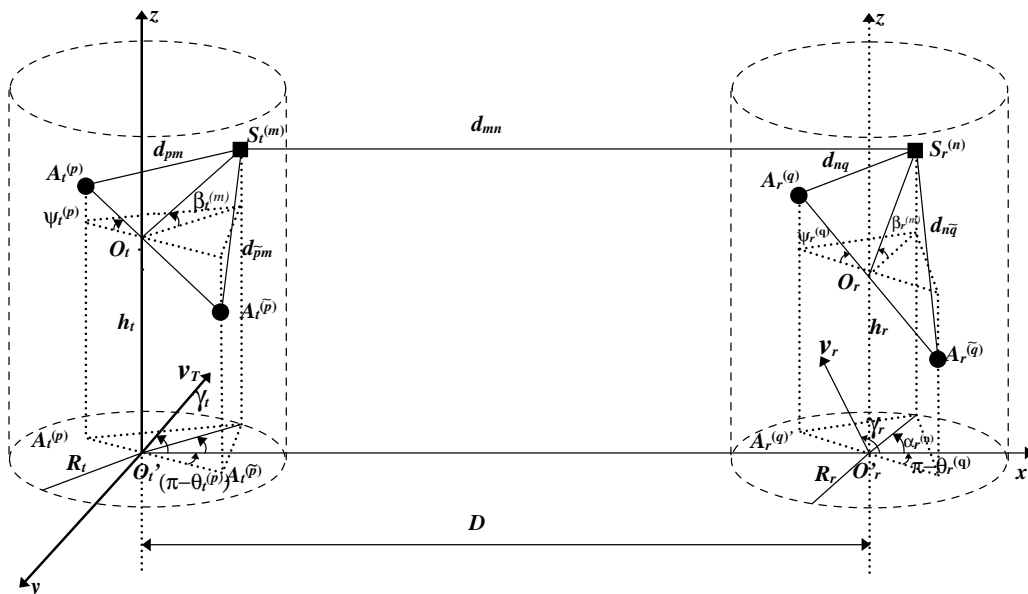

FIGURE 4.1: Proposed 3D Elliptical Channel Model for MIMO Mobile-to-Mobile Channels with $P = Q = 2$ antenna elements.
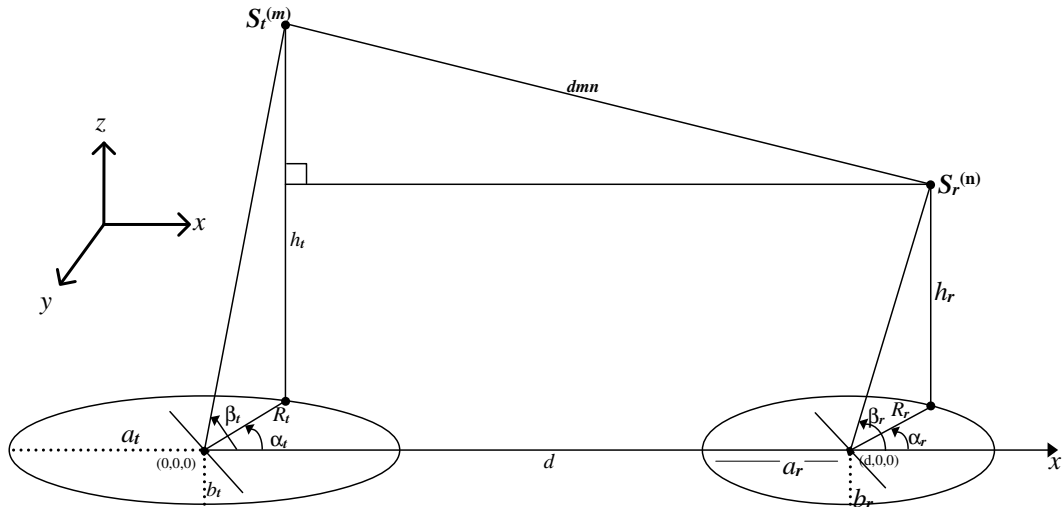
FIGURE 4.2: 2D view of proposed elliptical channel model for MIMO M2M channels.

that is transmitted from the transmit antenna array element $A_t^{(p)}$, first strikes at the scatterer $S_t^{(p)}$ present on the surface of elliptical cylindrical surrounding the transmitter node and then travels towards the scatter $S_r^{(q)}$ located on the surface of elliptical cylindrical surrounding the receiver node, and then finally reaches the receiving antenna array element $A_r^{(q)}$. During propagation, the distances covered by the wavelets from $A_t^{(p)}$ to $A_r^{(q)}$ and $A_t^{(\tilde{p})}$ to $A_r^{(\tilde{q})}$, are denoted by d_{max}^{pq} and $d_{max}^{\tilde{p}\tilde{q}}$, respectively. Therefore, the phase change due to the distance traveled by the wavelet can be written as $(2\pi/\lambda)d_{max}^{pq}$ and $(2\pi/\lambda)d_{max}^{\tilde{p}\tilde{q}}$, where $2\pi/\lambda$ is called wavenumber. Moreover, the joint gain and phase shift due to the collision of the wavelet with $S_t^{(p)}$ and $S_t^{(q)}$ can be expressed as $1/\sqrt{MN}$ and ϕ_{mn} respectively. Other sources of phase shift in M2M communication is due to the motion of transmitter and receiver, which can be expressed as $2\pi f_{Tmax}\cos(\alpha_t^{(m)}-\gamma_t)\cos\beta_t^{(m)}t$ and $2\pi f_{Rmax}\cos(\alpha_R^{(n)}-\gamma_r)\cos\beta_r^{(n)}t$. Where, $f_{Tmax} = v_t/\lambda$ and $f_{Rmax} = v_R/\lambda$ represents the maximum Doppler frequency caused by the motion of mobile nodes. Moreover, for the ease of derivations of the different expressions of the proposed channel model, following valid assumptions are considered

1. Each multipath component of the propagating signal undergoes two bounces while traveling from the transmitter mobile node to the receiver mobile node.

2. Infinite number of scatterers are uniformly distributed on the elliptical cylindrical surfaces with uniformly distributed phases.

3. Equal distributed power is reflected from all the scatterers.

4. All the waves reaching at the receiver antenna elements are equal in power.

5. The scatterers are fixed and MSs are quasi-stationary for a short period of time.

Finally, with the help of above assumptions the diffused components of the transmission link from $A_t^{(p)}$ to $A_r^{(q)}$ can be expressed as,

$$
\begin{aligned}
h_{pq}(t) = \lim_{M,N\to\infty} \frac{1}{\sqrt{MN}} \sum_{m=1}^{M} \sum_{n=1}^{N} & G_{pq} e^{-j\frac{2\pi}{\lambda}(d_{pm}+d_{mn}+d_{nq})+j\phi_{mn}} \\
& \times e^{j2\pi t f_{Tmax}\cos(\alpha_t^{(m)}-\gamma_t)\cos\beta_t^{(m)}} \times e^{j2\pi t f_{Rmax}\cos(\alpha_R^{(n)}-\gamma_r)\cos\beta_r^{(n)}}
\end{aligned}
\tag{4.1}
$$

The expressions of the distances d_{pm}, $d_{\tilde{p}m}$, d_{nq} and $d_{n\tilde{q}}$ are obtained by solving the geometry of the proposed model as shown in Fig. 4.1. It is observed that these distances are the functions of random angles of azimuth and elevation of transmit antenna arrays, receive antenna arrays and scatter. The 3D polar coordinates of pth transmit and qth receive antenna elements in 3D space are denoted by $\left(d_{T_x}^{(p)}, d_{T_y}^{(p)}, d_{T_z}^{(p)}\right)$ and $\left(d_{R_x}^{(q)}, d_{R_y}^{(q)}, d_{R_z}^{(q)}\right)$, where $d_{T_x}^{(p)} = d(A_t^{(p)}, C_t)\cos\theta_t^{(p)}\cos\psi_t^{(p)}$, $d_{T_y}^{(p)} = d(A_t^{(p)}, C_t)\sin\theta_t^{(p)}\cos\psi_t^{(p)}$, $d_{T_z}^{(p)} = d(A_t^{(p)}, C_t)\sin\psi_t^{(p)}$, $d_{R_x}^{(q)} = d(A_r^{(p)}, C_r)\cos\theta_r^{(q)}\cos\psi_r^{(q)}$, $d_{R_y}^{(q)} = d(A_r^{(p)}, C_r)\sin\theta_r^{(q)}\cos\psi_r^{(q)}$, $d_{R_z}^{(q)} = d(A_r^{(p)}, C_r)\sin\psi_r^{(q)}$. Similarly, the coordinates of mth and nth scatterer in 3D space are denoted by $\left(d_{A_x}^{(m/\tilde{m})}, d_{A_y}^{(m/\tilde{m})}, d_{A_z}^{(m/\tilde{m})}\right)$ and $\left(d_{A_x}^{(n/\tilde{n})}, d_{A_y}^{(n/\tilde{n})}, d_{A_z}^{(n/\tilde{n})}\right)$, where $d_{A_x}^{(m/\tilde{m})} = R_{d,t}\cos\alpha_t^{(m/\tilde{m})}$, $d_{A_y}^{(m/\tilde{m})} = R_{d,t}\sin\alpha_t^{(m/\tilde{m})}$, $d_{A_z}^{(m/\tilde{m})} = R_{d,t}\tan\beta_t^{(m/\tilde{m})}$, $d_{A_x}^{(n/\tilde{n})} = d+R_{d,r}\cos\alpha_r^{(n/\tilde{n})}$, $d_{A_y}^{(n/\tilde{n})} = R_{d,r}\sin\alpha_r^{(n/\tilde{n})}$, $d_{R_z}^{(n/\tilde{n})} = R_{d,r}\tan\beta_t^{(n/\tilde{n})}$. These polar coordinates depend upon the orientation and configuration of the antenna arrays. The dynamic radii $R_{d,r}$ and $R_{d,t}$ of the transmit and receive ellipses can be written in terms of minor a_i and major b_i axis as, $a_i b_i / \sqrt{a_i^2 \sin^2\alpha_i + b_i^2 \cos^2\alpha_i}$ [129]. Using the distance formula, and binomial approximation $\sqrt{(1+x)} \approx 1 + x/2$ if $(x \ll 1)$, the approximated distances can be expressed as,

$$d_{p/\tilde{p},m} \approx \frac{R_{d,t}}{\cos \beta_t^{(m)}} - d(A_t^{(p)}, C_t) \sin \psi_t^{(p)} \sin \beta_t^{(m)} - d(A_t^{(p)}, C_t) \cos \psi_t^{(p)} \cos \beta_t^{(m)} \cos(\alpha_t^{(m)} - \theta_t^{(p)})$$

(4.2)

$$d_{n,q/\tilde{q}} \approx \frac{R_{d,r}}{\cos \beta_r^{(n)}} - d(A_r^{(p)}, C_r) \sin \psi_r^{(q)} \sin \beta_r^{(n)} - d(A_r^{(p)}, C_r) \cos \psi_r^{(q)} \cos \beta_r^{(n)} \cos(\alpha_r^{(n)} - \theta_r^{(q)})$$

(4.3)

The propagation path length, d_{mn}, from $S_t^{(p)}$ to $S_t^{(q)}$ is greater than $\max(d_{pm}, d_{nq})$ and contributes significantly in the phase shift to the received signal. It is the function of random angles $\beta_t^{(m)}, \alpha_t^{(m)}, \beta_r^{(n)}$ $\alpha_r^{(n)}, \beta_r^{(q)}, \beta_t^{(m)}$ and dynamic radii of the ellipses and can be obtained by solving the geometry as shown in Fig. 4.2. With the help of approximations used in (4.2) and (4.3), the simplified form of d_{mn} can be expressed as,

$$\begin{aligned} d_{mn} \approx d &+ \frac{R_{d,r}^2}{2d} + \frac{R_{d,t}^2}{2d} - \frac{R_{d,r}R_{d,t}\cos(\alpha_r^{(n)} - \alpha_t^{(m)})}{d} - R_{d,t}\cos \alpha_t^{(m)} + R_{d,r}\cos \alpha_r^{(n)} \\ &+ \frac{(R_{d,t}\tan \beta_t^{(m)})^2}{2d} + \frac{(R_{d,r}\tan \beta_r^{(n)})^2}{2d} - \frac{R_{d,t}\tan \beta_t^{(n)} R_{d,r}\tan \beta_r^{(m)}}{d}. \end{aligned}$$

(4.4)

$$\begin{aligned} d_{mn} \approx d &- \frac{R_{d,r}R_{d,t}\cos(\alpha_r^{(n)} - \alpha_t^{(m)})}{d} - R_{d,t}\cos \alpha_t^{(m)} + R_{d,r}\cos \alpha_r^{(n)} \\ &+ \frac{R_{d,t}^2 \sec^2 \beta_t^{(m)}}{2d} + \frac{R_{d,r}^2 \sec^2 \beta_r^{(n)}}{2d} - \frac{R_{d,t}\tan \beta_t^{(m)} R_{d,r}\tan \beta_r^{(n)}}{d}. \end{aligned}$$

(4.5)

Substituting values of d_{pm}, d_{nq} and d_{mn} in (4.1), we get,

$$\begin{aligned} h_{pq}(t) = \lim_{M,N \to \infty} \frac{1}{\sqrt{MN}} \sum_{m=1}^{M} \sum_{n=1}^{N} a_{p,m} b_{n,q} c_{p,q} e^{j\phi_{mn}} \\ \times e^{j2\pi[f_{Tmax}\cos(\alpha_t^{(m)} - \gamma_t)\cos \beta_t^{(m)} + f_{Rmax}\cos(\alpha_R^{(n)} - \gamma_r)\cos \beta_r^{(n)}]t} \end{aligned}$$

(4.6)

.

where,

$$a_{p,m} = e^{\frac{-j\pi}{\lambda}\left(\frac{d}{2} + \frac{2R_{d,t}}{\cos \beta_t^{(m)}}\right)} e^{j\frac{2\pi}{\lambda}\left(-R_{d,t}\cos \alpha_t^{(m)}\right)} e^{j\frac{2\pi}{\lambda}d_{T_x^p}\cos \alpha_t^{(m)}\cos \beta_t^{(m)}} e^{j\frac{2\pi}{\lambda}d_{T_y^p}\sin \alpha_t^{(m)}\cos \beta_t^{(m)}}$$

$$e^{j\frac{2\pi}{\lambda}d_{T_z^p}\sin \beta_t^{(m)} + \frac{(R_{d,t}\sec \beta_r^{(p)})^2}{2d}}$$

$$b_{n,q} = e^{\frac{-j\pi}{\lambda}\left(\frac{d}{2} + \frac{2R_{d,r}}{\cos \beta_r^{(n)}}\right)} + e^{j\frac{2\pi}{\lambda}\left(R_{d,r}\cos \alpha_r^{(n)}\right)} e^{j\frac{2\pi}{\lambda}d_{R_x^q}\cos \alpha_r^{(n)}\cos \beta_r^{(n)}} e^{j\frac{2\pi}{\lambda}d_{R_y^q}\sin \alpha_r^{(n)}\cos \beta_r^{(n)}}$$

$$e^{j\frac{2\pi}{\lambda}d_{R_z^q}\sin \beta_r^{(n)} + \frac{(R_{d,r}\sec \beta_r^{(n)})^2}{2d}}$$

$$c_{p,q} = e^{\frac{-j\pi}{\lambda} \left(\frac{R_{d,t} \tan \beta_t^{(p)} R_{d,r} \tan \beta_r^{(n)}}{d} + \frac{R_{d,r} R_{d,t} \cos(\alpha_r^{(n)} - \alpha_t^{(m)})}{d} \right)}$$

The proposed geometrical can be also extended for $P \times Q$ antenna arrays structure. The polar coordinates of antenna elements is denoted by $(d_{T_x/R_x}^{(p/q)}, d_{T_x/R_x}^{(p/q)}, d_{T_x/R_x}^{(p/q)})$ where, $d_{T_x/R_x}^{(p/q)} = \delta_{(t/r)} \left(0.5 A_{(t/r)} - .5 - p(q) \right) \cos \theta_{t/r}^{(p/q)} \cos \psi_{t/r}^{(p/q)}$, $d_{T_x/R_x}^{(p/q)} = \delta_{(t/r)}$ $\left(0.5 A_{(t/r)} - .5 - p(q) \right) \sin \theta_{t/r}^{(p/q)} \cos \psi_{t/r}^{(p/q)}$, $d_{T_x/R_x}^{(p/q)} = \delta_{(t/r)} \left(0.5 A_{(t/r)} - .5 - p(q) \right) \sin \psi_{t/r}^{(p/q)}$. The parameter $p, \tilde{p} \in \{1, ... P\}$ and $q, \tilde{q}$ takes values from $\{1, ... Q\}$. The coordinates for $\tilde{p}$ element and $\tilde{q}$ element can be obtained by replacing $\delta_{(t/r)}$ with $-\delta_{(t/r)}$. Where, $\delta_{(t/r)}$ is the spacing between two adjacent elements of transmitter (receiver) antenna arrays.

4.4 Derivation of Space-time correlation function of the proposed model

The normalized space-time correlation function between diffused channel coefficients $h_{pq}(t)$ and $h_{\tilde{p}\tilde{q}}(t)$ for the proposed 3D model can be found using the following relation,

$$\rho_{pq,\tilde{p}\tilde{q}}[\tau] = \frac{E[h_{pq}(t) h_{\tilde{p}\tilde{q}}^*(t + \tau)]}{\sqrt{E[|h_{pq}(t)|]^2 E[|h_{\tilde{p}\tilde{q}}(t)|]^2}} \tag{4.7}$$

where, $E[\cdot]$ is the statistical expectation operator and can be applied only to all random variables and $(\cdot)^*$ symbolizes as the complex conjugate operation. Using (4.6) and (4.7), the space-time correlation function can be formulated as,

$$\begin{aligned}
\rho_{pq,\tilde{p}\tilde{q}}[\tau] = \lim_{M,N \to \infty} \frac{1}{MN} \sum_{m=1}^{M} \sum_{n=1}^{N} E\Big[a_{p,m} b_{n,q} c_{p,q} a_{\tilde{p},m}^* b_{n,\tilde{q}}^* c_{\tilde{p}\tilde{q}}^* \\
\times e^{-2j\pi\tau \left(f_{Tmax} \cos(\alpha_t^{(m)} - \gamma_t) \cos \beta_t^{(m)} + f_{Rmax} \cos(\alpha_R^{(n)} - \gamma_r) \cos \beta_r^{(n)} \right)} \Big],
\end{aligned} \tag{4.8}$$

It is assumed that infinite number of scattering objects reside around each MS, which implies that the scattering distributions may be transformed from discrete to continuous that in turn forces to change the discrete random variables (e.g., $\alpha_t^{(m)}$, $\beta_t^{(m)}$) into continuous random variables (α_t, β_t). Furthermore, we assume that azimuth and elevation angles are independent of each other, therefore, $f(\alpha_t, \beta_t)$

and $f(\alpha_R, \beta_r)$ can be written in product form as $f(\alpha_t)f(\beta_t)$ and $f(\alpha_R)f(\beta_r)$, respectively. Hence, for the continuous time random variables, the above equation can be written in integration form as,

$$
\begin{aligned}
\rho_{pq,\tilde{p}\tilde{q}}(\tau) \approx & \int_{-\beta_{Rm}}^{\beta_{Rm}} \int_{-\beta_{Tm}}^{\beta_{Tm}} \int_{-\pi}^{\pi} \int_{-\pi}^{\pi} e^{-2j\pi\tau(f_{Tmax}\cos(\alpha_t-\gamma_t)\cos\beta_t)} \\
& \times e^{\frac{j2\pi}{\lambda}\left(d_{Tx}^{(p,\tilde{p})}\cos\alpha_t\cos\beta_t+d_{Tz}^{(p,\tilde{p})}\sin\beta_t+\frac{(R_{d,t}\sec\beta_t)^2}{2d}\right)} e^{\frac{j2\pi}{\lambda}d_{Ty}^{(p,\tilde{p})}\sin\alpha_t\cos\beta_t} \\
& \times e^{-2j\pi\tau(f_{Rmax}\cos(\alpha_R-\gamma_r)\cos\beta_r)} e^{\frac{j2\pi}{\lambda}\left(d_{Ty}^{(p,\tilde{p})}\sin\alpha_t\cos\beta_t+d_{Rz}^{(q,\tilde{q})}\sin\beta_r+\frac{(R_{d,r}\sec\beta_r)^2}{2d}\right)} \\
& \times e^{\frac{j2\pi}{\lambda}d_{Rx}^{(p,\tilde{p})}\sin\alpha_r\cos\beta_r} f(\alpha_t)f(\beta_t)f(\alpha_R)f(\beta_r)\mathrm{d}\alpha_t\mathrm{d}\beta_t\mathrm{d}\alpha_R\mathrm{d}\beta_r
\end{aligned}
\tag{4.9}
$$

where, $\beta_{m,R}$, $\beta_{m,T}$ represents the maximum elevation angles of the scatters present around transmit and receiver mobile nodes and $d_{Tx}^{(p,\tilde{p})} = d_{Tx}^{(p)} - d_{Tx}^{(\tilde{p})}$, $d_{Ty}^{(p,\tilde{p})} = d_{Ty}^{(p)} - d_{Ty}^{(\tilde{p})}$, $d_{Tz}^{(p,\tilde{p})} = d_{Tz}^{(p)} - d_{Tz}^{(\tilde{p})}$, $d_{Rx}^{(q,\tilde{q})} = d_{Rx}^{(q)} - d_{Rx}^{(\tilde{q})}$, $d_{Ry}^{(q,\tilde{q})} = d_{Ry}^{(q)} - d_{Ry}^{(\tilde{q})}$, $d_{Rz}^{(q,\tilde{q})} = d_{Rz}^{(q)} - d_{Rz}^{(\tilde{q})}$. Furthermore, different scattering distribution have been proposed in the literature for isotropic and non-isotropic environments [6]. In urban areas streets, canyons and highways are more likely non-isotropic environments. So, in the proposed research work, eccentricity-based (i.e., ϵ_i) modified von Mises distribution for azimuth AoA/AoD is used [130]. The PDF of azimuth AoA/AoD at each MS can be written as, $p(\alpha_i) = \frac{1}{2\pi I_0(\epsilon_i^2)}e^{\epsilon_i^2\cos\alpha_i}$, $i = t, r$, where, $\epsilon_i = \sqrt{1 - b_i^2/a_i^2}$, the azimuth angle $\alpha_i \in [-\pi, \pi)$ and $I_0(\cdot)$ is the zeroth-order modified Bessel function of the first kind. Similarly, It has been observed from the experiments that the elevation AoA of incoming signals ranges from 0° to 20° [131] and the distance between two MSs is much larger than each of their antenna heights; therefore, using the small angle approximation $\sin\beta_i \approx \beta_i$, $\cos\beta_i \approx 1$, $\sec_i^2\beta = 1 + \beta_i/2$ and substituting PDF of elevation AoA(AoD), i.e., $f(\beta_i) = \frac{\pi}{4\beta_{im}}\cos\left(\frac{\pi}{2}\frac{\beta_i}{\beta_{im}}\right)$ as proposed in [132], where, the absolute values of elevation angles $(\beta_{i_m}, i \in T, R)$ lies in the

range $0^0 \leq \beta_{i_m} \leq 20^0$, in equation (5.9) we get,

$$\rho_{pq,\tilde{p}\tilde{q}}[\tau] \approx \frac{1}{4\pi^2 I_o(\epsilon_t^2)\pi I_o(\epsilon_r^2)} \int_{-\pi}^{\pi} \exp\left[c_t \cos\alpha_t + d_t \sin\alpha_t\right] d\alpha_t$$
$$\int_{-\pi}^{\pi} \exp\left[c_r \cos\alpha_r + d_r \sin\alpha_r\right] d\alpha_r$$
$$\int_{-\beta_{R_m}}^{\beta_{R_m}} \int_{-\beta_{T_m}}^{\beta_{T_m}} \times e^{\frac{j2\pi}{\lambda}\left(d_{Tz}^{(p,\tilde{p})} + \frac{R_{d,t}^2}{4d}\right)\beta_t} \times e^{\frac{j2\pi}{\lambda}\left(d_{Rz}^{(q,\tilde{q})} + \frac{R_{d,r}^2}{4d}\right)\beta_r}$$

$$\frac{\pi}{4\beta_{Tm}}\cos\left(\frac{\pi\beta_t}{2\beta_{Tm}}\right)\frac{\pi}{4\beta_{Rn}}\cos\left(\frac{\pi\beta_r}{2\beta_{Rn}}\right)d\beta_t d\beta_r$$

(4.10)

where,

$c_t = \frac{j2\pi d_{Tx}^{(p,\tilde{p})}}{\lambda} - 2j\pi\tau f_{Tmax}\cos\gamma_t + \epsilon_t^2,$

$d_t = \frac{j2\pi d_{Ty}^{(p,\tilde{p})}}{\lambda} - 2j\pi\tau f_{Tmax}\sin\gamma_t,$

$c_r = \frac{j2\pi d_{Rz}^{(q,\tilde{q})}}{\lambda} - 2j\pi\tau f_{Rmax}\cos\gamma_r + \epsilon_r^2,$

$d_r = \frac{j2\pi d_{Rw}^{(q,\tilde{q})}}{\lambda} - 2j\pi\tau f_{Rmax}\sin\gamma_r.$

Equation (4.10) can be further simplified by introducing trigonometric transformation and the equality $\int_{-\pi}^{\pi} \exp\left[c_i \cos\alpha_i + d_i \sin\alpha_i\right] d\alpha_i = I_0(2\pi\sqrt{c_i^2 + d_i^2})$ [133].

$$\rho_{pq,\tilde{p}\tilde{q}}[\tau] \approx \frac{I_o(2\pi\sqrt{c_t^2 + d_t^2})}{2\pi I_o(\epsilon_t^2)} \int_{-\beta_{Tm}}^{\beta_{Tm}} \frac{\pi}{4\beta_{Tm}}\cos\left(\frac{\pi\beta_t}{2\beta_{Tm}}\right) e^{\frac{j2\pi}{\lambda}\left(d_{Tz}^{(p,\tilde{p})}\beta_t + \frac{R_{d,t}^2}{4d}\right)\beta_t} d\beta_t$$
$$\times \frac{I_o(2\pi\sqrt{c_r^2 + d_r^2})}{2\pi I_o(\epsilon_r^2)} \int_{-\beta_{Rm}}^{\beta_{Rm}} \frac{\pi}{4\beta_{Rn}}\cos\left(\frac{\pi\beta_r}{2\beta_{Rn}}\right) e^{\frac{j2\pi}{\lambda}\left(d_{Rz}^{(q,\tilde{q})}\beta_r + \frac{R_{d,r}^2}{4d}\right)\beta_r} d\beta_r$$

(4.11)

It is seen that the joint correlation function in (4.11) is the product of transmit and receive correlation functions, that can be written as,

$$\rho_{pq,\tilde{p}\tilde{q}}[\tau] \approx \rho(\phi_t, \beta_t, \delta_t, \tau)\rho(\phi_r, \beta_r, \delta_r, \tau)$$

(4.12)

where,

$$\rho(\phi_t, \beta_t, \delta_t, \tau) \approx \frac{2\pi I_o(\sqrt{c_t^2 + d_t^2})}{2\pi I_o(\epsilon_t^2)} \int_{-\beta_{Tm}}^{\beta_{Tm}} \frac{\pi}{4\beta_{Tm}}\cos\left(\frac{\pi\beta_t}{2\beta_{Tm}}\right) e^{\frac{j2\pi}{\lambda}\left(d_{Tz}^{(p,\tilde{p})}\beta_t + \frac{R_{d,t}^2}{4d}\right)\beta_t} d\beta_t$$

(4.13)

Integrating (4.13) with respect to β_t, and introduce approximations for the complex error function as in [134], the simplified expression can be written as,

$$
\rho(\phi_t, \beta_t, \delta_t, \tau) \approx \frac{2\pi I_o\left(\sqrt{c_t^2 + d_t^2}\right)}{2\pi I_o(\epsilon_t^2)} \left(\frac{d^2\lambda^2 \cos(\frac{\pi(4d_{Tz}^{(p,\tilde{p})}d + R_{d,t}^2)\beta_{Tm}}{2d\lambda})}{d^2\lambda^2 - (R_{d,t}^2 + 4d_{Tz}^{(p,\tilde{p})}d)^2\beta_{Tm}^2} \right) \tag{4.14}
$$

$$
\rho(\phi_t, \beta_{Tm}, \delta_t, \tau) \approx \frac{I_o\left(2\pi\sqrt{c_t^2 + d_t^2}\right)}{2\pi I_o(\epsilon_t^2)} \left(\frac{\cos\left(\frac{2\pi}{\lambda}\beta_{Tm}d_{Tz}^{(p,\tilde{p})} + \frac{\pi\beta_{Tm}R_{d,t}^2}{2d\lambda}\right)}{1 - \left(\frac{R_{d,t}^2\beta_{Tm}}{d\lambda} + \frac{4\beta_{Tm}d_{Tz}^{(p,\tilde{p})}}{\lambda}\right)^2} \right) \tag{4.15}
$$

The closed-form expression for the receive space-time correlation function can be obtained by replacing the index t with index r, and the joint space time correlation function (4.13) can be written as

$$
\rho_{pq,\tilde{p}\tilde{q}}[\tau] \approx \frac{I_o\left(2\pi\sqrt{c_t^2+d_t^2}\right)}{2\pi I_o(\epsilon_t^2)} \frac{I_o\left(2\pi\sqrt{c_r^2+d_r^2}\right)}{2\pi I_o(\epsilon_r^2)} \left(\frac{\cos\left(\frac{2\pi}{\lambda}\beta_{Rm}d_{Rz}^{(q,\tilde{q})} + \frac{\pi\beta_{Rm}R_{d,r}^2}{2d\lambda}\right)}{1 - \left(\frac{R_{d,r}^2\beta_{Rm}}{d\lambda} + \frac{4\beta_{Rm}d_{Rz}^{(q,\tilde{q})}}{\lambda}\right)^2} \right) \\
\left(\frac{\cos\left(\frac{2\pi}{\lambda}\beta_{Tm}d_{Tz}^{(p,\tilde{p})} + \frac{\pi\beta_{Tm}R_{d,t}^2}{2d\lambda}\right)}{1 - \left(\frac{R_{d,t}^2\beta_{Tm}}{d\lambda} + \frac{4\beta_{Tm}d_{Tz}^{(p,\tilde{p})}}{\lambda}\right)^2} \right) \tag{4.16}
$$

The existing 3D cylindrical channel model [85] can become the spacial case of our proposed geometrical channel model. By using the assumption that is the radii are much smaller than the distance d (i.e., $\max\{R_{d,r}, R_{d,t}\} \ll d$) moreover,to avoid keyhole behavior of the wireless channel the distance $d < 4R_{d,t}R_{d,r}Q/(\lambda(P-1)(Q-1))$. Using this assumption the expression (4.16) can be reduced to space time correlation function (34) of [85] for isotropic propagation environments.

$$
\rho_{pq,\tilde{p}\tilde{q}}[\tau] \approx \frac{I_o\left(2\pi\sqrt{c_t^2+d_t^2}\right)}{2\pi I_o(\epsilon_t^2)} \frac{I_o\left(2\pi\sqrt{c_r^2+d_r^2}\right)}{2\pi I_o(\epsilon_r^2)} \frac{\cos\left(\frac{2\pi}{\lambda}\beta_{Rm}d_{Rz}^{(q,\tilde{q})}\right)}{1 - \left(\frac{4\beta_{Rm}d_{Rz}^{(q,\tilde{q})}}{\lambda}\right)^2} \frac{\cos\left(\frac{2\pi}{\lambda}\beta_{Tm}d_{Tz}^{(p,\tilde{p})}\right)}{1 - \left(\frac{4\beta_{Tm}d_{Tz}^{(p,\tilde{p})}}{\lambda}\right)^2} \tag{4.17}
$$

When MSs reside on such highways where the low elevated scattering objects are non isotropically distributed around transmitter and receive. The probability of elevation plane waves can be negligible. In that case the elevation angles β_{R_m}, β_{T_m} can be illuminated in the proposed space time correlation functions (4.16). The resultant expression is the space time correlation function given by Wani *et al.* in [130], which is the special case of the proposed channel model.

$$\rho_{pq,\tilde{p}\tilde{q}}[\tau] \approx \frac{I_o\left(2\pi\sqrt{c_t^2+d_t^2}\right)}{2\pi I_o(\epsilon_t^2)} \frac{I_o\left(2\pi\sqrt{c_r^2+d_r^2}\right)}{2\pi I_o(\epsilon_r^2)} \tag{4.18}$$

The expression (4.18) can be further explored for the space time correlation functions in isotropic scattering environments that is proposed by Pätzold *et al.* [135] by keeping eccentricity $\epsilon_r, \epsilon_t = 1$.

4.5   Results and Description

In this section, The theoretical results obtained from the derived correlation functions (4.15) are described and its impact on the MIMO channel capacity. It can be observed that the derived joint correlation expressions (4.16) is the function of various parameters that are linked with physical MIMO system and the propagation channel environment. For the ease of discussion our focus is mainly on the receive correlation function (4.14), the transmit correlation can be directly obtained by replacing subscript index r with t. In all simulations, a normalized sampling period $f_{R_{max}} T_s = .01$, is used (where $f_{R_{max}}, f_{T_{max}}$ are the maximum Doppler frequencies and T_s is the sampling period). Furthermore, the orientation angle of the antenna arrays, elevation angle of scatterers and other parameters are mentioned on the respective plots for each simulation. Different 2D and 3D plots of the correlations among MIMO channel coefficients are obtained for observation and discussion. The simulation plots of space-time correlation among receive antenna array elements is shown in Fig. 4.3, and 4.4. It is observed from the graph that the correlation decays rapidly in both space and temporal domains by increasing

distance (δ_r) between antenna array elements and normalized time delay. The temporal correlation is dependent on the velocity v_r, AoA/AoD of multipaths, carrier frequency f_c and the speed of light c. Therefore, for the design of MIMO M2M communication system in the rich scattering environment, antenna spacing, and velocity of the MSs are the constraints that have significant impact on the system performance.

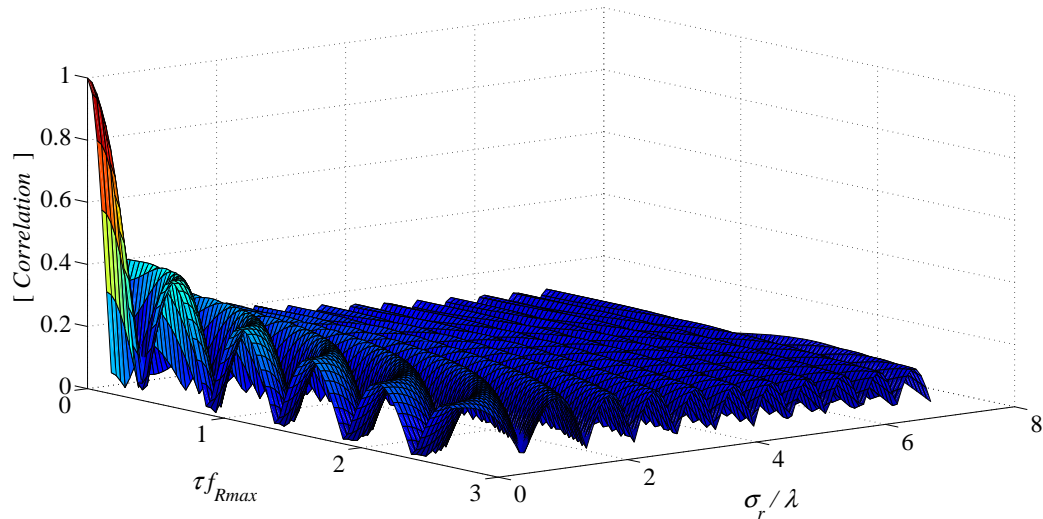FIGURE 4.3: 3D space time correlation function $\rho_r(\delta_r, \tau)$ of 2×2 MIMO M2M channel, $(\beta_r = 20^o, \alpha_r = 60^o, \psi_r = 30^o, \theta_r = 60^o, a_r = 100m, b_r = 50m)$
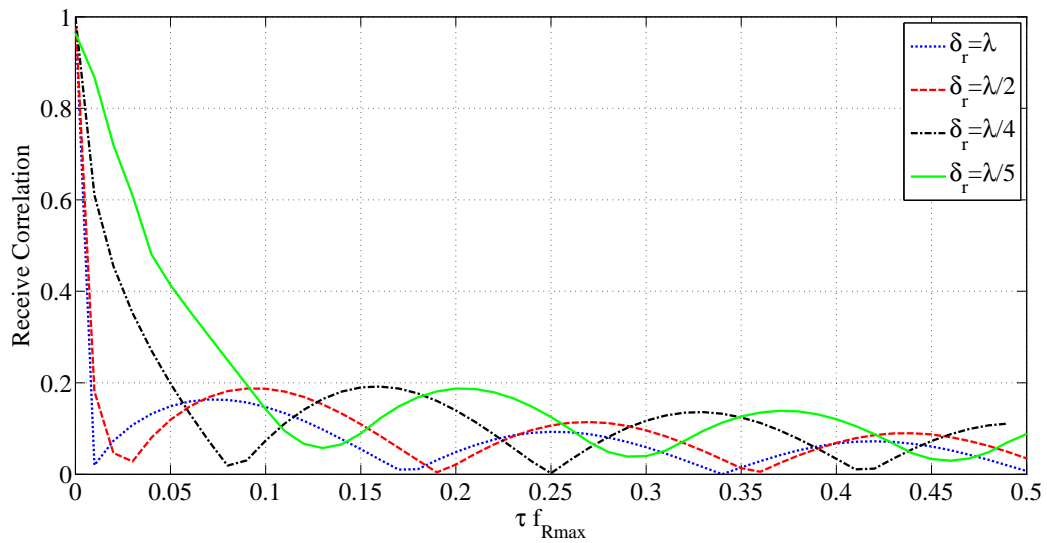

FIGURE 4.4: Effect of spacing between antenna elements on correlation function. The curves are obtained using the parameter $\beta_r = 20^o, \alpha_r = 60^o, \psi_r = 30^o, \theta_r = 60^o, a_r = 100m, b_r = 50m$.

Similarly, the correlations among receive antenna elements are obtained by varying the eccentricity (ϵ_r) of the receiver ellipse as shown in Fig. 4.5. It is observed from the graph that the correlation has a decreasing trend as of eccentricity is decreased from 0.9 (elliptical channel model) to 0 (circle model). This indicates that the capacity is degraded when the mobile units resides in the narrow streets or canyons, similar findings were observed by Abouda *et al.* in [136]. Therefore, for the design and implementation of MIMO M2M communication system for such propagation environments, the simulation results based on elliptical channel model are more appropriate than circular channel model. Correlation among antenna
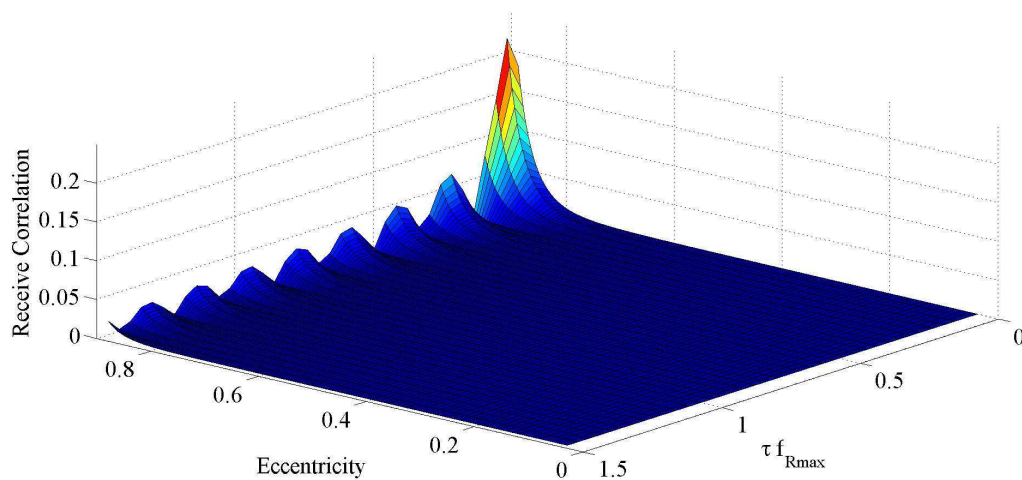
FIGURE 4.5: 3D space time correlation function with respect to eccentricity, $\delta_r = 0.5\lambda, \beta_r = 20^o, \alpha_r = 60^o, \psi_r = 30^o, \theta_r = 60^o$.

elements is also evaluated for different relative velocities of the mobile nodes. It is discerned from the simulation results as shown in Fig. 4.6, that the correlation has a decreasing trend with the increasing relative velocity of the mobile nodes. Similar observations were reported in [137, 138]; however, increasing velocity leads to other severe constraints in the wireless channel that degrade the system throughput.

The proposed 3D channel model is transformed into existing 2D elliptical geometrical channel model [130] and circular geometrical channel model [135] by replacing the elevation angle $\beta_i = 0^o$ and $a_i = b_i$ where, $i = r, t$. In mobile communication environments the subscribers are predominantly on the move in the streets and canyons of urban or suburban areas. The elliptical geometry is appropriate shape, which correlates more closely the layout of such propagation environments than
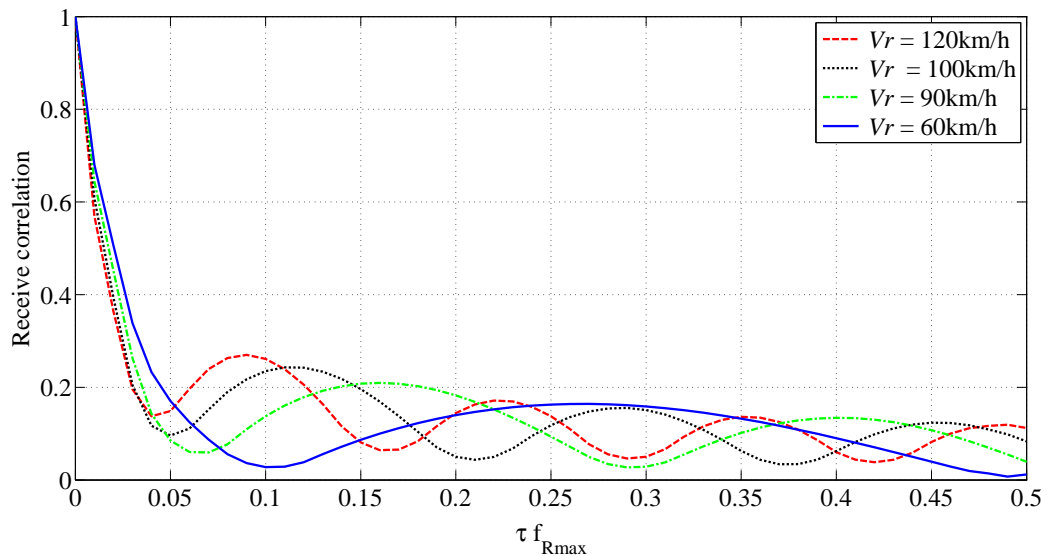
FIGURE 4.6: 2D space-time correlation function for different velocities, $(\delta_r = 0.5\lambda,\ \beta_r = 20^o, \alpha_r = 60^o, \psi_r = 30^o, \theta_r = 60^o, a_r = 100m, b_r = 50m)$

the circular shape. Therefore, the simulation results obtained using elliptical-based geometrical models can provide better understanding of the propagation channel. In MIMO communication systems the capacity of the MIMO system is dependent on the correlations among MIMO links, that in turn depend on the transmit and receiver correlations. Hence, capacity analysis of the MIMO system can be also done on the correlation graph.
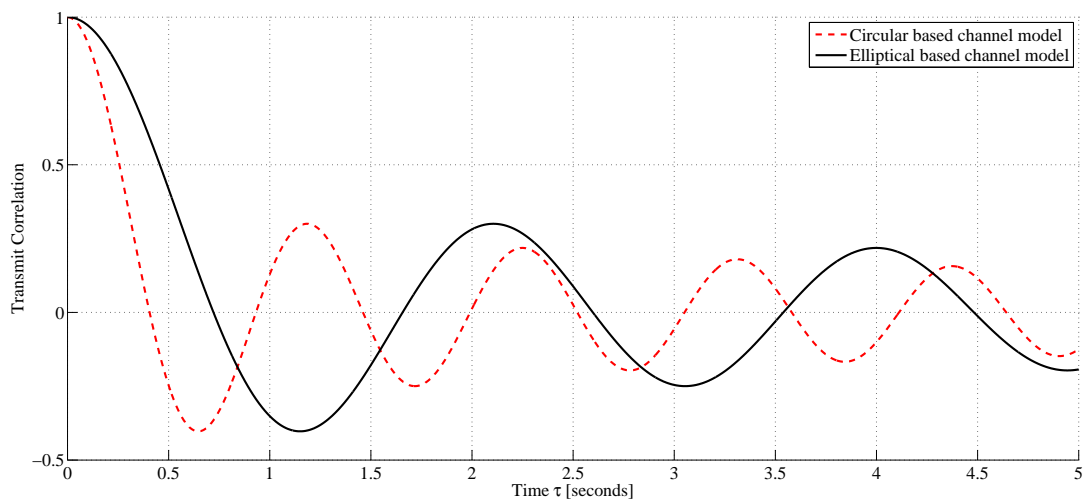
FIGURE 4.7: Comparison of transmit correlation function of circular-based channel model with the elliptical based channel model, $\delta_r = 0.5\lambda,\ \alpha_r = 60^o, f_c = 3MHz, \psi_r = 30^o, \theta_r = 60^o, \beta_r = 20^o$

The simulation results of correlation functions of the deduced 2D geometrical channel model at low carrier frequency is depicted in Fig. 4.7. It is observed from the graph that the transmit correlation using circular-based channel model is lower as compared to elliptical-based channel model. Since, the streets and canyons can be modeled more appropriately using elliptical shape as discussed earlier. Therefore, the simulation results based on the elliptical geometry can predict more appropriately the achievable capacity of MIMO M2M communication systems in streets and canyons.
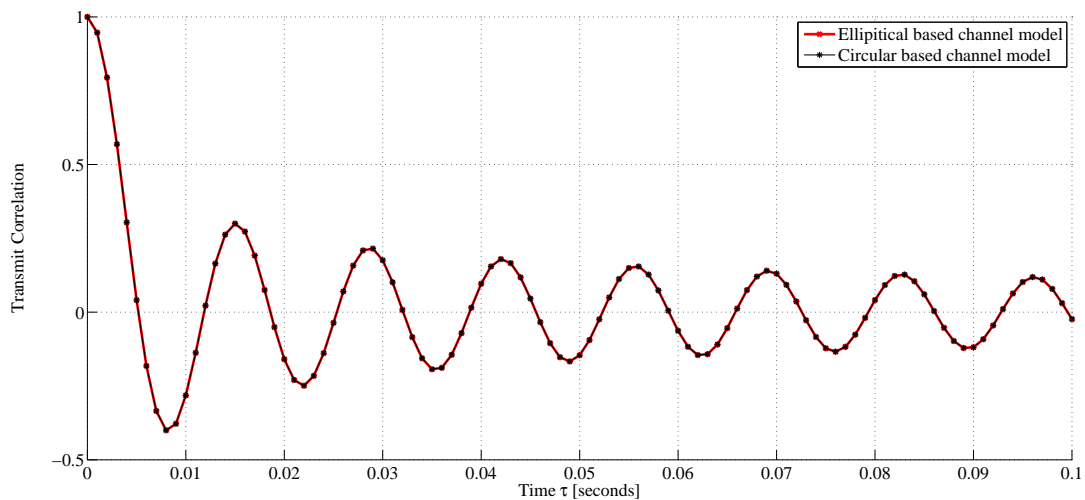
FIGURE 4.8: Comparison of transmit correlation function of circular-based channel model with the elliptical based channel model, $\delta_r = 0.5\lambda$, $\alpha_r = 60^o$, $f_c = 900MHz$, $\psi_r = 30^o$, $\theta_r = 60^o$, $\beta_r = 20^o$

Fig. 4.8, shows the effect of high carrier frequency on the transmit correlation among antenna elements. It is clear from the figure that high carrier frequency shows no effect on the transmit correlation, no matter whether elliptical or circular shape is considered. This implies that geometrical shape does not have prominent effect on the correlation curves at high carrier frequency. Similarly, the similar results are observed for the correlations among the receive antenna elements.

By adjusting the parameters of the proposed model the correlation curves are validated by comparing with the measurement results obtained from experimental campaigns carried out for COST2100 channel model in the outdoor communication environment [1]. It is observed from Fig. 4.9, that the proposed model is in close agreement with the measurement data.
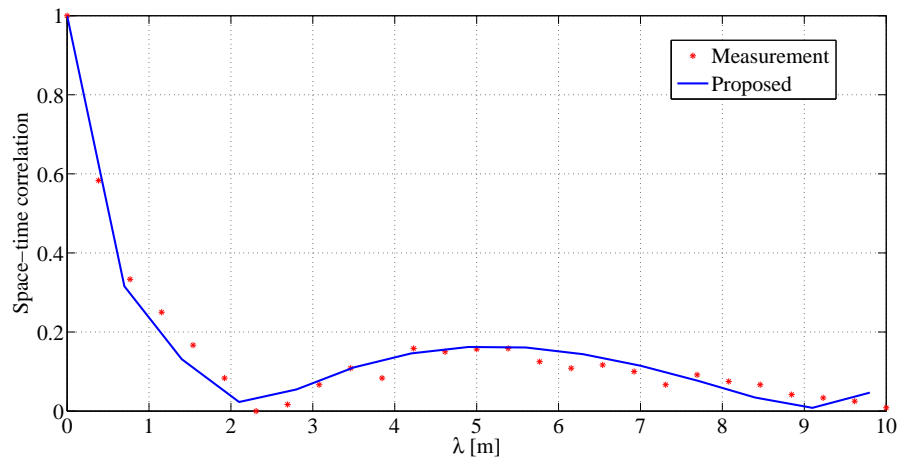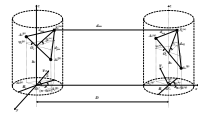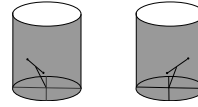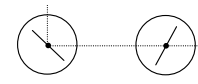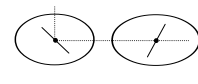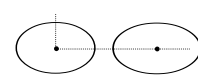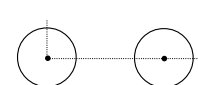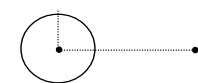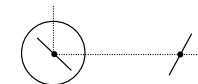
FIGURE 4.9: Comparison of space time correlation function of the proposed
model with the measurement results in [1],

Furthermore, the proposed model is more dynamic in nature, i.e. various other ex-
isting geometrical channel models can become the special cases of it. By adjusting
the appropriate values for $a_i, b_i, \psi_i, \beta_i, \delta_i, (i = t, r)$ parameters in equation (4.16)
of the proposed geometrical channel model. Following 2D and 3D regular shape
geometrical channel models can be deduced from the proposed channel model.

TABLE 4.2: Comparison of the proposed model with the existing 2D and 3D channel models.

Scattering Model	Communication Scenarios	Corresponding Substitutions	Respective Scattering Models	Geometry of Scattering Regions
Proposed	MIMO M2M	-	3D Elliptical-based Cylindrical Model	
Zajić *et al.* [85]	MIMO M2M	$a_r = b_r,\ a_t = b_t$	3D Circular-based Cylindrical Model	
Pätzold *et al.* [135], Stüber *et al.* [139] and Zajić *et al.* [140]	MIMO M2M	$a_t = b_t,\ a_r = b_r,\ \beta_t = \beta_r = 0^o$	2D Circular Model	
Wani *et al.* [130]	MIMO M2M	$a_t \neq b_t,\ a_r \neq b_r,\ \beta_t = \beta_r = 0^o$	2D Elliptical Model	
Baltzis *et al.* [103]	SISO M2M	$a_t \neq b_t,\ a_r \neq b_r,\ \beta_t = \beta_r = 0^o,\ \delta_r = \delta_t = 0$	2D Elliptical Model	
Paul, *et al.* [141]	SISO M2M	$a_t = b_t,\ a_r = b_r,\ \delta_t = \delta_r = \beta_t = \beta_r = 0^o$	2D Circular Model	
Baltzis *et al.* [99]	SISO F2M	$a_r = b_r,\ a_t = b_t = 0,\ \beta_t = \beta_r = \delta_t = \delta_r = f_{T_{max}} = 0^o$	2D Model	
Abidi *et al.* [97]	F2M MIMO	$a_t = b_t,\ a_r = b_r = 0,\ \beta_t = \beta_r = 0^o$	2D Circular Model	

4.6 Conclusion

Geometrical modeling of the mobile communication fading channels has been remained a hot topic in the research arena since the last few decades. Various 2D and 3D geometrical channel models have been proposed in the literature for MIMO M2M communication environments. However, to provide better understanding for the design and performance investigation of the future communication systems, a well designed channel model is required that can provide a deep knowledge of the multipath fading channel statistics. Models available in the literature may be suitable for some specific communication scenarios, but may not be desirable for the fast moving subscribers while they are on a call. Because, these fast moving mobile subscribers predominatingly resides in the streets, canyons and highways of the urban and suburban areas. To model such metropolitan areas, elliptical geometry is better appropriate that provides close statistical analysis of the MIMO M2M communication channel.

In this chapter, an eccentricity based 3D cylindrical geometrical model for MIMO M2M communication scenario is proposed. The geometry of the proposed model is rotatable above x-y plane and its dimensions are adjustable in all axes corresponds to the physical propagation scenario. Based on the proposed model, the expressions of joint and marginal correlation functions among transmitter and receiver antenna array elements are formulated. The resultant correlation function is converted into space-time correlation function of circular-based cylindrical channel model and 2D elliptical based channel models. The expression of correlation function is simulated by changing various parameters and obtained correlation results are meticulously described. Moreover, for the validation of proposed model, correlation results are compared with the measurement data, which shows a close agreement. Furthermore, different existing 2D and 3D geometrical channel models can be obtained by varying few of the channel parameters.

Chapter 5

Geometrical Modeling of Scattering Environment For Highways in Umbrella Cell Based MIMO Communication Systems

This chapter presents a 3D elliptic cylindrical geometrical channel model for scattering environment under the umbrella-cell. Section 5.1 provides brief introduction and importance of the umbrella cell. Section 5.2 describes the system model of the proposed geometrical channel model. The Section 5.3 and Section 5.4 provides the details of mathematical derivation of the space-time correlation function. Section 5.5 describes theoretical results of the obtained space-time correlation function and finally, Section 5.6 provides summary of the chapter.

5.1 Introduction

F2M communication systems have been growing tremendously since the last few decades, because of its potential of facilitating communication links between machines, robots, aircrafts, ships and automobiles, etc. Cellular mobile communication (CMC) system is one of the applications of F2M communication systems. Where, a fixed base station (BS) is mounted with a high elevated scatterer-free antenna whereas, MSs are mounted with low elevated antennas and are usually located in the rich scattering regions [142]. Because of the marvelous applications of CMC, the number of mobile subscribers has shown exponential increasing trend in the recent years. Moreover, each mobile subscriber demands discriminate features like multimedia applications, live video streaming, internet access and other data-hungry applications that forces the system to increase its spectral efficiency and link performance. In CMC systems, capacity (in terms of number of subscribers) [143] can be increased by sub-dividing larger cells into the smaller ones like microcells, picocells, or femtocells [5, 144]. On one hand, smaller cell size enhances the system capacity but on the other hand, it increases rate of occurrence of handoff [42]. In the fast moving communication scenario, these frequent handoff phenomena increase burden on the MSC and decrease the spectrum efficiency [44]. To overcome this handoff problem, fast moving subscribers are handed over to an umbrella cell while they are on call. Moreover, multiple antennas on both sides of the communication link can fulfill the data-rate demands of each mobile subscriber as long as the array elements are spatially uncorrelated [127]. Therefore, for the beneficial design of an umbrella cell, depth knowledge of the propagation channel between the BS and MS is extremely important. Various approaches like deterministic, stochastic and geometrical-based channel modeling approaches have been published in the literature to analyze the statistics of propagation channel [145, 146]. As discussed in previous chapters that elliptical geometry has more similarity with the layout of streets, canyons and express ways, where usually mobile subscribers reside. An elliptical geometrical shape is more suitable to model the scattering environment along the highways. The high-rise scattering objects along

the highways like buildings, mountains, and trees are modeled using the elliptical-based cylindrical shape. The elevated walls of the cylinder represent these elevated scatterers. Furthermore, higher data rate can be achieved using multiple antenna array system on each end of the communication link.

5.2   System Model

This section presents a detailed description of the system model of the proposed fixed-to-mobile (F2M) MIMO elliptical-based cylindrical geometrical channel model for umbrella-cell as shown in Fig. 5.1. In this proposed, channel model the mobile subscriber is supposed to be located at the center of elliptical cylinder holding low elevated antenna array and the base BS is located on the top of tower of height h_t, fixed with multiple antenna array structure. The eccentricity ϵ_r models the azimuth dimensions of the elliptical scattering region around the MS ; whereas, the height h_r of the elliptical cylinder models its elevation. The BS and MS are equipped with P and Q number of antenna array elements respectively, for the sake of simplicity, we take $P = Q = 2$, however, the results can be derived for any configuration. The antenna array elements of BS and MS are symbolized as $A_t^{(p)}$ and $A_r^{(q)}$, and spacings between them are denoted by δ_t and δ_r, respectively. The MS is assumed to be located at $(0, 0, 0)$ and BS $(D, 0, 0)$, at an arbitrary time instant, in the Cartesian coordinate system, and the azimuth distance between the center of cylinder to base-station is denoted by D. Moreover it is also assumed that the MS is moving with the speed of v_r in the direction of γ_r. The description of other variables used in the proposed geometry are listed in Table 5.1.

5.3   Derivation of Channel Parameters

The derivation of the space-time correlation among MIMO antenna elements is based on the reference system model depicted in Fig. 5.1. The multipath signals are arrived at $A_t^{(p,\tilde{p})}$ from $A_r^{(q,\tilde{q})}$ via striking at the scattering point $S_r^{(n)}$ that is

TABLE 5.1: Notations of various channel parameters used in the system model.

Symbols	Description.
$R_{d,r}$	The variable radius of the receiver ellipses.
$A_t^{(p)}$, $A_r^{(q)}$	Antenna array elements at BS and MS, respectively.
$S_r^{(n)}$	Represents the n-th scatter located on the surface of elliptic cylinder.
δ_t	The spacing between p-th and $\tilde{p}$-th antenna elements at Tx.
δ_r	The spacing between q-th and $\tilde{q}$-th antenna elements at Rx.
$\theta_r^{(q)}, \theta_t^{(p)}$	The azimuth angle of q-th receive and p-th transmit antenna element with respect to x-axis, respectively.
$\psi_r^{(q)}, \psi_t^{(p)}$	The elevation angle of q-th receive and p-th transmit antenna element with respect to x-y plane, respectively.
v_r	Velocities of the MS.
γ_r	The moving direction of the MS.
$\alpha_r^{(n)}, \beta_r^{(n)}$	AoA of multipath in azimuth and elevation plane respectively.
d_{max}^{pq}	The distance between p-th antenna element to q-th antenna element, $d_{qn} + d_{np}$.
$d_{max}^{\tilde{p}\tilde{q}}$	The distance between $\tilde{p}$-th antenna element to $\tilde{q}$-th antenna element, $d_{\tilde{q}n} + d_{n\tilde{p}}$.
a_r, b_r	Represents the major and minor axes of ellipse respectively.
ϵ_r	Represents the eccentricity of the ellipse surrounding the MS.

situated at the surface of elliptical cylinder. The phase change due to the distance traveled by the signal can be written as $(2\pi/\lambda)d_{max}^{pq}$ and $(2\pi/\lambda)d_{max}^{\tilde{p}\tilde{q}}$, where $2\pi/\lambda$ is called wavenumber. The signals channel gain and phase shift due to the collision of the signal with $S_r^{(n)}$ can be written as $1/\sqrt{N}$ and ω_n, respectively. Phase change also occur due to the motion of MS and can be expressed as $2\pi f_{Rmax}\cos(\alpha_r^{(n)} - \gamma_r)\cos\beta_r^{(n)}t$, where, $f_{Rmax} = v_r/\lambda$ represents the maximum Doppler frequency caused by the motion of receiver mobile node. It is also assumed that both antenna element spacing δ_t, δ_r are much smaller than b_r. The AoA in azimuth plane and elevation plane are assumed to be random variable and independent of each other [147]. Moreover, ω_n is also supposed to be a random variable that is uniformly distributed over $[-\pi, \pi]$ and is also independent from AoA. Furthermore, for the ease of derivation of the space-time correlation among MIMO antenna arrays of the proposed channel model, the following valid assumptions are considered:

1. The proposed eccentricity-based channel model is assumed to be a single-bounced.

FIGURE 5.1: The proposed elliptical-based cylindrical channel model for umbrella cell in macrocellular communication environment.

2. Infinity number of scattering points are uniformly distributed on the surface of the elliptical cylindrical geometry.

3. Uniform power is reflected from all scatterers.

4. The MS is surrounded by stationary scattering points.

5. Each scatterer behaves as an omni-directional source.

Finally, with the help of above assumptions, the diffused components of the transmission link from $A_t^{(p)}$ to $A_r^{(q)}$ can be expressed as,

$$h_{pq}(t) = \lim_{N \to \infty} \frac{1}{\sqrt{N}} \sum_{n=1}^{N} e^{-j\frac{2\pi}{\lambda}(d_{qn}+d_{np})+j\omega_n} \times e^{j2\pi t f_{Rmax}\cos(\alpha_R^{(n)}-\gamma_r)\cos\beta_r^{(n)}} \qquad (5.1)$$

The distances d_{qn}, $d_{\tilde{q}n}$, d_{np} and $d_{n\tilde{p}}$ are obtained by solving the geometry of the proposed model as shown in Fig. 5.1. The 3D polar coordinates of qth receive antenna element and pth transmit antenna element are denoted by $\left(d_{R_x}^{(q)}, d_{R_y}^{(q)}, d_{R_z}^{(q)}\right)$ and $\left(d_{T_x}^{(p)}, d_{T_y}^{(p)}, d_{T_z}^{(p)}\right)$, respectively. Where, $d_{Rx}^{(q)} = \delta_r \cos\theta_r^{(q)} \cos\psi_r^{(q)}$, $d_{Ry}^{(q)} = \delta_r \sin\theta_r^{(q)} \cos\psi_r^{(q)}$, $d_{Rz}^{(q)} = \delta_r \sin\psi_r^{(q)}$, $d_{Tx}^{(p)} = \delta_t \cos\theta_t^{(p)} \cos\psi_t^{(p)}$, $d_{Ty}^{(p)} = \delta_t \sin\theta_t^{(p)} \cos\psi_t^{(p)}$, $d_{Tz}^{(p)} = \delta_t \sin\psi_t^{(p)}$. Similarly, the coordinates of nth scatterer in 3D space is denoted by $\left(d_{R_x}^{(n \ or \ \tilde{n})}, d_{R_y}^{(n \ or \ \tilde{n})}, d_{R_z}^{(n \ or \ \tilde{n})}\right)$, where $d_{R_x^{(n \ or \ \tilde{n})}} = R_{d,r} \cos\alpha_r^{(n \ or \ \tilde{n})}$, $d_{R_y^{(n \ or \ \tilde{n})}} = R_{d,r} \sin\alpha_r^{(n \ or \ \tilde{n})}$, $d_{R_z^{(n \ or \ \tilde{n})}} = R_{d,r} \tan\beta_r^{(n \ or \ \tilde{n})}$.

These polar coordinates depend upon the orientation and configuration of the antenna arrays. Moreover, the variable radios $R_{d,r}$ of and receive ellipse can be written in terms of minor b_r and major a_r axes as, $a_r b_r / \sqrt{a_r^2 \sin^2\alpha_r + b_r^2 \cos_r^2\alpha_r}$ [129]. Using the distance formula, and binomial approximation $\sqrt{(1+x)} \approx 1+x/2$ if $(x \ll 1)$, the approximated distances can be expressed as,

$$d_{pn} \approx \frac{R_{d,r}}{\cos\beta_r^{(n)}} - \delta_r \sin\psi_r^{(p)} \sin\beta_r^{(n)} - \delta_r \cos\theta_r^{(q)} \cos\psi_r^{(q)} \cos\alpha_r^{(n)} \cos\beta_r^{(n)}$$
$$-\delta_r \sin\theta_r^{(q)} \cos\psi_r^{(q)} \sin\alpha_r^{(n)} \cos\beta_r^{(n)} \tag{5.2}$$

$$d_{nq} \approx D + \frac{\delta_t^2}{2D} + \frac{h_t^2}{2D} + \frac{R_{d,r}^2 \sec^2\beta_r^{(n)}}{2D} - \frac{\delta_t R_{d,r} \tan\beta_r^{(n)} \sin\psi_t}{D} + \delta_t \cos\psi_t^{(p)} \cos\theta_t^{(p)}$$
$$-R_{d,r} \cos\alpha_r^{(n)} - \frac{\delta_t R_{d,r} \cos\alpha_r^{(n)} \cos\theta_t^{(p)} \cos\psi_t^{(p)}}{D} + \frac{h_t R_{d,r} \sin\theta_t^{(p)} \cos\psi_t^{(p)}}{D}$$
$$-\frac{h_t R_{d,r} \sin\alpha_r^{(n)}}{D} - \frac{\delta_t R_{d,r} \sin\alpha_r^{(n)} \sin\phi_t^{(p)} \cos\psi_t^{(p)}}{D} \tag{5.3}$$

The distances $d_{\tilde{q}n}$ and $d_{n\tilde{p}}$ can be also obtained using the same geometry. Furthermore, for the ease of understanding and avoiding complexity, equation (5.1) can be rewritten as,

$$h_{pq}(t) \approx \lim_{N \to \infty} \frac{1}{\sqrt{N}} \sum_{n=1}^{N} G_{rt} e^{j2\pi t f_{Rmax} \cos(\alpha_R^{(n)} - \gamma_r) \cos\beta_r^{(n)}} \tag{5.4}$$

where, $G_{rt} = e^{-j\frac{2\pi}{\lambda}(d_{pn}+d_{nq})}$.

5.4   Derivation of the Correlation function

The normalized space-time correlation function between diffused channel coefficients $h_{pq}(t)$ and $h_{\tilde{p}\tilde{q}}(t)$ for the proposed 3D MIMO F2M non-isotropic scattering propagation environment can be obtained using the following relation given in [85, 88],

$$\rho_{pq,\tilde{p}\tilde{q}}(\tau) = \frac{E\{h_{pq}(t)h_{\tilde{p}\tilde{q}}^*(t+\tau)\}}{\sqrt{E\{|h_{pq}(t)|\}^2 E\{|h_{\tilde{p}\tilde{q}}(t)|\}^2}} \tag{5.5}$$

where, $E\{\cdot\}$ is the statistical expectation operator and can be applied to all random variables, $(\cdot)^*$ symbolizes the complex conjugate operation and $p, \tilde{p} \in \{1,...,P\}$, $q, \tilde{q} \in \{1,...,Q\}$. Using equation 5.5 and 5.4 the expression for the space-time correlation function can be written as,

$$\rho_{pq,\tilde{p}\tilde{q}}(\delta_r, \delta_t, \tau) = \lim_{N\to\infty} \frac{1}{N}\sum_{n=1}^{N} G_{rt}G_{rt}^* e^{j2\pi\tau f_{Rmax}\cos(\alpha_R^{(n)}-\gamma_r)\cos\beta_r^{(n)}} \tag{5.6}$$

In cellular networks, the fast moving vehicles are usually present in the streets, canyons and on the highways. The distribution of the AoA in such regions depend on the scattering objects like vegetation, buildings and side-barrier walls, etc., present along the roadside premises. Consequently, we can assume that infinity high-rise scattering objects are present around the MS, which implies that the discrete scattering distributions may be transformed to a continuous scattering distributions that in turn forces us to change the discrete random variables $\alpha_r^{(n)}$ and $\beta_r^{(n)}$ into continuous random variables α_r and β_r, respectively. Furthermore, we assume that azimuth and elevation angles are independent of each other; therefore, the joint PDF of AoA at MS $f(\alpha_r, \beta_r)$ can be written in product form as $f(\alpha_r)f(\beta_r)$, where, $f(\alpha_r)$ and $f(\beta_r)$ are the PDF of AoA in azimuth plane and elevation plane respectively. Therefore, the equation (5.6) can be written in integration form as,

$$\rho_{pq,\tilde{p}\tilde{q}}(\delta_r, \delta_t, \tau) \approx \int_{-\beta_{R_m}}^{\beta_{R_m}} \int_{-\pi}^{\pi} e^{-2j\pi\tau(f_{Tmax}\cos(\alpha_r - \gamma_r)\cos\beta_r)}$$

$$\times e^{\frac{j2\pi}{\lambda}\left(d_{Rx}^{(q,\tilde{q})}\cos\alpha_r \cos\beta_r + \frac{R_{d,r}d_{Tx}^{(p,\tilde{p})}}{D}\cos\alpha_r\right)} e^{\frac{j2\pi}{\lambda}\left(d_{Ry}^{(q,\tilde{q})}\sin\alpha_r \cos\beta_r + \frac{R_{d,r}d_{Ty}^{(p,\tilde{p})}}{D}\sin\alpha_r\right)}$$

$$e^{\frac{j2\pi}{\lambda}\left(d_{Rz}^{(q,\tilde{q})}\sin\beta_r + \frac{R_{d,r}d_{Tz}^{(p,\tilde{p})}\tan\beta_r}{D} + \frac{R_{d,r}^2 \sec^2\beta_r}{2D}\right)} f(\alpha_r)f(\beta_r)\mathrm{d}\alpha_r \mathrm{d}\beta_r$$

$$(5.7)$$

where, $d_{Rx}^{(q,\tilde{q})} = d_{Rx}^{(q)} - d_{Rx}^{(\tilde{q})}$, $d_{Ry}^{(q,\tilde{q})} = d_{Ry}^{(q)} - d_{Ry}^{(\tilde{q})}$, $d_{Rz}^{(q,\tilde{q})} = d_{Rz}^{(q)} - d_{Rz}^{(\tilde{q})}$, $d_{Tx}^{(p,\tilde{p})} = d_{Tx}^{(p)} - d_{Tx}^{(\tilde{p})}$, $d_{Ty}^{(p,\tilde{p})} = d_{Ty}^{(p)} - d_{Ty}^{(\tilde{p})}$, $d_{Tz}^{(p,\tilde{p})} = d_{Tz}^{(p)} - d_{Tz}^{(\tilde{p})}$, and β_{R_m} is the maximum elevation AoA of the scatterers causes at the MS. To describe isotropic and non-isotropic scattering environments, various distributions have been proposed in the literature for AoA/AoD [6, 88, 148]. In urban or suburban areas the physical layouts of the streets, canyons and highways in the azimuth plane resemble elliptical shapes. Thus the roadside scatterers can be modeled non-isotropically distributed. Hence, eccentricity-based modified von Mises distribution proposed in [130], is more appropriate for such nonisotropic scattering environments to model azimuth AoA/AoD. The expression of PDF of azimuth AoA/AoD at MS is, $p(\alpha_r) = \frac{1}{2\pi I_0(\epsilon_r^2)}e^{\epsilon_r^2 \cos\alpha_r}$, where, $\epsilon_r = \sqrt{1 - b_r^2/a_r^2}$, the azimuth angle $\alpha_r \in [-\pi, \pi]$ and $I_0(\cdot)$ is the zeroth-order modified Bessel function of the first kind. Similarly, different scattering distributions have been also proposed in the literature for elevation AoA [88, 123]. In addition, Parsons *et al.* in [132] proposed PDF of elevation AoA $f(\beta_r) = \frac{\pi}{4\beta_{r_m}}\cos\left(\frac{\pi}{2}\frac{\beta_r}{\beta_{r_m}}\right)$, where, the absolute values of elevation angles β_{r_m} lie in the range $0^0 \leq \beta_{r_m} \leq 20^0$ [131].

$$\rho_{pq,\tilde{p}\tilde{q}}(\delta_r, \delta_t, \tau) = \frac{1}{2\pi I_0(\epsilon_r^2)} \int_{-\beta_{R_m}}^{\beta_{R_m}} \int_{-\pi}^{\pi} e^{-2j\pi\tau\left(f_{Rmax}(\cos\alpha_r \cos\gamma_r \cos\beta_r + \sin\alpha_r \sin\gamma_r \cos\beta_r)\right)}$$

$$\times e^{\frac{j2\pi}{\lambda}\left(d_{Rx}^{(q,\tilde{q})}\cos\alpha_r \cos\beta_r + \frac{R_{d,r}d_{Tx}^{(p,\tilde{p})}}{D}\cos\alpha_r\right)} e^{\frac{j2\pi}{\lambda}\left(d_{Ry}^{(q,\tilde{q})}\sin\alpha_r \cos\beta_r + \frac{R_{d,r}d_{Ty}^{(p,\tilde{p})}}{D}\sin\alpha_r\right)}$$

$$e^{\frac{j2\pi}{\lambda}\left(d_{Rz}^{(q,\tilde{q})}\sin\beta_r + \frac{R_{d,r}d_{Tz}^{(p,\tilde{p})}\tan\beta_r}{D} + \frac{R_{d,r}^2 \sec^2\beta_r}{2D}\right)} e^{\epsilon_r^2 \cos\alpha_r} \frac{\pi}{4\beta_{R_m}}\cos\left(\frac{\pi}{2}\frac{\beta_r}{\beta_{R_m}}\right)\mathrm{d}\alpha_r \mathrm{d}\beta_r$$

$$(5.8)$$

The integration in (5.8) lacks the closed-form solution for the space-time correlation functions among the MIMO antenna elements. Hence, we integrate this equation numerically by using small angle approximation i.e., $\sin\beta_r \approx \beta_r$, $\cos\beta_r \approx 1$, $\sec^2\beta_r = 1 + \beta_r/2$. This assumption of small elevation angles is valid for the proposed model because the distance between the MS and BS is much larger than the antenna heights. By incorporating these approximations, we get the following expression,

$$\rho_{pq,\tilde{p}\tilde{q}}(\delta_r, \delta_t, \tau) \approx \frac{1}{2\pi I_0(\epsilon_r^2)} \int_{-\beta_{R_m}}^{\beta_{R_m}} \int_{-\pi}^{\pi} e^{-2j\pi\tau \left(f_{Tmax}(\cos\alpha_r \cos\gamma_r + \sin\alpha_r \sin\gamma_r) \right)}$$

$$\times e^{\frac{j2\pi}{\lambda}\left(d_{R_x}^{(q,\tilde{q})} \cos\alpha_r + \frac{R_{d,r}d_{Tx}^{(p,\tilde{p})}}{D} \cos\alpha_r \right)} e^{\frac{j2\pi}{\lambda}\left(d_{R_y}^{(q,\tilde{q})} \sin\alpha_r + \frac{R_{d,r}d_{Ty}^{(p,\tilde{p})}}{D} \sin\alpha_r \right)}$$

$$e^{\frac{j2\pi}{\lambda}\left(d_{R_z}^{(q,\tilde{q})} \beta_r + \frac{R_{d,r}d_{Tz}^{(p,\tilde{p})}\beta_r}{D} + \frac{R_{d,r}^2 \beta_r}{4D} \right)} e^{\epsilon_r^2 \cos\alpha_r} \frac{\pi}{4\beta_{R_m}} \cos\left(\frac{\pi}{2}\frac{\beta_r}{\beta_{R_m}} \right) \mathrm{d}\alpha_r \mathrm{d}\beta_r \tag{5.9}$$

The above integrations for variables α_r and β_r can be written separately as,

$$\rho_{pq,\tilde{p}\tilde{q}}(\delta_r, \delta_t, \tau) \approx \frac{1}{2\pi I_0(\epsilon_r^2)} \int_{-\pi}^{\pi} e^{-2j\pi\tau \left(f_{Rmax}(\cos\alpha_r \cos\gamma_r + \sin\alpha_r \sin\gamma_r) \right)}$$

$$\times e^{\frac{j2\pi}{\lambda}\left(d_{R_x}^{(q,\tilde{q})} + \frac{R_{d,r}d_{Tx}^{(p,\tilde{p})}}{D} + \epsilon_r^2 \right) \cos\alpha_r} e^{\frac{j2\pi}{\lambda}\left(d_{R_y}^{(q,\tilde{q})} + \frac{R_{d,r}d_{Ty}^{(p,\tilde{p})}}{D} \right) \sin\alpha_r} \mathrm{d}\alpha_r$$

$$\int_{-\beta_{R_m}}^{\beta_{R_m}} e^{\frac{j2\pi\beta_r}{\lambda}\left(d_{R_z}^{(q,\tilde{q})} + \frac{R_{d,r}d_{Tz}^{(p,\tilde{p})}}{D} + \frac{R_{d,r}^2}{4D} \right)} \frac{\pi}{4\beta_{R_m}} \cos\left(\frac{\pi}{2}\frac{\beta_r}{\beta_{R_m}} \right) \mathrm{d}\beta_r \tag{5.10}$$

By substituting, $x_1 = \frac{j2\pi}{\lambda}\left(d_{R_x}^{(q,\tilde{q})} + \frac{R_{d,r}d_{Tx}^{(p,\tilde{p})}}{D} \right) - 2j\pi\tau f_{Rmax} \cos\gamma_r + \epsilon_r^2$, $x_2 = \frac{j2\pi}{\lambda}\left(d_{R_y}^{(q,\tilde{q})} + \frac{R_{d,r}d_{Ty}^{(p,\tilde{p})}}{D} \right) - 2j\pi\tau f_{Rmax} \sin\gamma_r$, $x_3 = \frac{j2\pi}{\lambda}\left(d_{R_z}^{(q,\tilde{q})} + \frac{R_{d,r}d_{Tz}^{(p,\tilde{p})}}{D} + \frac{R_{d,r}^2}{4D} \right)$ in (5.10), we get the following expression,

$$\rho_{pq,\tilde{p}\tilde{q}}(\delta_r, \delta_t, \tau) \approx \frac{1}{2\pi I_0(\epsilon_r^2)} \int_{-\pi}^{\pi} e^{x_1 \cos\alpha_r + x_2 \sin\alpha_r} \mathrm{d}\alpha_r \int_{-\beta_{R_m}}^{\beta_{R_m}} e^{x_3 \beta_r} \frac{\pi}{4\beta_{R_m}} \cos\left(\frac{\pi}{2}\frac{\beta_r}{\beta_{R_m}} \right) \mathrm{d}\beta_r \tag{5.11}$$

Equation (5.11) can be written in simplified form by using Bessel function notations given in [119],

$$\rho_{pq,\tilde{p}\tilde{q}}(\delta_r, \delta_t, \tau) \approx \frac{I_o\left(\sqrt{x_1^2 + x_2^2}\right)}{I_0(\epsilon_r^2)} \frac{\cos(\frac{2\pi}{\lambda}\beta_{Rm}x_3)}{\left[1 - (\frac{4\beta_{Rm}x_3}{\lambda})^2\right]} \qquad (5.12)$$

5.5 Results and Description

In this section, the theoretical results of the space-time correlation function are presented and elaborate the impact of various channel parameters on the correlations among MIMO antenna elements. It is observed that the derived expression (5.12) is the function of various model parameters and physical dimensions of the propagation channel. The values of the parameters used in plotting different curves of space-time correlations are mentioned in the caption of each plot. A normalized sampling period (step size) $f_{R_{max}}T_s = .01$, is used for plotting the curves. Various 2D and 3D plots of the correlations among MIMO antenna elements are presented for discussion and observation.

The correlations among MIMO antenna elements shown in Fig. 5.2, 5.3, 5.4, and 5.5, are plotted against the orientation of antenna arrays in the azimuth and elevation planes. The plot depicted in Fig. 5.2, shows clearly that the correlation is maximum when the elevation angles of any antennas is set at 0° or 180°, and the correlations show a decreasing trend with the increase in elevation angle of any the antenna from 0° to 90°. Therefore, for the design of an umbrella cell in cellular mobile communication, antenna orientation has significant impact on the system performance.

The proposed elliptical cylindrical channel model is generic in nature and can be reduced to cylindrical model proposed by Liu Feng *et al.* in [2] by keeping eccentricity $\epsilon_r = 0$ and distance D= 5km. The joint correlation graph is plotted against elevation angles of transmit and receive antenna arrays, shown in Fig. 5.3. Resultant plot is well matched with the correlation plot given in [2]. This implies
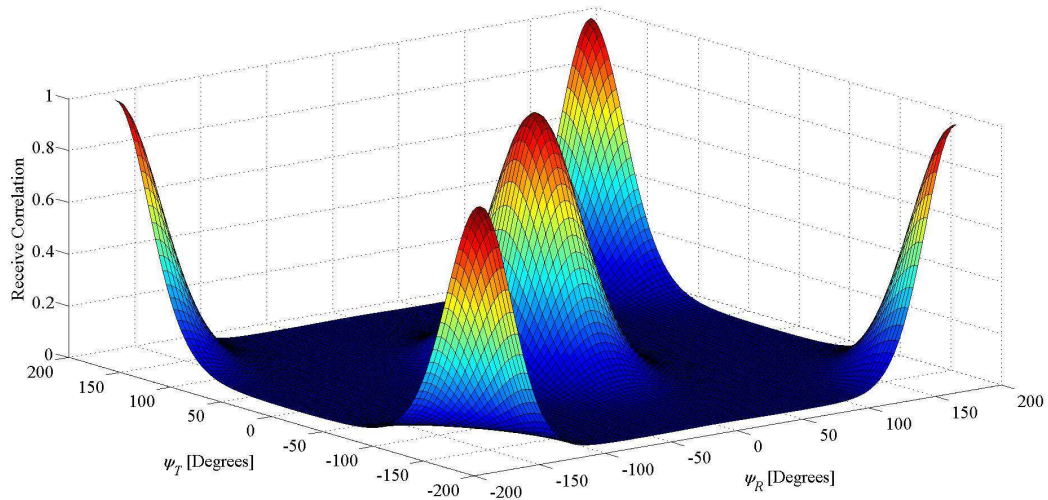
FIGURE 5.2: 3D space time correlation function with respect elevation angles of transmit and receive antenna arrays, $(\delta_r = \delta_t = \lambda/2, \beta_r = 20^o$, $\alpha_r = \pi/4, \psi_r = 30^o, \theta_r = \theta_t = 2\pi/3, a_r = 500m, b_r = 200m)$
.
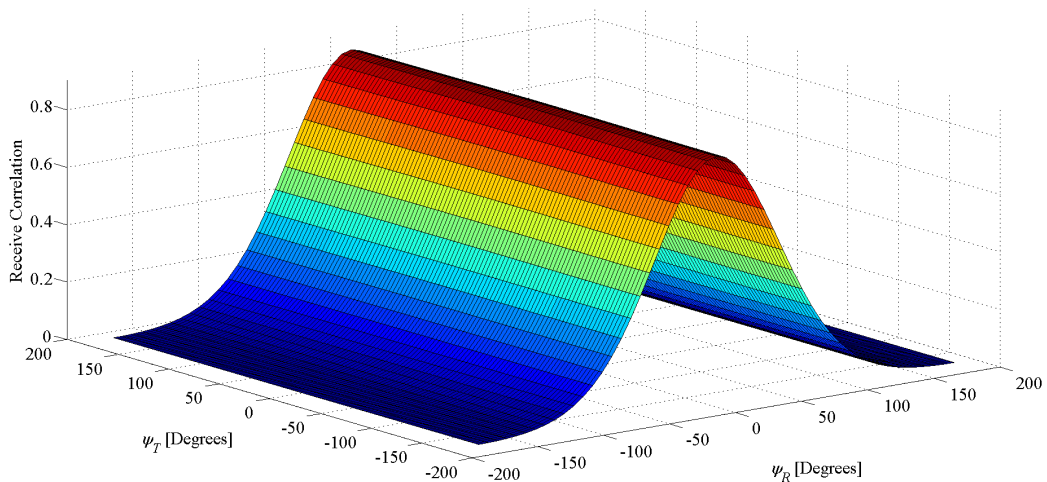
FIGURE 5.3: Receive correlation with respect to elevation angles of transmit and receive antenna arrays [2], $\delta_r = \delta_t = \lambda/2, \beta_r = 20^o, \alpha_r = \pi/4, \theta_r$ $= \theta_t = 2\pi/3, a_r = b_r = 100m, D = 5km$
.

that the channel model given in [2] is the special case of our proposed channel model.

Similarly, 3D plot shown in Fig. 5.4, of joint space-time correlation function is taken against azimuth AoA , and its 2D slices are plotted in Fig. 5.5(a), and 5.5(b). It is observed from the plots that the correlation among the MIMO antenna array elements are dependent on the PDF of AoA (α_r) in azimuth plane of the
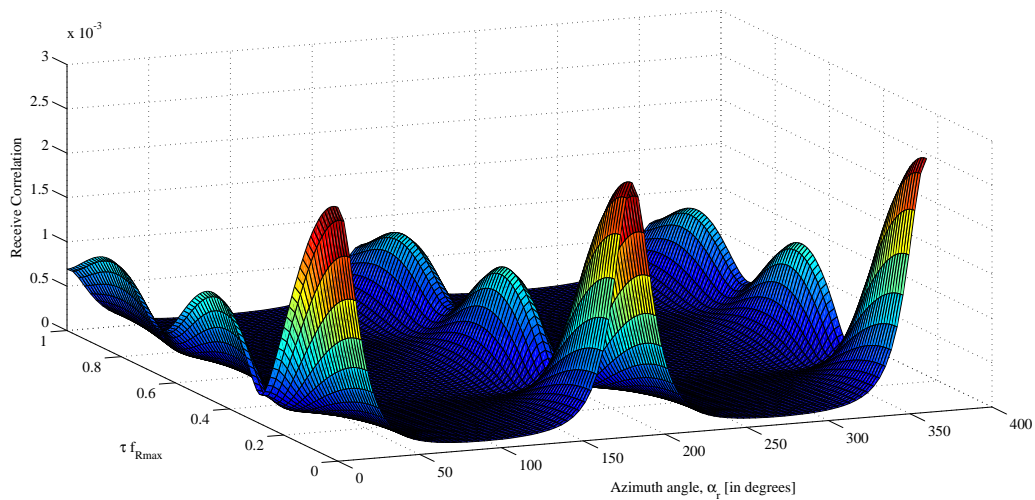
FIGURE 5.4: Joint space-time correlation function of azimuth AoA and normalized time delay ($\delta_r = \delta_t = \lambda/2, \beta_r = 20^o, \psi_r = 30^o, \theta_r = \theta_t = 2\pi/3,$ $a_r = b_r = 100m$).
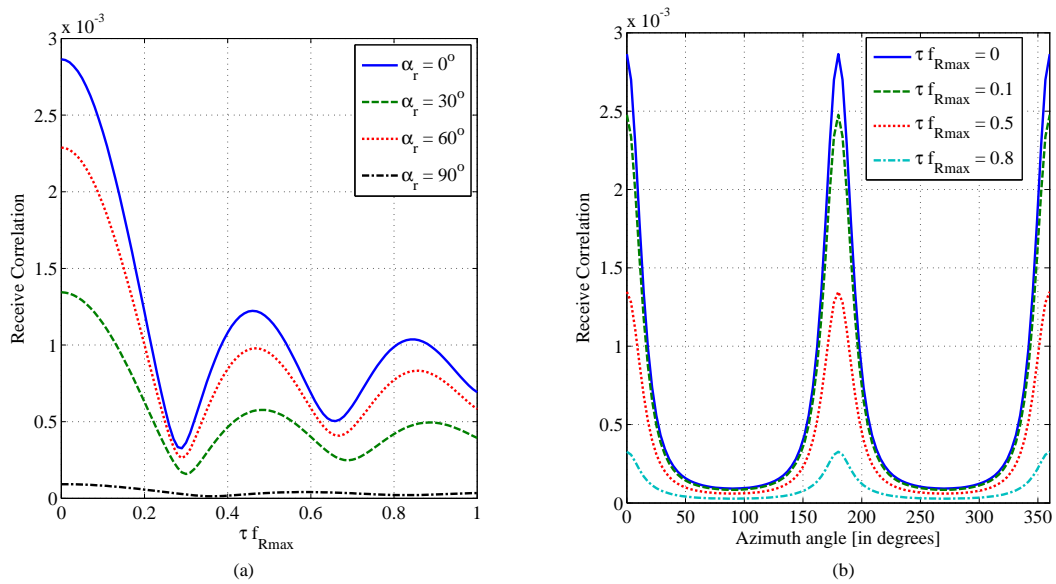
FIGURE 5.5: 2D space time correlation function with respect azimuth AoA, ($\delta_r = \delta_t = \lambda/2, \beta_r = 20^o, \psi_r = 30^o, \theta_r = \theta_t = 2\pi/3, a_r = b_r = 100m$)

nonisotropic scattering environments; a similar observation was reported in [149, 150].

The antenna spacing is another most important system parameter that has significant effect on the correlations among the MIMO antenna elements [32, 40]. The graph shown in Fig. 5.6, demonstrates the effect of antenna spacing on antenna correlations. It is seen as the spacing is increased, the correlation shows a
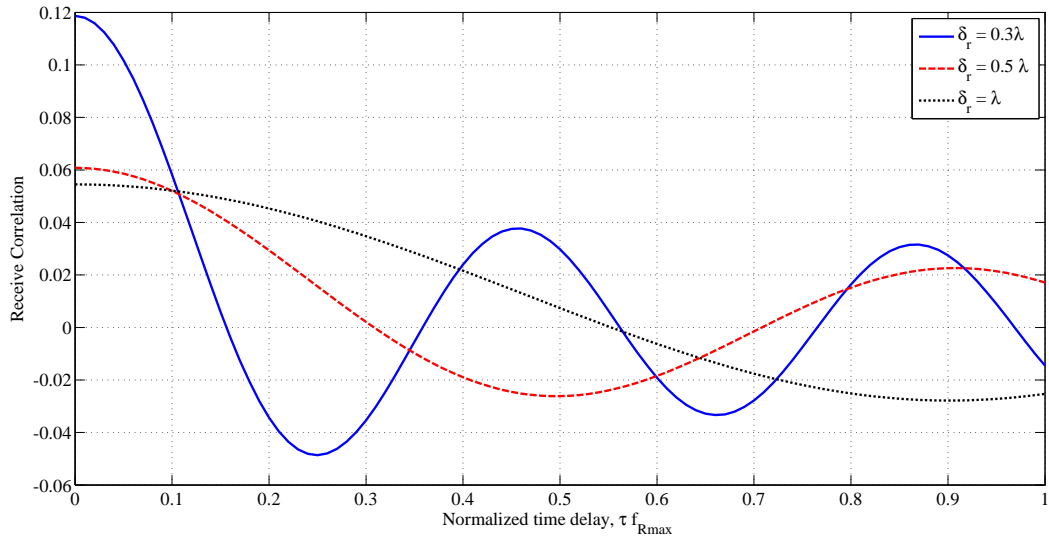
FIGURE 5.6: Effect of antenna spacing on space-time correlation function, $\beta_r = 20^o, \psi_r = 30^o, \theta_r = \theta_t = 2\pi/3, \psi_t = \theta_r = \pi/2, a_r = 500m, b_r = 100m$

decreasing trend and vice versa. Hence, keeping the antenna elements at appropriate spacing, maximum throughput can be achieved from the MIMO systems. Moreover, the proposed 3D eccentricity based channel model is transformed into 3D circular based geometrical channel model given in [2], by making eccentricity equal to zero and radius equal $200m$. It is observed from the graph that elliptical geometry shows significant increase in correlation as compared to circular geometry. It thus confirms the statement that elliptical geometry is more appropriate shape to model scattering environments of streets, canyons or highways in umbrella cellular environment; therefore, the results of our proposed channel model are more justified than circular ones to design and analyze MIMO M2M communication links.
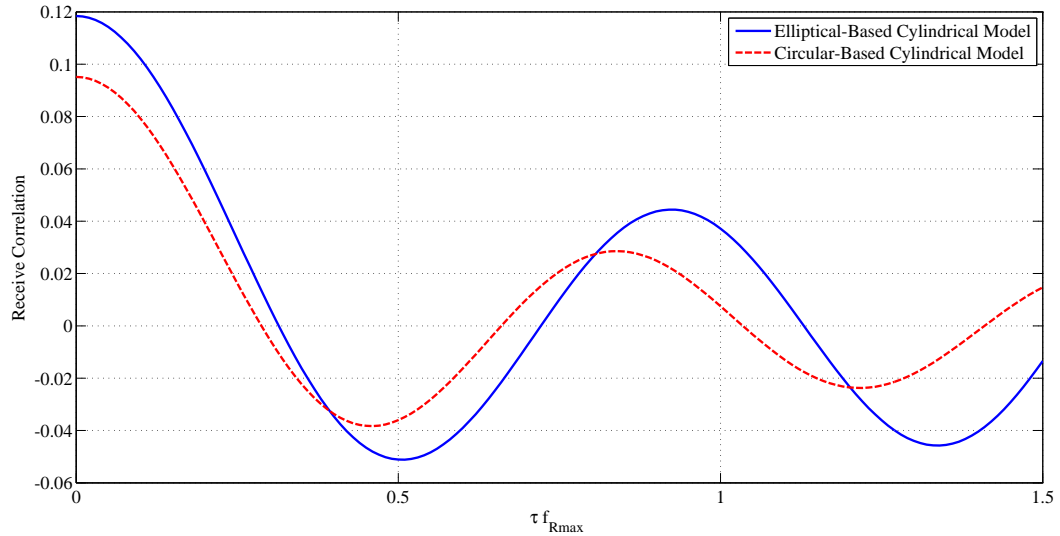
FIGURE 5.7: Comparison of space-time correlation function of proposed elliptical based cylindrical models with the circular based cylindrical channel models [2], $\delta_t = \lambda/2, \beta_r = 20^o, \theta_r = 30^o, \psi_r = 30^o, \theta_r = \theta_t = 120^o$

5.6 Conclusion

In this chapter, a single bounce 3D eccentricity-based cylindrical geometrical channel model for MIMO F2M propagation environment has been presented. The proposed elliptic cylindrical geometry is rotatable along the horizontal plane about vertical axis and its dimensions are adjustable corresponding to the physical propagation environment. Based on the proposed model, expressions of joint and marginal space-time correlation functions among the transmitter and receiver antenna array elements have been formulated. Various curves are generated using the obtained theoretical expressions for the joint and marginal correlation functions for different values of the channel parameters. The resultant correlation plots are thoroughly elaborated over the system performance. Moreover, 2D and 3D F2M geometrical channel models in the literature can be extracted from the proposed geometrical model by changing some of the parameters of its geometry.

Chapter 6

Conclusion and Future Directions

This chapter begins with Section 6.1 that summarizes the developed research work carried out in this dissertation and Section 6.2 provides future directions and recommendations.

6.1 Conclusion

In this dissertation, geometrically modeling of MIMO M2M and MIMO F2M radio fading propagation channels are targeted. Geometrical modeling approach is considered to be sophisticated and is well-suitable for mobile propagation channels. In mobile communication scenario, majority of the mobile-subscribers usually exist in streets, canyons, or on highways in urban or suburban areas. Where, the scatterers are usually non-isotropically distributed along the propagation path. Elliptical geometry has close resemblance with such non-isotropic propagation environments and has potential to accommodates most of scattering objects that are located at the road-side areas.

Exploiting the advantages of elliptical shape, initially, a 2D eccentricity-based geometrical channel model for MIMO M2M communications in non-isotropic scattering environments has been developed. It has been assumed that MSs reside at the center of two different ellipses holding low elevated antenna array structures.

The scattering objects are assumed to be uniformly distributed on the boundary of ellipses. In addition, it is considered that the ellipses around the MSs are flexible and rotatable in azimuth plane according to direction of motion of the MSs. Moreover, the ellipses are adjustable in dimensions according to the physical lengths of scattering regions around the MSs. In the developed eccentricity-based channel model, mathematical expression for the PDF of AoA/AoD is derived, which is further verified through simulation results. Moreover, with the help of the proposed geometry, an empirical expression for the PDF of AoA/AoD is formulated that is utilized for the joint and marginal correlation functions among the MIMO antenna elements. Furthermore, the proposed 2D eccentricity-based geometry is extended to 3D elliptic cylindrical geometry to accommodate the high-rise infrastructures, vegetation and other scattering objects along the roadside premises that have significant impact on the AoA/AoD of the multipath signals in the elevation plane. In the proposed 3D channel model, the eccentricities are used to model the physical dimensions of the scattering areas around the MSs in azimuth plane whereas the height of the elliptic-cylinder represents the elevation of roadside objects.

The MSs with low-elevated MIMO antenna arrays are assumed to be located at the centers of the elliptical cylinders and scatterers are considered to be uniformly distributed along the surfaces of each cylinder independently. MSs are assumed to be located in two different streets, canyons or highways having any size and density of scattering objects. Using the 3D developed channel model, expressions for the joint and marginal cross-correlation functions (CCFs) are derived. The derived expressions are plotted using various channel parameters to observe their effect on the antenna correlations. The result of antenna correlation is then compared with the measured data that shows a close agreement with it. Moreover, some of the existing 2D and 3D channel models in the literature are deduced by changing few of the channel parameters in the proposed channel model.

Furthermore, the fast-moving vehicles on highways in macrocellular environment create frequent handoffs during the call. The frequent handoffs impose burden on MSC and generate massive overhead traffic in cellular communication systems. Hence, these fast-moving subscribers are handed over to high-powered BS of an

umbrella cell that not only reduces the frequency of handoff but also increases the link coverage. Therefore, for the design and development of an umbrella cell of macrocellular communication networks, a 3D elliptical-based geometrical cylindrical channel model is developed. This system incorporates a novel idea of modeling scattering environments around the fast-moving vehicles on highways equipped with multiple antenna systems. In this case, it is assumed that the fast-moving subscriber is located at the center of elliptical cylinder and is equipped with low elevated multiple-antenna arrays. Whereas, the base-station is located on the top of a high-rise structure with multiple antenna arrays. Using the proposed model, expressions for the joint and marginal space-time correlation functions among MIMO antenna elements are derived. These correlation functions are helpful to design and develop MIMO systems for the high-speed mobile subscribers in a rich scattering environments.

6.2   Future Directions

Developing a communication system for data-hungry M2M/F2M communication systems with QoS is a challenging task in the research arena. Therefore, for the performance analysis and design of a communication system, various 2D and 3D geometrical channel models have been proposed in the literature. Like all other existing channel models available in the literature, the proposed model are also based on some assumptions that are more or less valid in a specific propagation scenarios. Hence, these proposed channel models can provide an appropriate framework to develop statistics of wireless channel parameters in a particular propagation environments considering both isotropic and non-isotropic scattering environments. The geometry of the proposed models have close resemblance with the layout of metropolitan regions, where the fast moving subscribers mostly reside while they are either on the call or using real-time data applications. However, for ease of derivations of the proposed channel models, single-bounce or double-bounce reflected multipaths are only taken in to consideration. In multipath propagation environments such channel models may not provide the statistics of channel

parameters accurately. Hence, the issues and challenges like multi-bounce scattering, Doppler effect and time variation of the propagation channel, etc., may be addressed collectively in future in a single channel model.

Therefore, to provide a GBSCM that can exactly assess the performance of a radio communication link on the basis of statistics of channel parameters is still undoubtedly a challenging problem in the literature.

Bibliography

[1] M. Zhu, G. Eriksson, and F. Tufvesson, "The COST 2100 channel model: Parameterization and validation based on outdoor MIMO measurements at 300 MHz," *IEEE Trans. Wireless Commun.*, vol. 12, no. 2, pp. 888–897, 2013.

[2] L. Feng, P. Fan, C. Wang, and A. Ghazal, "A 3D GBSM for high-speed train communication systems under deep cutting scenarios," in *Proc. International Workshop on High Mobility Wireless Communications (HMWC).* IEEE, 2015, pp. 86–90.

[3] K. Rundstedt, "Measurements and channel modelling of microwave line-of-sight MIMO links," Ph.D. dissertation, Masters thesis, Chalmers University of Technology, Sweden, 2014.

[4] J. Harri, F. Filali, and C. Bonnet, "Mobility models for vehicular ad hoc networks: a survey and taxonomy," *IEEE Commun. Surveys Tuts.*, vol. 11, no. 4, pp. 19–41, 2009.

[5] T. S. Rappaport, *Wireless communications: principles and practice.* Prentice Hall PTR New Jersey, 1996, vol. 2.

[6] N. M. Khan, M. T. Simsim, and P. B. Rapajic, "A generalized model for the spatial characteristics of the cellular mobile channel," *IEEE Trans. Veh. Technol.*, vol. 57, no. 1, pp. 22–37, 2008.

[7] Y. Akaiwa, "Digital mobile radio communication systems," *Introduction to Digital Mobile Communication, Second Edition*, pp. 543–612.

[8] A. Kuchar, J.-P. Rossi, and E. Bonek, "Directional macro-cell channel characterization from urban measurements," *IEEE Trans. Antennas Propag.*, vol. 48, no. 2, pp. 137–146, 2000.

[9] H. Furukawa and Y. Akaiwa, "A microcell overlaid with umbrella cell system," in *Proc. IEEE Veh. Technol. Conf.*, 1994, pp. 1455–1459.

[10] S. Misra, P. V. Krishna, and V. Saritha, "Lacav: an energy-efficient channel assignment mechanism for vehicular ad hoc networks," *The Journal of Supercomputing*, vol. 62, no. 3, pp. 1241–1262, 2012.

[11] N. D. Tripathi, J. H. Reed, and H. F. VanLandinoham, "Handoff in cellular systems," *IEEE Pers. Commun.*, vol. 5, no. 6, pp. 26–37, 1998.

[12] P. Crichton, R. S. Oberoi, and H. Thomas, "Handover based on measured time of signals received from neighboring cells," Feb. 24 1998, US Patent 5,722,072.

[13] K. Ivanov and G. Spring, "Mobile speed sensitive handover in a mixed cell environment," in *Proc. IEEE Vehicular Technology Conference*, vol. 2, 1995, pp. 892–896.

[14] Y.-u. Chung and D. Cho, "Velocity estimation using adaptive array antennas," in *Proc. IEEE Vehicular Technology Conference*, vol. 4, 2001, pp. 2565–2569.

[15] Y. u. Chung, D. J. Lee, D. H. Cho, and B. C. Shin, "Macrocell/microcell selection schemes based on a new velocity estimation in multitier cellular system," *IEEE Trans. Veh. Technol.*, vol. 51, no. 5, pp. 893–903, 2002.

[16] R. Mishra, N. Chaki, and S. Choudhury, "Study on handover mechanism in cellular network: An experimental approach," in *Applied Computation and Security Systems.* Springer, 2015, pp. 203–212.

[17] C. W. Lee, M. C. Chuang, M. C. Chen, and Y. S. Sun, "Seamless handover for high-speed trains using femtocell-based multiple egress network interfaces," *IEEE Trans. Commun.*, vol. 13, no. 12, pp. 6619–6628, 2014.

[18] H. Q. Ngo, E. G. Larsson, and T. L. Marzetta, "Energy and spectral efficiency of very large multiuser MIMO systems," *IEEE Trans. Commun.*, vol. 61, no. 4, pp. 1436–1449, 2013.

[19] S. Abbas, D. Selvathi, V. Nandhini, and S. Thiruvengadam, "Synthesis and implementation of spatial multiplexing blocks for 3GPP-LTE using FPGA," in *Prof. IEEE Int. Communication and Network Technologies (ICCNT)*, 2014, pp. 243–248.

[20] D. W. Bliss, K. W. Forsythe, A. O. Hero, and A. F. Yegulalp, "Environmental issues for MIMO capacity," *IEEE Trans. Signal Process.*, vol. 50, no. 9, pp. 2128–2142, 2002.

[21] D. Tse and P. Viswanath, *Fundamentals of wireless communication.* Cambridge university press, 2005.

[22] J. H. Winters, "On the capacity of radio communication systems with diversity in a rayleigh fading environment," *IEEE J. Sel. Areas Commun.*, vol. 5, no. 5, pp. 871–878, 1987.

[23] G. J. Foschini and M. J. Gans, "On limits of wireless communications in a fading environment when using multiple antennas," *Wireless Pers. Commun.*, vol. 6, no. 3, pp. 311–335, 1998.

[24] T. L. Marzetta and B. M. Hochwald, "Capacity of a mobile multiple-antenna communication link in rayleigh flat fading," *IEEE Trans. Inf. Theory*, vol. 45, no. 1, pp. 139–157, 1999.

[25] G. G. Raleigh and J. M. Cioffi, "Spatio-temporal coding for wireless communication," *IEEE Trans. Commun.*, vol. 46, no. 3, pp. 357–366, 1998.

[26] B. Holter, "On the capacity of the MIMO channel: A tutorial introduction," in *Proc. IEEE Norwegian Symposium on Signal Processing*, 2001, pp. 167–172.

[27] V. Tarokh, N. Seshadri, and A. R. Calderbank, "Space-time codes for high data rate wireless communication: Performance criterion and code construction," *IEEE Trans. Inf. Theory*, vol. 44, no. 2, pp. 744–765, 1998.

[28] G. J. Foschini, "Layered space-time architecture for wireless communication in a fading environment when using multi-element antennas," *Bell labs technical journal*, vol. 1, no. 2, pp. 41–59, 1996.

[29] V. Tarokh, H. Jafarkhani, and A. R. Calderbank, "Space-time block codes from orthogonal designs," *IEEE Trans. Inf. Theory*, vol. 45, no. 5, pp. 1456–1467, 1999.

[30] J. O. Nielsen, B. Yanakiev, S. C. Del Barrio, and G. F. Pedersen, "On antenna design objectives and the channel capacity of MIMO handsets," *IEEE Trans. Antennas Propag.*, vol. 62, no. 6, pp. 3232–3241, 2014.

[31] D.-S. Shiu, G. J. Foschini, M. J. Gans, and J. M. Kahn, "Fading correlation and its effect on the capacity of multielement antenna systems," *IEEE Trans. Commun.*, vol. 48, no. 3, pp. 502–513, 2000.

[32] A. Goldsmith, S. A. Jafar, N. Jindal, and S. Vishwanath, "Fundamental capacity of MIMO channels," *IEEE J. Select. Areas Commun*, 2002.

[33] X. Cheng, Y. He, and M. Guizani, "3-D geometrical model for multi-polarized MIMO systems," *IEEE Access*, vol. X, no. X, pp. 1–20, 2017.

[34] D. Chizhik, F. Rashid-Farrokhi, J. Ling, and A. Lozano, "Effect of antenna separation on the capacity of blast in correlated channels," *IEEE Commun. Lett.*, vol. 4, no. 11, pp. 337–339, 2000.

[35] E. Telatar, "Capacity of multi-antenna gaussian channels," *Eur. Trans. on Telecommun.*, vol. 10, no. 6, pp. 585–595, 1999.

[36] A. F. Molisch, *Wireless communications.* John Wiley & Sons, 2007.

[37] G. D. Durgin and T. S. Rappaport, "Theory of multipath shape factors for small-scale fading wireless channels," *IEEE Trans. Antennas Propag.*, vol. 48, no. 5, pp. 682–693, 2000.

[38] W. C. Lee, *Mobile communications engineering*. McGraw-Hill Professional, 1982.

[39] F. Adachi, M. Feeney, J. Parsons, and A. Williamson, "Cross-correlation between the envelopes of 900 MHz signals received at a mobile radio base station site," *IEE Proc. F Communications, Radar and Signal Processing*, vol. 133, no. 6, pp. 506–512, 1986.

[40] R. Janaswamy, "Effect of element mutual coupling on the capacity of fixed length linear arrays," *IEEE Antennas Wireless Propag. Lett.*, vol. 1, no. 1, pp. 157–160, 2002.

[41] C. E. Shannon, R. G. Gallager, and E. R. Berlekamp, "Lower bounds to error probability for coding on discrete memoryless channels. I," *Information and Control*, vol. 10, no. 1, pp. 65–103, 1967.

[42] L. Wang, G. Min, and D. Kouvatsos, "Performance analysis of a dynamic handoff scheme in wireless networks with heterogeneous call arrival processes," *Telecommunication Systems*, vol. 39, no. 2, pp. 157–167, 2008.

[43] S. Tekinay and B. Jabbari, "Handover and channel assignment in mobile cellular networks," *IEEE Commun. Mag.*, vol. 29, no. 11, pp. 42–46, 1991.

[44] P. Marichamy, S. Chakrabarti, and S. Maskara, "Overview of handoff schemes in cellular mobile networks and their comparative performance evaluation," in *Proc. IEEE Veh. Technol. Conf.*, vol. 3, 1999, pp. 1486–1490.

[45] A. S. Anpalagan and I. Katzela, "Overlaid cellular system design with cell selection criteria for mobile wireless users," in *Proc. IEEE Electrical and Computer Engineering*, vol. 1. IEEE, 1999, pp. 24–28.

[46] J. D. Gibson, *Mobile communications handbook*. CRC press, 2012.

[47] A. Bencheikh, "Handoff management in a multi-layer wireless network," Aug. 2014.

[48] E. Inaty, "A finite state markov chain-based umbrella cell channel model for fast mobile users," in *Proc. IEEE Wireless Communications, Networking and Mobile Computing (WiCOM)*, 2006, pp. 1–5.

[49] A. Richardson, "Method and system of setting transmitter power levels," Nov. 11 2014, uS Patent 8,886,249.

[50] C. Budianu and L. Tong, "Channel estimation for space-time orthogonal block codes," *IEEE Trans. Signal Process.*, vol. 50, no. 10, pp. 2515–2528, 2002.

[51] J. G. Andrews, A. Ghosh, and R. Muhamed, *Fundamentals of WiMAX: understanding broadband wireless networking.* Pearson Education, 2007.

[52] L. Cheng, D. D. Stancil, and F. Bai, "A roadside scattering model for the vehicle-to-vehicle communication channel," *IEEE Journal on Selected Areas in Communications*, vol. 31, no. 9, pp. 449–459, 2013.

[53] A. Molisch, F. Tufvesson, J. Kåredal, and C. F. Mecklenbräuker, "A survey on vehicle-to-vehicle propagation channels," *IEEE Commun. Mag.*, vol. 16, no. 6, pp. 12–22, 2009.

[54] L. Wang, X. Qi, J. Xiao, K. Wu, M. Hamdi, and Q. Zhang, "Exploring smart pilot for wireless rate adaptation," 2016.

[55] R. S. Blum and J. H. Winters, "On optimum MIMO with antenna selection," in *Proc. IEEE International Conference on Communications (ICC) 2002*, vol. 1, pp. 386–390.

[56] R. B. Ertel, P. Cardieri, K. W. Sowerby, T. S. Rappaport, and J. H. Reed, "Overview of spatial channel models for antenna array communication systems," *IEEE Pers. Commun.*, vol. 5, no. 1, pp. 10–22, 1998.

[57] N. M. Khan, "Modeling and characterization of multipath fading channels in cellular mobile communication systems," Ph.D. dissertation, University of New South Wales, 2006.

[58] H. Asplund, A. A. Glazunov, A. F. Molisch, K. I. Pedersen, and M. Stein-bauer, "The COST259 directional channel model-part II: macrocells," *IEEE Trans. Wireless Commun.*, vol. 5, no. 12, pp. 3434–3450, 2006.

[59] V. Abhayawardhana, I. Wassell, D. Crosby, M. Sellars, and M. Brown, "Comparison of empirical propagation path loss models for fixed wireless access systems," in *Proc. IEEE Vehicular Technology Conference*, vol. 1. IEEE, 2005, pp. 73–77.

[60] G. E. Athanasiadou, A. R. Nix, and J. P. McGeehan, "A microcellular ray-tracing propagation model and evaluation of its narrow-band and wide-band predictions," *IEEE J. Sel. Areas Commun.*, vol. 18, no. 3, pp. 322–335, 2000.

[61] H. Kokoszkiewicz, "MIMO geometrically based channel model," Ph.D. dissertation, POLITECHNIKA WARSZAWSKA, 2005.

[62] G. E. Corazza, V. Degli-Esposti, M. Frullone, and G. Riva, "A characterization of indoor space and frequency diversity by ray-tracing modeling," *IEEE Journal on selected areas in communications*, vol. 14, no. 3, pp. 411–419, 1996.

[63] S. Y. Seidel and T. S. Rappaport, "A ray tracing technique to predict path loss and delay spread inside buildings," in *Proc. IEEE Global Telecommun. Conf. (GLOBECOM)*, 1992, pp. 649–653.

[64] P. Bello, "Characterization of randomly time-variant linear channels," *IEEE Trans. Commun. Systems*, vol. 11, no. 4, pp. 360–393, 1963.

[65] C.-X. Wang, X. Cheng, and D. I. Laurenson, "Vehicle-to-vehicle channel modeling and measurements: recent advances and future challenges," *IEEE Communications Magazine*, vol. 47, no. 11, 2009.

[66] L. Song and J. Shen, *Evolved cellular network planning and optimization for UMTS and LTE.* CRC Press, 2010.

[67] L. Vuokko, P. Vainikainen, and J.-i. Takada, "Clusters extracted from measured propagation channels in macrocellular environments," *IEEE Transactions on Antennas and Propagation*, vol. 53, no. 12, pp. 4089–4098, 2005.

[68] X. Cheng, C.-X. Wang, D. I. Laurenson, S. Salous, and A. V. Vasilakos, "An adaptive geometry-based stochastic model for non-isotropic MIMO mobile-to-mobile channels," *IEEE Trans. Wireless Commun.*, vol. 8, no. 9, pp. 4824–4835, 2009.

[69] J. Karedal, F. Tufvesson, N. Czink, A. Paier, C. Dumard, T. Zemen, C. F. Mecklenbräuker, and A. F. Molisch, "Measurement-based modeling of vehicle-to-vehicle MIMO channels," in *Proc. IEEE International Conference on Communications*. IEEE, 2009, pp. 1–6.

[70] R. Janaswamy, "Angle of arrival statistics for a 3D spheroid model," *IEEE Trans. Veh. Technol.*, vol. 51, no. 5, pp. 1242–1247, 2002.

[71] A. Mohammadi and F. M. Ghannouchi, *RF transceiver design for MIMO wireless communications*. Springer Science & Business Media, 2012, vol. 145.

[72] G. Del Galdo, "Geometry based channel modeling for multi-user MIMO systems and applications." ISLE, 2007.

[73] J. B. Andersen and P. C. F. Eggers, "A heuristic model of power delay profiles in landmobile communications," in *Proc. URSI Symposium on Electromagnetic Theory*, 1992.

[74] A. S. Akki and F. Haber, "A statistical model of mobile-to-mobile land communication channel," *IEEE Trans. Veh. Technol.*, vol. 35, no. 1, pp. 2–7, Feb. 1986.

[75] M. Pätzold, B. O. Hogstad, N. Youssef, and D. Kim, "A MIMO mobile-to-mobile channel model: Part I- the reference model," in *Proc. IEEE 16th International Symp. on Personal, Indoor and Mobile Radio Communications (PIMRC)*, vol. 1, 2005, pp. 573–578.

[76] C. Wei, H. Zhiyi, and Z. Lili, "A reference model for MIMO mobile-to-mobile fading channel," in *Proc. International Conference on Wireless Communications, Networking and Mobile Computing*, 2007, pp. 228–231.

[77] M. Riaz and N. M. Khan, "Closed-form expressions for correlation function and power density spectrum in MIMO mobile-to-mobile channels using two-erose-ring model," in *Proc. IEEE International Conference on Information and Communication Technologies (ICICT)*, 2011, pp. 1–5.

[78] B. S. Paul, A. Hasan, H. Madheshiya, and R. Bhattacharjee, "Time and angle of arrival statistics of mobile-to-mobile communication channel employing circular scattering model," *IETE Journal of Research*, vol. 55, no. 6, p. 275, 2009.

[79] B. S. Paul, R. Bhattacharjee *et al.*, "Time and angle of arrival statistics of mobile-to-mobile communication channel employing dual annular strip model," *IETE Journal of Research*, vol. 56, no. 6, p. 327, 2010.

[80] A. Chelli and M. Pätzold, "A non-stationary MIMO vehicle-to-vehicle channel model based on the geometrical t-junction model," in *Proc. IEEE International Conference on Wireless Communications and Signal Processing (WCSP)*. IEEE, 2009, pp. 1–5.

[81] J. F. Ossanna, "A model for mobile radio fading due to building reflections: Theoretical and experimental fading waveform power spectra," *Bell System Technical Journal*, vol. 43, no. 6, pp. 2935–2971, 1964.

[82] T. Aulin, "A modified model for the fading signal at a mobile radio channel," *IEEE Trans. Veh. Technol*, vol. 28, no. 3, pp. 182–203, 1979.

[83] F. Vatalaro and A. Forcella, "Doppler spectrum in mobile-to-mobile communications in the presence of three-dimensional multipath scattering," *IEEE Trans. Veh. Technol.*, vol. 46, no. 1, pp. 213–219, Feb. 1997.

[84] A. G. Zajić and G. L. Stuber, "A three dimensional parametric model for wideband MIMO mobile-to-mobile channels," in *Proc. International Conference on IEEE GLOBECOM.* IEEE, 2007, pp. 3760–3764.

[85] A. G. Zajić and G. L. Stüber, "Three-dimensional modeling, simulation, and capacity analysis of space-time correlated mobile-to-mobile channels," *IEEE Trans. Veh. Technol.*, vol. 57, no. 4, pp. 2042 –2054, Jul. 2008.

[86] A. G. Zajić and G. L. Stuber, "Three-dimensional modeling and simulation of wideband MIMO mobile-to-mobile channels," *IEEE Trans. Wireless Commun.*, vol. 8, no. 3, pp. 1260–1275, 2009.

[87] N. Avazov and M. Pätzold, "A novel wideband MIMO car-to-car channel model based on a geometrical semi-circular tunnel scattering model," *IEEE Trans. Veh. Technol.*, vol. 65, no. 3, pp. 1070–1082, 2016.

[88] A. Abdi and M. Kaveh, "A space-time correlation model for multielement antenna systems in mobile fading channels," *IEEE J. Sel. Areas Commun.*, vol. 20, no. 3, pp. 550–560, 2002.

[89] M. Pätzold and B. O. Hogstad, "A space-time channel simulator for MIMO channels based on the geometrical one-ring scattering model," *Wireless Communications and Mobile Computing*, vol. 4, no. 7, pp. 727–737, 2004.

[90] M. Zhang, P. J. Smith, and M. Shafi, "An extended one-ring MIMO channel model," *IEEE Trans. Commun.*, vol. 6, no. 8, pp. 2759–2764, 2007.

[91] X. Cheng, C.-X. Wang, and D. I. Laurenson, "A generic space-time-frequency correlation model and its corresponding simulation model for narrowband MIMO channels," in *Proc. European Conference on Antennas Propag.* IET, 2007, pp. 1–6.

[92] A. Ghazal, C.-X. Wang, B. Ai, D. Yuan, and H. Haas, "A nonstationary wideband MIMO channel model for high-mobility intelligent transportation systems," *IEEE Trans. Intell. Transp. Syst.*, vol. 16, no. 2, pp. 885–897, 2015.

[93] H. Jiang, V. C. Leung, C. Gao, and T. Tang, "MIMO-assisted handoff scheme for communication-based train control systems," *IEEE Trans. Veh. Technol.*, vol. 64, no. 4, pp. 1578–1590, 2015.

[94] A. Y. Olenko, K. T. Wong, and E. Hui-On Ng, "Analytically derived uplink/downlink ToA and 2D-DoA distributions with scatterers in a 3D hemispheroid surrounding the mobile," *IEEE Trans. Antennas Propag.*, vol. 54, no. 9, pp. 2446–2454, Sep. 2006.

[95] J. C. Liberti and T. S. Rappaport, "A geometrically based model for line-of-sight multipath radio channels," in *Proc. IEEE Veh. Technol. Conf.*, vol. 2, 1996, pp. 844–848.

[96] R. B. Ertel and J. H. Reed, "Angle and time of arrival statistics for circular and elliptical scattering models," *IEEE J. Sel. Areas Commun.*, vol. 17, no. 11, pp. 1829–1840, 1999.

[97] P. Petrus, J. H. Reed, and T. S. Rappaport, "Geometrical-based statistical macrocell channel model for mobile environments," *IEEE Trans. Commun.*, vol. 50, no. 3, pp. 495–502, 2002.

[98] N. M. Khan, M. T. Simsim, and R. Ramer, "Modeling spatial aspects of mobile channel for macrocells using Gaussian scattering distribution," in *Proc. IEEE International Symposium on Wireless Communication Systems (ISWCS'06.)*. IEEE, 2006, pp. 616–620.

[99] K. Baltzis, "On the geometric modeling of the uplink channel in a cellular system." *Journal of Engineering Science & Technology Review*, vol. 1, no. 1, 2008.

[100] I. Jaafar, H. Boujemâa, and M. Siala, "Angle and time of arrival statistics for hollow-disc and elliptical scattering models," in *Proc. 2nd Int. Conf. Signals, Circuits Syst*, 2008, pp. 1–4.

[101] C. Ziółkowski and J. M. Kelner, "Geometry-based statistical model for the temporal, spectral, and spatial characteristics of the land mobile channel," *Wireless Pers. Commun.*, vol. 83, no. 1, pp. 631–652, 2015.

[102] K. B. Baltzis, "A generalized elliptical scattering model for the spatial characteristics of mobile channels," *Wireless Pers. Commun.*, pp. 1–14, 2011.

[103] ——, "A simplified geometric channel model for mobile-to-mobile communications," *Radioengineering*, vol. 20, no. 4, pp. 961–967, 2011.

[104] M. Riaz, S. J. Nawaz, and N. M. Khan, "3D ellipsoidal model for mobile-to-mobile radio propagation environments," *Wireless Pers. Commun.*, vol. 72, no. 4, pp. 2465–2479, 2013.

[105] M. Riaz, N. M. Khan, and S. J. Nawaz, "A generalized 3D scattering channel model for spatiotemporal statistics in mobile-to-mobile communication environment," *IEEE Trans. Veh. Technol.*, vol. 64, no. 10, pp. 4399–4410, 2015.

[106] A. Ahmed, S. J. Nawaz, and S. M. Gulfam, "A 3D propagation model for emerging land mobile radio cellular environments," *PLOS ONE*, vol. 10, no. 8, p. e0132555, 2015.

[107] S. J. Nawaz, M. Riaz, N. M. Khan, and S. Wyne, "Temporal analysis of a 3D ellipsoid channel model for the vehicle-to-vehicle communication environments," *Wireless Pers. Commun.*, vol. 82, no. 3, pp. 1337–1350, 2015.

[108] Z. Sun and I. F. Akyildiz, "A mode-based approach for channel modeling in underground tunnels under the impact of vehicular traffic flow," *IEEE Trans. Commun.*, vol. 10, no. 10, pp. 3222–3231, 2011.

[109] X. Wang, E. Anderson, P. Steenkiste, and F. Bai, "Improving the accuracy of environment-specific vehicular channel modeling," in *Proc. International workshop on Wireless network testbeds, experimental evaluation and characterization.* ACM, 2012, pp. 43–50.

[110] J. Karedal, F. Tufvesson, N. Czink, A. Paier, C. Dumard, T. Zemen, C. F. Mecklenbrauker, and A. F. Molisch, "A geometry-based stochastic MIMO model for vehicle-to-vehicle communications," *IEEE Trans. Wireless Commun.*, vol. 8, no. 7, pp. 3646–3657, 2009.

[111] M. Pätzold and B. O. Hogstad, "A wideband MIMO channel model derived from the geometric elliptical scattering model," *Wireless Communications and Mobile Computing*, vol. 8, no. 5, pp. 597–605, 2008.

[112] A. Attia, A. A. Elmoslimany, A. Elkeyi, T. Elbatt, F. Bai, and C. Saraydar, "MIMO vehicular networks: research challenges and opportunities," *Journal of communications*, vol. 7, no. 06, pp. 500–513, 2012.

[113] M. D. Soltani, M. Alimadadi, and A. Mohammadi, "Modeling of mobile scatterer clusters for doppler spectrum in wideband vehicle-to-vehicle communication channels," *IEEE Commun. Lett.*, vol. 18, no. 4, pp. 628–631, 2014.

[114] M. Ghoraishi, J. Takada, and T. Imai, "Stochastic channel model for dense urban line-of-sight street microcell," *Technical Document of COST*, vol. 2100, pp. 26–28, 2007.

[115] M. Patzöld, B. O. Hogstad, and N. Youssef, "Modeling, analysis, and simulation of MIMO mobile-to-mobile fading channels," *IEEE Trans. Wireless Commun.*, vol. 7, no. 2, pp. 510–520, 2008.

[116] L. Lahtin, "Radio network structures for high traffic density areas," in *Proc. Third Nordic Seminar on Digital Land Mobile Radio Communication*, no. 14.10, 1988.

[117] K. I. Pedersen, P. E. Mogensen, and B. H. Fleury, "A stochastic model of the temporal and azimuthal dispersion seen at the base station in outdoor propagation environments," *IEEE Trans. Veh. Technol.*, vol. 49, no. 2, pp. 437–447, 2000.

[118] A. Abdi, J. A. Barger, and M. Kaveh, "A parametric model for the distribution of the angle of arrival and the associated correlation function and power spectrum at the mobile station," *IEEE Trans. Veh. Technol.*, vol. 51, no. 3, pp. 425–434, 2002.

[119] I. S. Gradshtejn and I. M. Ryzhik, *Table of integrals, series and products.* Academic Press, 1965.

[120] A. G. Zajić and G. L. Stüber, "Space-time correlated MIMO mobile-to-mobile channels," in *Proc. IEEE 17th International Symp. on Personal, Indoor and Mobile Radio Communications (PIMRC)*, 2006, pp. 1–5.

[121] A. Chelli and M. Patzöld, "A MIMO mobile-to-mobile channel model derived from a geometric street scattering model," in *Proc. Wireless Communication Systems (ISWCS)*, 2007, pp. 792–797.

[122] A. S. Akki, "Statistical properties of mobile-to-mobile land communication channels," *IEEE Trans. Veh. Technol.*, vol. 43, no. 4, pp. 826–831, Nov 1994.

[123] R. H. Clarke and W. L. Khoo, "3-D mobile radio channel statistics," *IEEE Trans. Veh. Technol.*, vol. 46, no. 3, pp. 798–799, 1997.

[124] W. C. Jakes and D. C. Cox, *Microwave mobile communications.* Wiley-IEEE Press, 1994.

[125] F. Qu, F.-Y. Wang, and L. Yang, "Intelligent transportation spaces: vehicles, traffic, communications, and beyond," *IEEE Commun. Mag.*, vol. 48, no. 11, pp. 136–142, 2010.

[126] N. Avazov and M. Pätzold, "Design of wideband MIMO car-to-car channel models based on the geometrical street scattering model," *Modelling and Simulation in Engineering*, vol. 2012, p. 5, 2012.

[127] D. Gesbert, H. Bolcskei, D. Gore, and A. Paulraj, "MIMO wireless channels: Capacity and performance prediction," in *IEEE, Global Telecommunications Conference (GLOBECOM).*, vol. 2. IEEE, 2000, pp. 1083–1088.

[128] D. Gesbert, H. Bolcskei, D. A. Gore, and A. J. Paulraj, "Outdoor MIMO wireless channels: Models and performance prediction," *IEEE Trans. Commun.*, vol. 50, no. 12, pp. 1926–1934, 2002.

[129] L. Rade and B. Westergren, *Mathematics handbook for science and engineering.* Springer Science & Business Media, 2013.

[130] M. Y. Wani, M. Riaz, and N. M. Khan, "Modeling and characterization of MIMO mobile-to-mobile communication channels using elliptical scattering geometry," *Wireless Pers. Commun.*, vol. 91, no. 2, pp. 509–524, 2016.

[131] Y. Yamada, Y. Ebine, and N. Nakajima, "Base station/vehicular antenna design techniques employed in high-capacity land mobile communications system," *Review of the Electrical Communication Laboratories*, vol. 35, no. 2, pp. 115–121, 1987.

[132] J. Parsons and A. Turkmani, "Characterisation of mobile radio signals: model description," in *Proc. IEE Communications, Speech and Vision*, vol. 138, no. 6. IET, 1991, pp. 549–556.

[133] A. Jeffrey and D. Zwillinger, *Table of integrals, series, and products.* Academic Press, 2007.

[134] S. Abrarov and B. Quine, "Accurate approximations for the complex error function with small imaginary argument," *arXiv preprint arXiv:1411.1024*, 2014.

[135] M. Pätzold, B. O. Hogstad, and N. Youssef, "Modeling, analysis, and simulation of MIMO mobile-to-mobile fading channels," *IEEE Trans. Wireless Commun.*, vol. 7, no. 2, pp. 510–520, 2008.

[136] A. A. Abouda, "Characterization of MIMO channel capacity in urban microcellular environment," Ph.D. dissertation, Electrical and Communications Engineering, Helsinki University of Technology, 2007.

[137] L. Haibin, X. Liangjun, Y. Jibing, and Z. Linhua, "Modeling and analysis on mobile-to-mobile cascade channel of amplify-and-forward two-way relay

networks," in *Proc. National Doctoral Academic Forum on Information and Communications Technology.* IET, 2013, pp. 1–6.

[138] M. J. Chu and W. E. Stark, "Effect of mobile velocity on communications in fading channels," *IEEE Trans. Veh. Technol.*, vol. 49, no. 1, pp. 202–210, 2000.

[139] H. Kang, G. Stuber, T. G. Pratt, and M. A. Ingram, "Studies on the capacity of MIMO systems in mobile-to-mobile environment," in *Wireless Communications and Networking Conference, 2004. WCNC. 2004 IEEE*, vol. 1. IEEE, 2004, pp. 363–368.

[140] A. G. Zajić and Stüber, "Space time correlated MIMO mobile to mobile channels."

[141] B. S. Paul, A. Hasan, H. Madheshiya, and R. Bhattacharjee, "Time and angle of arrival statistics of mobile-to-mobile communication channel employing circular scattering model," *IETE Journal of Research*, vol. 55, no. 6, pp. 275–281, 2009.

[142] V. H. Mac Donald, "Advanced mobile phone service: The cellular concept," *The Bell System Technical Journal*, vol. 58, no. 1, pp. 15–41, 1979.

[143] K. S. Gilhousen, I. M. Jacobs, R. Padovani, A. J. Viterbi, L. A. Weaver, and C. E. Wheatley, "On the capacity of a cellular CDMA system," *IEEE Trans. Veh. Technol.*, vol. 40, no. 2, pp. 303–312, 1991.

[144] P. Madhusudhanan, J. G. Restrepo, Y. Liu, T. X. Brown, and K. R. Baker, "Multi-tier network performance analysis using a shotgun cellular system," in *Proc. IEEE Global Telecommunications Conference (GLOBECOM).* IEEE, 2011, pp. 1–6.

[145] M. Boban, T. T. Vinhoza, M. Ferreira, J. Barros, and O. K. Tonguz, "Impact of vehicles as obstacles in vehicular ad hoc networks," *IEEE J. Sel. Areas Commun.*, vol. 29, no. 1, pp. 15–28, 2011.

[146] B. Talha and M. Pätzold, "Channel models for mobile-to-mobile cooperative communication systems: A state of the art review," *IEEE Veh. Technol. Mag.*, vol. 6, no. 2, pp. 33–43, 2011.

[147] A. Ahmed, S. J. Nawaz, N. M. Khan, M. N. Patwary, and M. Abdel-Maguid, "Angular characteristics of a unified 3-D scattering model for emerging cellular networks," in *Proc. IEEE International Conference on Communications (ICC).* IEEE, 2015, pp. 2450–2456.

[148] J. Salz and J. H. Winters, "Effect of fading correlation on adaptive arrays in digital mobile radio," *IEEE Trans. Veh. Technol.*, vol. 43, no. 4, pp. 1049–1057, 1994.

[149] A. Kuchar, E. A. Aparicio, J.-P. Rossi, and E. Bonek, "Azimuth, elevation, and delay of signals at mobile station site," in *Wireless Pers. Commun.* Springer, 2002, pp. 99–110.

[150] P. Petrus, J. H. Reed, and T. S. Rappaport, "Effects of directional antennas at the base station on the doppler spectrum," *IEEE Communications Letters*, vol. 1, no. 2, pp. 40–42, 1997.